

MaP Graduate Symposium

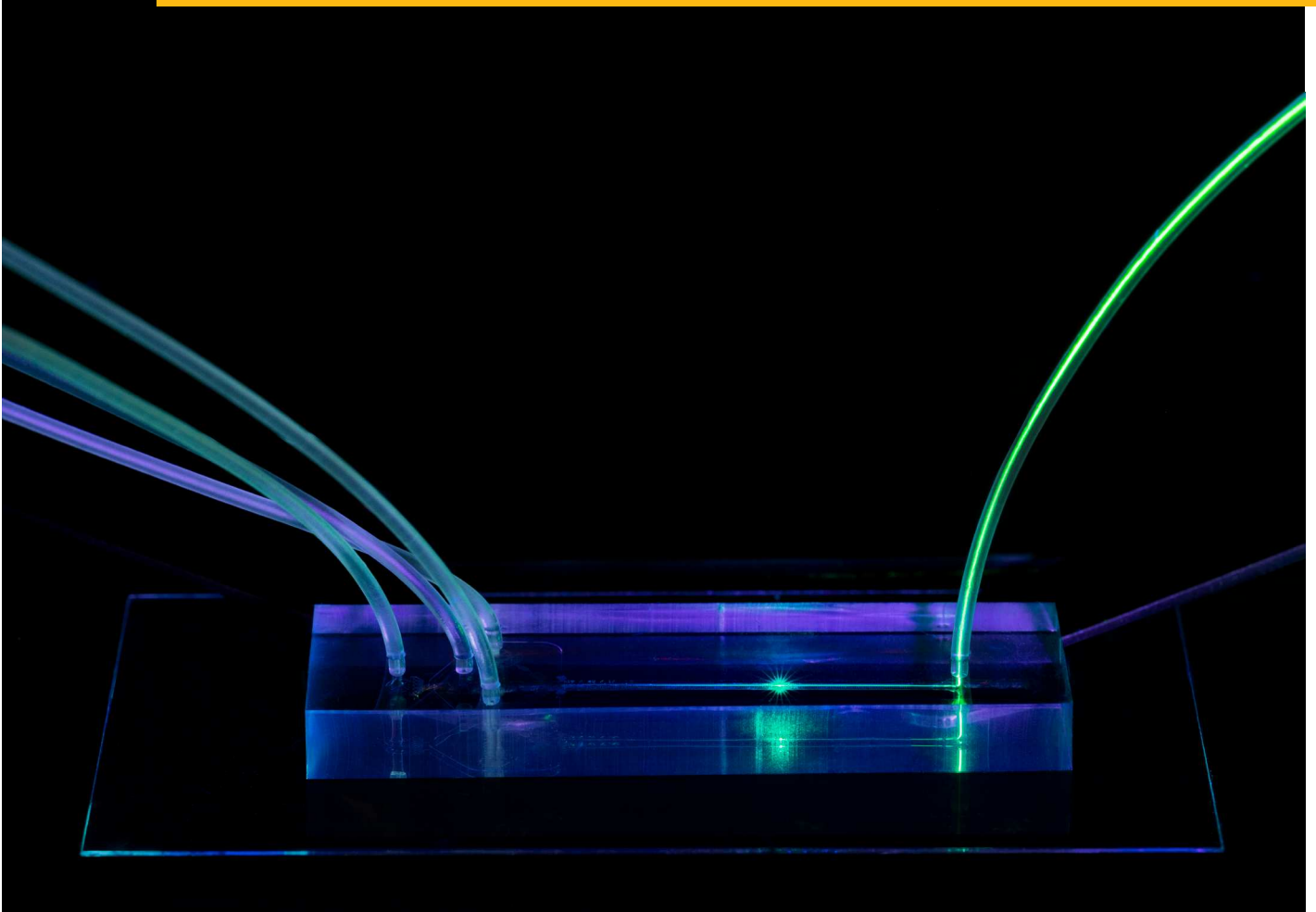
featuring the MaP Award 2022

The 17th Annual Gathering of the Materials & Processes community of ETH Zurich

1 September 2022

www.doctoral-school.ethz.ch/events/grad-symp

Symposium Booklet



The Light in the Channel | winner of MaP Art of Science Contest 2022 by Julie Probst (ETH Zurich)

Many thanks to our industry partners!



BOSCH

EPILATUS



SENSIRION

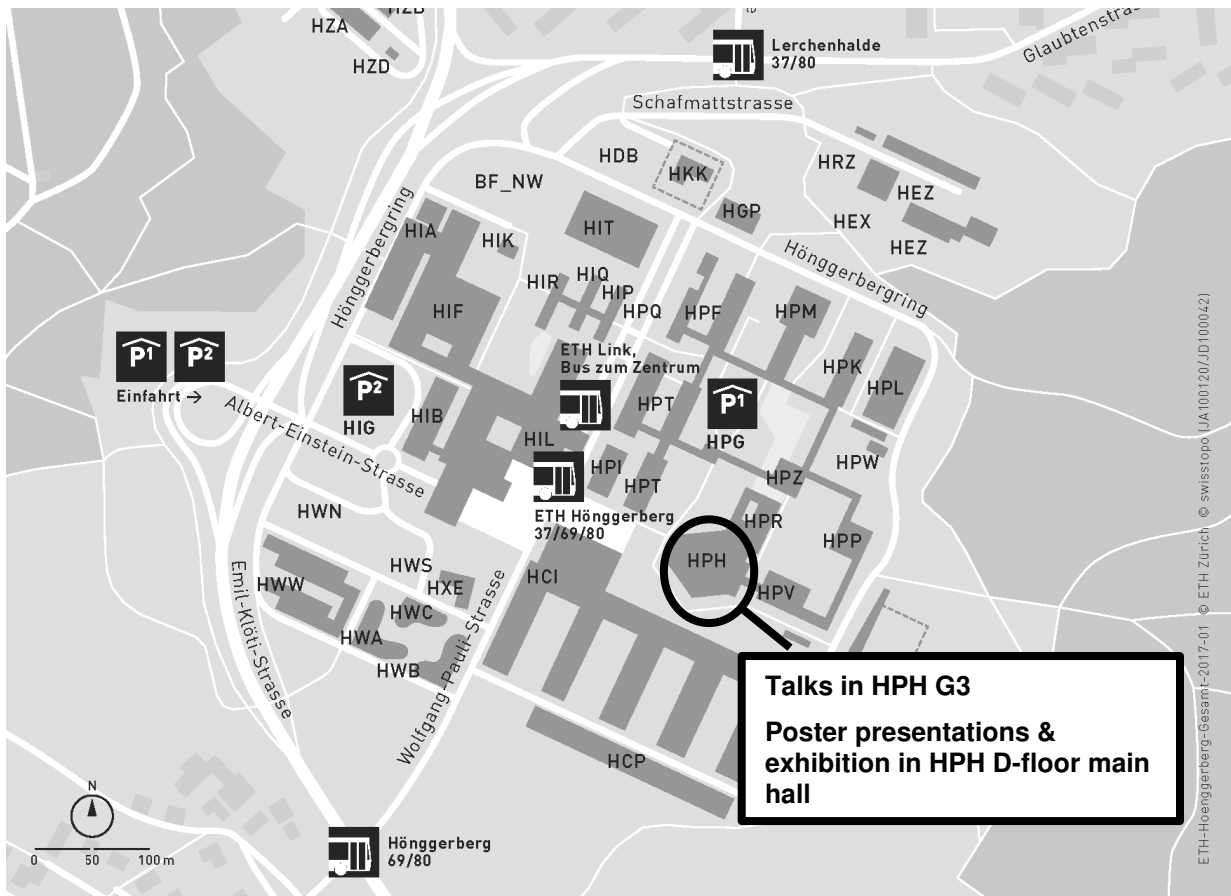


Geistlich

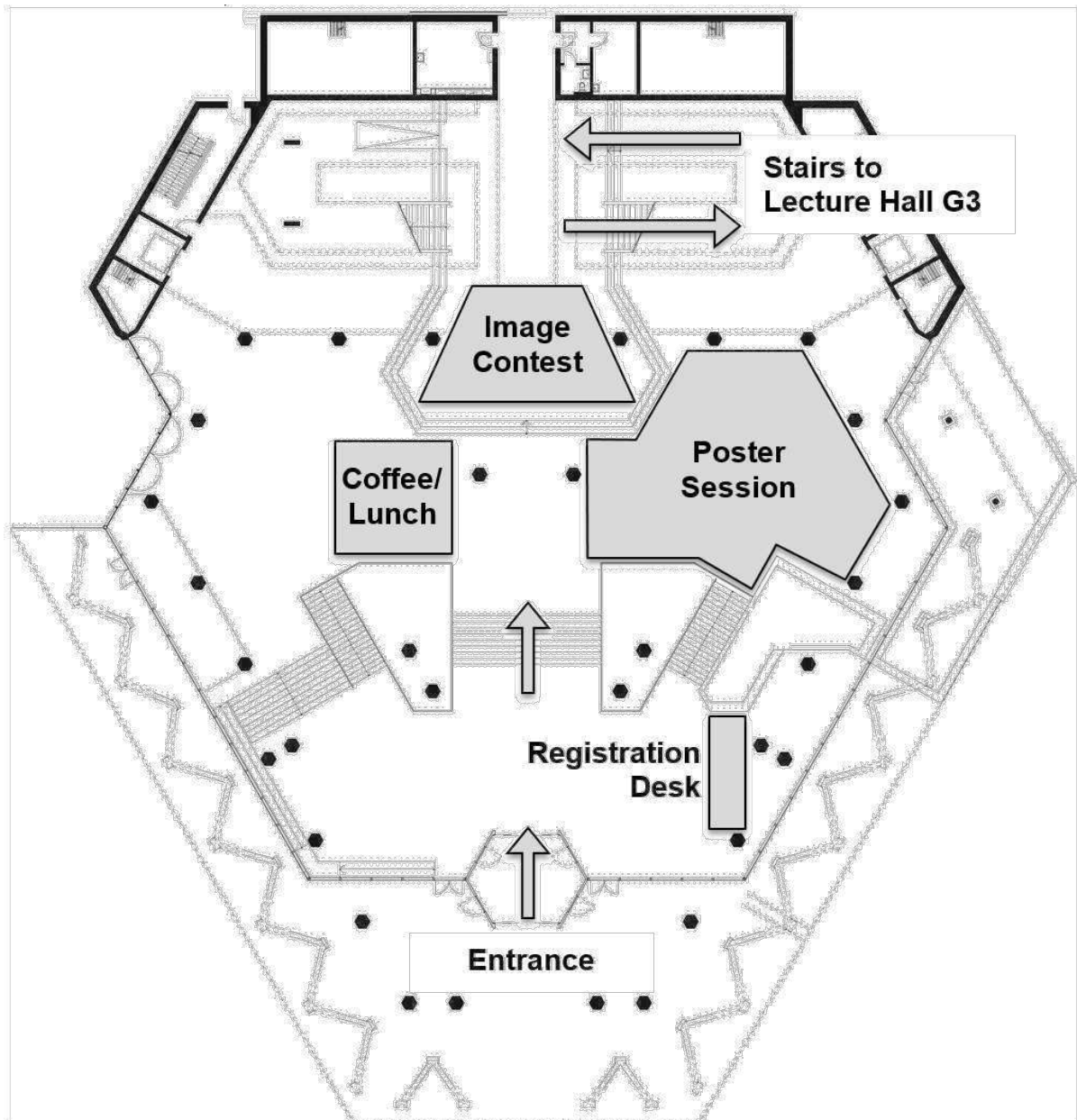
TABLE OF CONTENTS

| | |
|-----------------------------------|-----------|
| PROGRAMME | 5 |
| ABSTRACTS OF TALKS | 7 |
| SESSION 1: 09.00 – 10.00..... | 7 |
| SESSION 2: 11.00 – 12.00..... | 10 |
| MAP AWARD 2022..... | 13 |
| SESSION 3: 15.30– 16.30 | 15 |
| POSTER PRESENTATIONS | 18 |
| ABSTRACTS OF POSTERS | 23 |
| LIST OF PARTICIPANTS | 61 |

SITE MAP ETH HÖNGGERBERG



HPH D-FLOOR MAIN HALL



PROGRAMME

| | |
|-------|--|
| 08.00 | <i>Registration</i> |
| 08.45 | Opening Remarks |
| 09.00 | Alessandro Dutto , <i>Complex Materials, D-MATL</i> 3D Printing of Hierarchical Porous Ceramics for Thermal Insulation and Evaporative Cooling |
| | Dhananjay Deshmukh , <i>Macromolecular Engineering, D-MAVT</i> Acoustically Patterned Cells for Musculoskeletal Tissue Engineering |
| | Gianna Wolfisberg , <i>Soft and Living Materials, D-MATL</i> Understanding the Pancake-like Morphology of the Golgi Apparatus Compartments |
| | Oscar Cipolato , <i>Nanoparticle Systems Engineering, D-MAVT</i> Nanoparticle-Enhanced Laser Tissue Soldering |
| | Xiulin Chen , <i>Durability of Engineering Materials, D-BAUG & D-HEST</i> Amyloid Fibril-UiO-66-NH ₂ Aerogels for Environmental Remediation |
| 10.00 | <i>Coffee Break & Poster Session</i> |
| 11.00 | Carolina van Baalen , <i>Soft Materials and Interfaces, D-MATL</i> Confounding Interactions with Obstacles: How Colloidal Lattices Steer the Dynamics of Catalytic Microswimmers |
| | Prajwal Agrawal , <i>Acoustic Robotics System, D-MAVT</i> SonoPrint Acoustically-Assisted Volumetric 3D Printing |
| | Jean-Marc von Mentlen , <i>Materials and Device Engineering, D-ITET</i> Engineering of Sub-Nanometer Oxide Shell on Gold Nanoparticles |
| | Christian Gehre , <i>Bone Biomechanics, D-HEST</i> Sensitized Two-Photon Hydrogel Ablation for Laser-Guided Formation of 3D Bone Cell Networks |
| | Rani Boons , <i>Complex Materials, D-MATL</i> 3D Printing of Diatom-Laden Hydrogels for Water Quality Assessment |
| 12.00 | <i>Lunch & Poster Session</i> |

| MaP Award 2022 | |
|-----------------------|--|
| 13.30 | Dr. Alexandre Anthis , <i>Nanoparticle Systems Engineering, D-MAVT</i> Design & Formulation of Stimuli-Responsive Surgical Materials |
| | Dr. Tommaso Magrini , <i>Complex Materials, D-MATL</i> Tough & Transparent Nacre-Like Functional Composites |
| | Dr. Nives Strkalj , <i>Multifunctional Ferroic Materials, D-MATL</i> Emergence & Evolution of Ferroelectricity in Oxide Heterostructures |
| 14.45 | <i>Coffee Break</i> |
| 15.30 | Iacopo Mattich , <i>Complex Materials, D-MATL</i> Colloidal Self-Assembly Inside Droplets Under Magnetic Fields |
| | Riccardo Rizzo , <i>Tissue Engineering and Biofabrication, D-HEST</i> From Free-Radical to Radical-Free: A Biocompatible Paradigm Shift in Light-Mediated Biofabrication |
| | Sara Svanberg , <i>Bioanalytics Group, D-BSSE</i> A Novel Vascularization Model of the Human Dental Pulp and Periodontium |
| | Alexander Firlus , <i>Metal Physics and Technology, D-MATL</i> Anomalous Thermal Expansion of FeBYMo Bulk Metallic Glasses |
| | Donghoon Kim , <i>Multi-Scale Robotics, D-MAVT</i> Giant Shape-Memory Effect in Twisted Ferroic Nanocomposites |
| 16.35 | Flash Poster Presentations |
| 16.50 | Industry Presentations |
| 17.15 | Idea Pitches for a Novel Transdisciplinary Format Election MaP Student Representative |
| 17.40 | Award Ceremony |
| 18.00 | <i>Networking Apéro Riche</i> |

ABSTRACTS OF TALKS

Session 1: 09.00 – 10.00

Chair: Dr. Daniel Richards (Biochemical Engineering, D-CHAB)

3D Printing of Hierarchical Porous Ceramics for Thermal Insulation and Evaporative Cooling

Alessandro Dutto[1], Michele Zanini[1], Etienne Jeoffroy[1], Elena Tervoort[1], Saurabh A. Mhatre[2], Zachary B. Seibold[2], Martin Bechthold[2] and André R. Studart[1]

[1] *Complex Materials, D-MATL, ETH Zurich*

[2] *Graduate School of Design, Harvard University*

Confidential

Acoustically Patterned Cells for Musculoskeletal Tissue Engineering

Dhananjay V. Deshmukh[1,2], Peter Reichert[2], Joel Zvick[3], Céline Labouesse[1], Valentin Künzli[2], Oksana Dudaryeva[1], Ori Bar-Nur[3], Jurg Dual[2] and Mark W. Tibbitt[1]

[1] *Macromolecular Engineering, D-MAVT, ETH Zurich*

[2] *Institute for Mechanical Systems, D-MAVT, ETH Zurich*

[3] *Regenerative and Movement Biology, D-HEST, ETH Zurich*

Conventional 3D encapsulation of cells for tissue engineering often fails to capture the structural complexity of native tissues which is often critical for their functioning. For example, parallel alignment of myotubes enables uniaxial muscle contraction. These myotubes are formed by the fusion of muscle progenitor cells (myoblasts), a process in which cell–cell contact is important. [1] In our work we use acoustofluidics to pattern cells within a hydrogel to increase the local cell density to promote myotube formation while mimicking the structure of the native muscle.

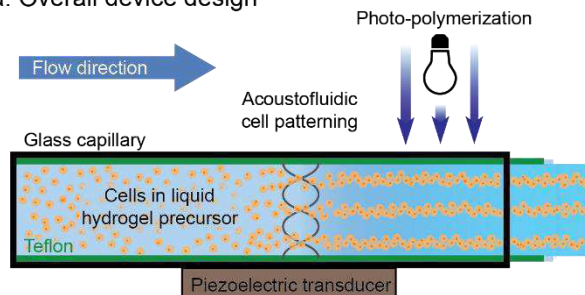
We engineered a Teflon-in-glass capillary device with a piezoelectric transducer glued onto a square glass capillary (Fig. a). [2] The glass capillary with the transducer enabled contactless and label free patterning of cells, while the Teflon tube ensured continuous extrusion of polymerized hydrogel fibers. Acoustofluidics allowed tunable patterning (variable spacing between parallel lines of cells) in the fluidic cavity. Acoustically patterned cells remained viable and spread inside the hydrogel fibers. With our device we patterned skeletal myoblasts in a hydrogel optimized for myotube formation. [3] We observed preferential myotube formation in the patterned regions (Fig. b). Further, spontaneous twitching of myotubes was seen in the patterned regions of the samples indicating muscle formation.

[1] R.S. Krauss, et. al., *Cold Spring Harb. Perspect. Biol.*, vol. 9, no. 2, (2017).

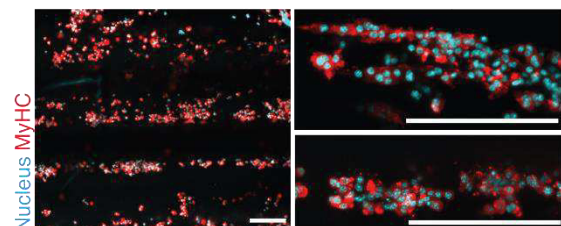
[2] D.V. Deshmukh et al., *Adv. Funct. Mater.*, 2113038 (2022).

[3] D.V. Deshmukh et. al., *Bioeng. Transl. Med.*, 5(3), (2020)

a. Overall device design



b. Functional myotubes



a. Cells in a liquid hydrogel precursor solution are patterned using an acoustic field, the patterned cell positions are retained by photo-polymerization of the hydrogel. The continuous flow in the device results in extrusion of the hydrogel fiber with patterned cells.

b. Myotube formation in patterned hydrogel samples. MyHC+ cells were observed in regions of high localized cell density. Scale bar, 200 μ m

Understanding the Pancake-Like Morphology of the Golgi Apparatus Compartments

Gianna Wolfisberg[1], Hendrik Spanke[1], Toshikaze Chiba[2], Naohito Urakami[3], Alexandre Torzynski[1], Masayuki Imai[2], Eric R. Dufresne[1] and Aleksander Rebane[1]

[1] *Soft and Living Materials, D-MATL, ETH Zurich*

[2] *Department of Physics, Tohoku University, Japan*

[3] *Department of Physics and Informatics, Yamaguchi University, Japan*

The Golgi Apparatus is a highly conserved membrane bound organelle involved in a complex cascade of protein post-translational modifications, with function being closely tied to morphology. Based on bending energy minimisation, one would expect membrane compartments of low volume-to-surface ratios, as found in the Golgi compartments (cisterna), to form a cup-like stomatocyte. In nature, however, the Golgi compartments have a flat pancake-like morphology. We investigate additional factors required for this flat pancake-like morphology. Therefore, we adhere giant unilamellar vesicles (GUVs) of varying volume-to-surface ratios to flat surfaces with varying adhesion energies. We find that by combining bending energy with adhesion, pancake-like shapes at lower volume-to-surface ratios can be achieved. However, it does not result in the ultra-flat morphology observed in the Golgi, implying that factors additional to bending and adhesion energy, such as the presence of rim stabilising proteins or lipids need to be considered.

Nanoparticle-Enhanced Laser Tissue Soldering

Oscar Cipolato[1,2], Lucas Dosnon[1] and Inge K. Herrmann[1,2]

[1] *Nanoparticle Systems Engineering Lab, D-MAVT, ETH Zurich*

[2] *Particles-Biology Interactions Lab, Materials Meet Life, Empa*

Confidential

Amyloid Fibril-UiO-66-NH₂ Aerogels for Environmental Remediation

Mohammad Peydayesh[1], Xiulin Chen[1,2], Julia Vogt[1], Felix Donat[3], Christoph R. Müller[3] and Raffaele Mezzenga[1,4].

[1] *D-HEST, ETH Zurich*

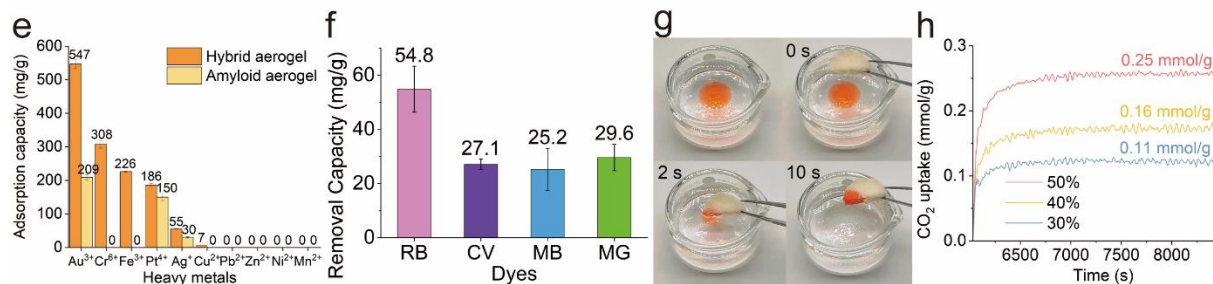
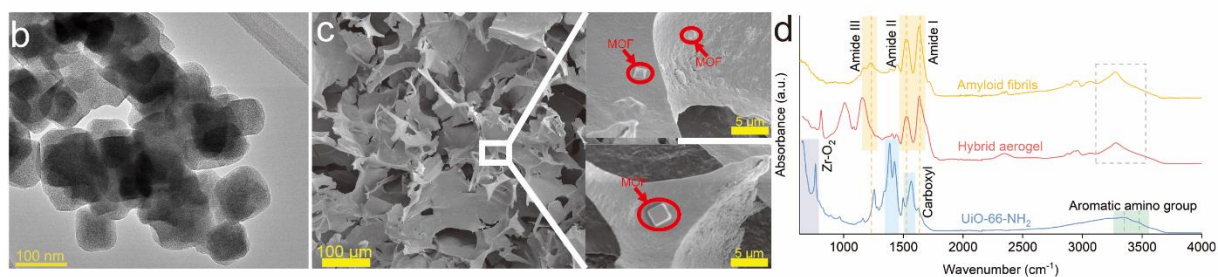
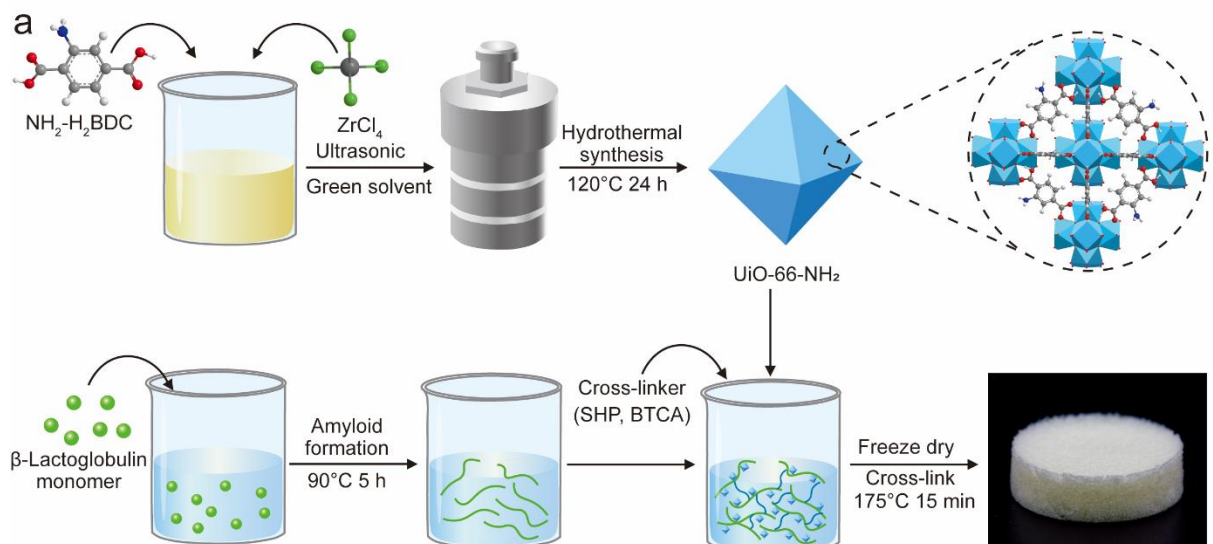
[2] *D-BAUG, ETH Zurich*

[3] *D-MAVT, ETH Zurich*

[4] *D-MATL, ETH Zurich*

Water scarcity and climate change are severe issues threatening the environment and society. Existing technologies for water treatment and CO₂ capture are not considered sustainable due to high energy demands and detrimental effects on the environment. Here, we introduce a sustainable hybrid aerogel based on UiO-66-NH₂/amyloid fibrils, in which UiO-66-NH₂ is a zirconium-based metal-organic framework (MOF) and amyloid fibrils are protein nano-assemblies produced from β -lactoglobulin. The hybrid aerogel's water purification and CO₂ capture performance were investigated. For heavy metals removal, high adsorption capacities for Au³⁺, Cr⁶⁺, Fe³⁺, and Pt⁴⁺ were achieved. The hybrid aerogel also exhibited excellent adsorption performance for dyes, such as Rhodamine B, Crystal violet, Methylene blue, and Malachite green. Furthermore, the organic solvents can be rapidly adsorbed on the water's surface within 10 seconds. Notably, three subsequent adsorption-regeneration experiments proved the recycling and reusability of the hybrid aerogel. Eventually, the CO₂ sorption experiments revealed the potential of the hybrid aerogel for CO₂ capture, thanks to binding phenomena between amino groups in UiO-66-NH₂ and CO₂. Altogether, these results introduce the hybrid aerogel as a sustainable and efficient solution for a broad range of environmental remediation.^[1]

[1] M. Peydayesh, et al., Chem. Commun. 58(33), 5104 (2022).



a) Fabrication process of hybrid UiO-66-NH_2 and amyloid fibrils aerogel. b) TEM images of UiO-66-NH_2 . c) SEM images of the inner structure of the hybrid aerogel, with the distribution of UiO-66-NH_2 . d) FTIR spectra of pure amyloid fibrils, hybrid aerogel, and UiO-66-NH_2 . e) Heavy metal adsorption capacity of the hybrid aerogel and pure amyloid aerogel. f) Dye removal performance of the hybrid aerogel. g) Rapid removal of organic solvents from water by the hybrid aerogel. h) CO_2 capture performance of hybrid aerogels with different MOF loadings.

Session 2: 11.00 – 12.00

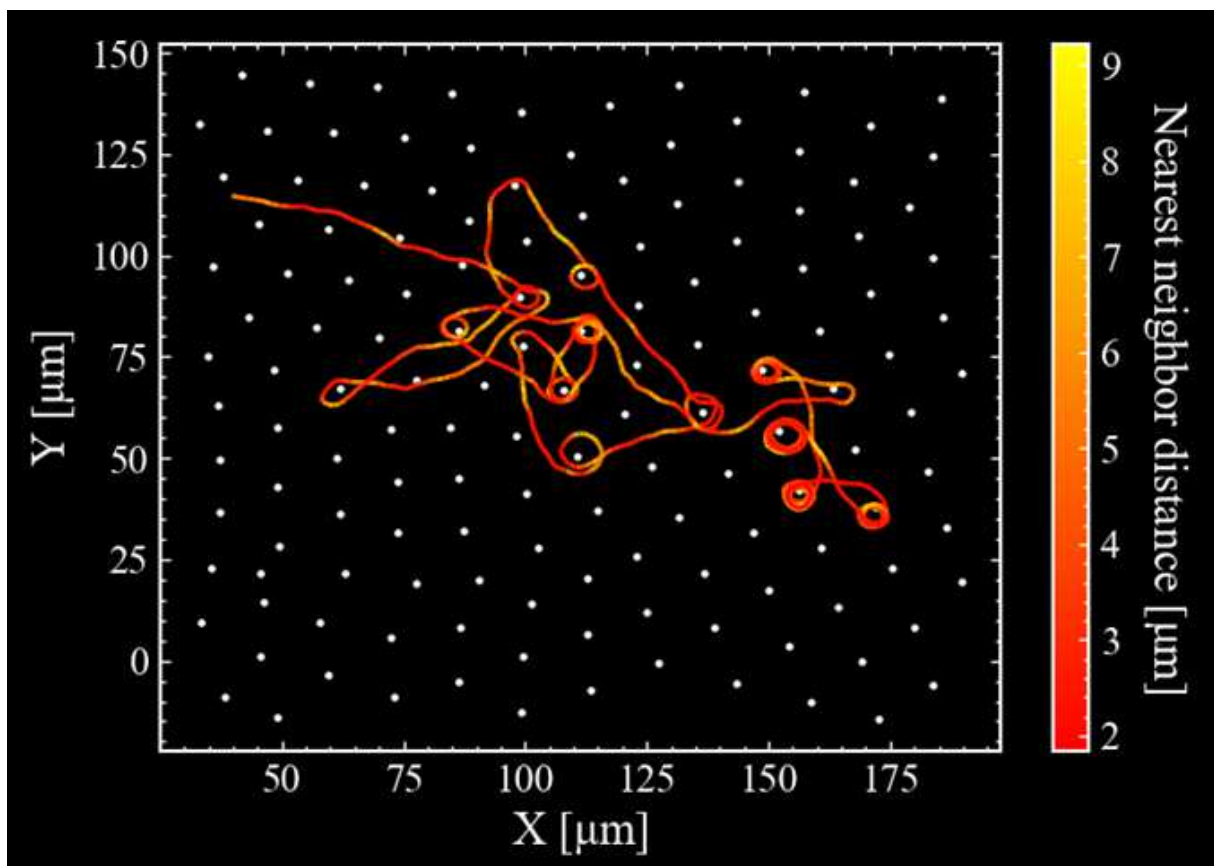
Chair: Dr. Eleonora Secchi (Environmental Microfluidics, D-BAUG)

Confounding Interactions with Obstacles: How Colloidal Lattices Steer the Dynamics of Catalytic Microswimmers

Carolina van Baalen and Lucio Isa

Soft Materials and Interfaces, D-MATL, ETH Zurich

Self-propelled particles, or so-called microswimmers, are capable of taking up energy from their local environment, and convert this into directed motion. Their inherent autonomy leads to confounding out-of-equilibrium behaviors, and capricious ways of interacting with boundaries and obstacles. Here we study how colloidal lattices can steer the dynamics of catalytic microswimmers hovering along a fluid-fluid interface. We find that the microswimmers radically change their way of interacting with the obstacles upon an increase in fuel concentration. At low concentrations, the obstacles marginally affect the swimming dynamics by weakly scattering the microswimmers upon a collision event. At higher fuel concentration, we observe a transition, where the microswimmers start to orbit strongly around the obstacles along their path. Counterintuitively, this leads to the scenario where increasing the amount of available fuel leads to a decrease in the efficiency of exploring space.



Trajectory of a microswimmer swimming inside a colloidal array (white dots). The trajectory is colour-coded according to the microswimmer distance to its nearest neighbour.

SonoPrint Acoustically-Assisted Volumetric 3D Printing

Prajwal Agrawal, Simon Dreher, Patrick Colgon and Daniel Ahmed

Acoustic Robotics for Life Science and Healthcare, D-MAVT, ETH Zurich

Confidential

Engineering of Sub-Nanometer Oxide Shell on Gold Nanoparticles

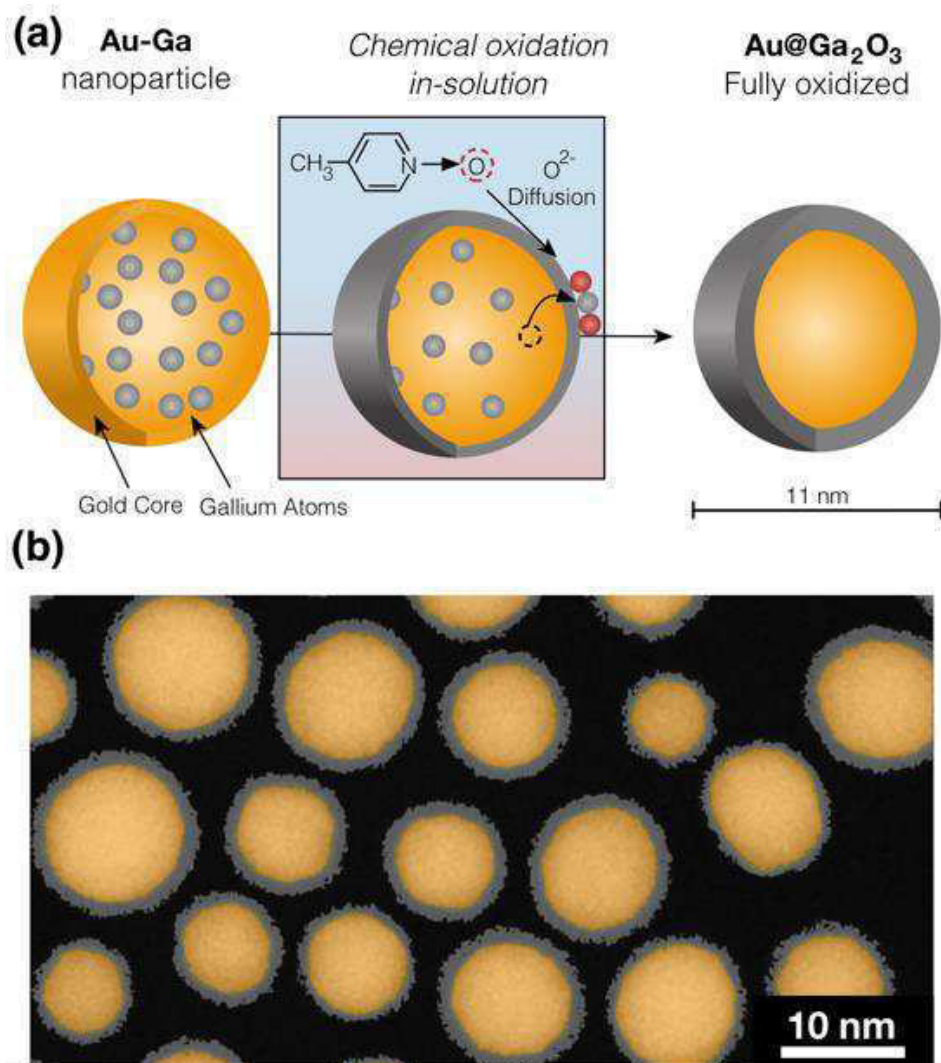
Jean-Marc von Mentlen[1], Jasper Clarysse[1], Annina Moser[1], Dhananjeya Kumar[2], Olesya Yarema[1], Takumi Sannomiya[3], Maksym Yarema[2] and Vanessa Wood[1]

[1] *Materials and Device Engineering, D-ITET, ETH Zurich*

[2] *Chemistry and Materials Design, D-ITET, ETH Zurich*

[3] *School of Materials and Chemical Technology, Department of Materials Science and Engineering, Tokyo Institute of Technology*

Metal oxide shells fully or partially covering gold nanoparticles are intensively studied for a wide range of applications in the fields of catalysis and plasmonics. When carefully designed, these coatings enhance the functionality and stability of the nanoparticles. Yet, facile and well controlled fabrication methods of thin metal oxide layers on metal nanoparticles are still lacking. Currently used methods struggle to produce uniform layers below 1 nm. In this work, we show an easy fabrication process to reliably engineer uniform Ga₂O₃ shells on Au nanoparticles with a thickness ranging from sub- to several monolayers. These thin shells are obtained by a liquid-phase chemical oxidation of alloyed Au-Ga nanoparticles. We demonstrate how the plasmonic properties of the nanoparticles can be used to understand the reaction process and quantitatively monitor the Ga₂O₃ shell growth. Finally, we show as a practical application that the Ga₂O₃ coating prevents the sintering of the Au nanoparticles, ensuring thermal stability up to at least 250°C. Dealloying of bimetallic nanoparticles by in-solution oxidation is a promising approach to obtain controlled metal-metal oxide core-shell nanoparticles.



(a) Schematic description of the formation of Au nanoparticles with uniform, sub-nm Ga₂O₃ shells.
(b) Colored STEM image of oxidized Au@Ga₂O₃ nanoparticles

Sensitized Two-Photon Hydrogel Ablation for Laser-guided Formation of 3D Bone Cell Networks

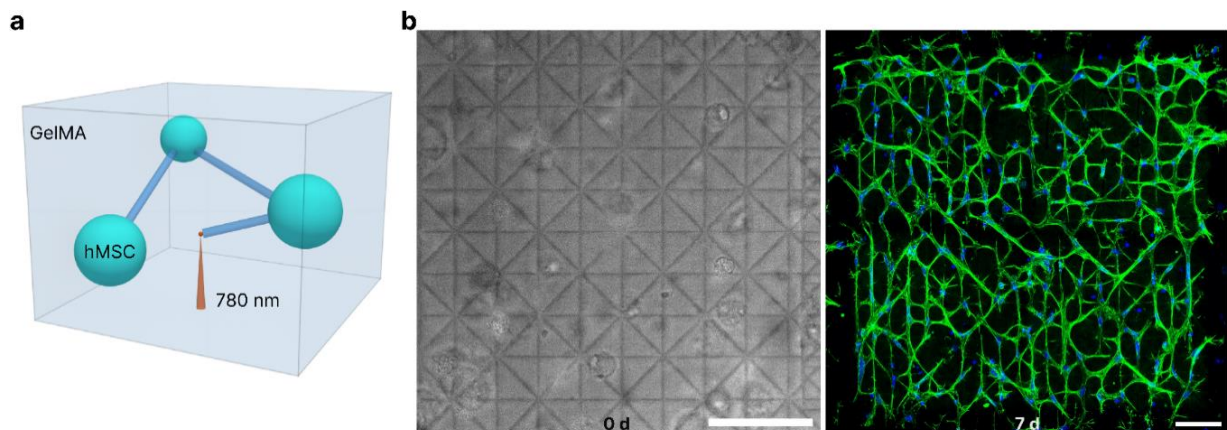
Christian Gehre, Wanwan Qiu, Ralph Müller and Xiao-Hua Qin

Bone Biomechanics, D-HEST, ETH Zurich

Osteocytes play a crucial role in maintaining bone's structural integrity and mechano-adaptation. By traversing the mineralized bone matrix with a multitude of dendrites, osteocytes form a complex 3D network of interconnected microchannels.¹ The inaccessible nature of this micron-scale network poses a major challenge to understand the mechanobiology in native bone tissues, creating the need for biomimetic *in vitro* models. Here we employ **sensitized two-photon hydrogel ablation** to create microchannels in 3D cell cultures, guiding the network formation of embedded bone cells in 3D for an *in vitro* bone model. We demonstrate that the presence of a soluble photosensitizer (P2CK)² drastically reduces the energy dosage necessary for photoablation, enabling cell-compatible photopatterning in soft GelMA hydrogels. To reconstruct a bone cell network *in vitro*, μm -scale channels were ablated within human mesenchymal stem cell-laden hydrogels, directing cell outgrowth at high spatial resolution. Cells spread into the channels within hours after sensitized low-dosage ablation, forming a functional cellular network with over 300 μm long protrusions, connected via gap junctions. Taken together, our results highlight the potential of sensitized two-photon hydrogel ablation for laser-assisted precision tissue engineering.

[1] L.F. Bonewald (2011) JBMR, 26:229.

[2] M. Lunzer et al. (2018) Angew Chem, 57:15122.



Guided 3D cell-cell networking via sensitized two-photon hydrogel micropatterning.

a) The 2P-laser ablates the GelMA hydrogel between cells, creating a void channel for guided outgrowth.

b) hMSC exposed to a grid with $1 \times 30 \mu\text{m}$ channel depth, forming an intricate network within 7 days. Left: Brightfield image of the ablated microchannel grid on day 0. Right: Actin (green) nuclei (blue) staining visualizing 3D network formation after 7 days of culture. Scale bars = 100 μm .

3D Printing of Diatom-Laden Hydrogels for Water Quality Assessment

Rani Boons[1,2], Fergal Coulter[1], Gilberto Siqueira[1,2], Gustav Nyström[2], Tanja Zimmermann[2,3] and André R. Studart[1]

[1] *Complex Materials, D-MATL, ETH Zurich*

[2] *Cellulose and Wood Materials Laboratory, Functional Materials, Empa*

[3] *D-MATL and STI, ETH Zurich and EPF Lausanne*

Confidential

MaP Award 2022 13.30– 14.45

Chair: Prof. Lucio Isa (Soft Materials and Interfaces, D-MATL)



Design & Formulation of Stimuli-Responsive Surgical Materials

Dr. Alexandre Anthis

Nanoparticle Systems Engineering, D-MAVT, ETH Zurich

Every year around the world approximately 14 million people undergo abdominal surgery. These operations while lifesaving for a multitude of diseases ranging from cancer to weight loss inducing gastric bypass, carry great intrinsic risks. These latter are associated with the leaking of digestive fluids through sutured or stapled reconnections, which can vastly prolong recovery but also cause premature death. As such, anastomotic leakage is one of the most dreaded complications following abdominal surgery, worldwide, with reported incidence rates reaching values on average >10% and an associated mortality of up to 27%. Due to the scarcity of tools capable of protecting patients from leaks, but also crucially due to the absence of technologies capable of detecting early such deteriorations, surgeons rely on inconveniently navigating ambiguity via the monitoring of surrogate markers and clinical symptoms. These latter oftentimes lack sensitivity and specificity, hence only offering late-stage detection of already fully developed leaks.

Towards addressing these issues the work within this thesis proposes and demonstrates the development of novel abdominal cavity adhesives, that remain attached to target tissues even in the face of serious digestive leaks. In addition, the materials presented are developed to allow the rapid and unambiguous assessment of the breaching of sutured reconnections, using readily available portable ultrasound sonography. As such for the first time, a suture support patch is presented capable of assisting surgeons in the management of patients while promises to widen the opportunity window to identify deteriorations before the clinical manifestation of symptoms.



Tough & Transparent Nacre-Like Functional Composites

Dr. Tommaso Magrini

Complex Materials, D-MATL, ETH Zurich

Bioinspired bulk composites have an internal architecture that replicates the microstructural features of biological composites: their inner structure provides them with high strength and high fracture toughness. Strength and toughness are fundamental in most structural applications; key to provide mechanical stability and reliability. Although research efforts have been mostly focused on the optimization of the mechanical performance of synthetic structural composites, the hallmark of biological composites is their ultimate ability to combine within the same material additional functionalities, such as color, self-healing capabilities, stimuli sensing, and shape responsiveness. However, the implementation of sensing and other optical properties in today's composites without sacrificing strength and toughness remains an open challenge. Rethinking materials processing to combine multiple functionalities within a single bioinspired composite has been the major drive of my doctoral studies. In my talk, I will showcase a new class of composites inspired by nature that replicate the microstructure of mother-of-pearl, also known as nacre, and that combine optical transparency, strength and fracture toughness. The remarkable resistance of these transparent composites against fracture makes them a promising alternative to commercially available display-protecting materials.

Finally, I will highlight the recent development of strong and tough composite materials that can signal, report and pre-emptively detect the presence of damage using a simple optical readout, such as a change in their color. The careful and timely detection of damage in these lightweight structural composites not only proves to be a useful tool for the analysis of complex fractures, but also ensures the safe use and the prevention of accidents during service life of the composites as lightweight structural components.



Emergence & Evolution of Ferroelectricity in Oxide Heterostructures

Dr. Nives Strkali

Multifunctional Ferroic Materials, D-MATL, ETH Zurich

The global demand for electric energy for electronic devices is on a constant rise and presents a societal challenge in the face of the climate crisis. The search for materials for energy-efficient devices is an important part of solving this challenge. Oxide heterostructures have emerged over the last decade as a promising platform for energy-efficient electronics. Among oxides, ferroelectric materials, owing to their spontaneous polarization that can be controlled by an electric field, stand out as natural memory elements for low-power devices. In devices, thin films of ferroelectric materials need to be prepared with a high degree of control over the ferroelectric response. Thin-film synthesis is the decisive point for setting the functional property that is obtained after the deposition. I co-developed the first tool to monitor polar order simultaneously with the film synthesis, which is pivotal for optimizing the ferroelectric response. Using a laser-optical approach, we observe the emergence and evolution of polarization in oxide heterostructures which not only complements the standard characterization but allows for better and faster optimization of polarization. Based on the information obtained during the synthesis, we tune the growth process to stabilize the coveted robust polarization. Ultimately, we provide new routes to engineer heterostructures displaying improved functionality.

Session 3: 15.30– 16.30

Chair: Dr. Minghan Hu (Soft Materials and Interfaces, D-MATL)

Colloidal Self-Assembly Inside Droplets Under Magnetic Fields

Iacopo Mattich[1], Golnaz Isapour[2], Joan Sendra[3], Henning Galinski[3], Marco Lattuada[4], Simone Schürle-Finke[5] and André R Studart[1]

[1] *Complex Materials, D-MATL, ETH Zurich*

[2] *Department of Mechanical Engineering, Massachusetts Institute of Technology*

[3] *Nanometallurgy, D-MATL, ETH Zurich*

[4] *Department of Chemistry, University of Fribourg.*

[5] *Institute for Translational Medicine, D-HEST, ETH Zurich*

Confidential

From Free-Radical to Radical-Free: A Biocompatible Paradigm Shift in Light-Mediated Biofabrication

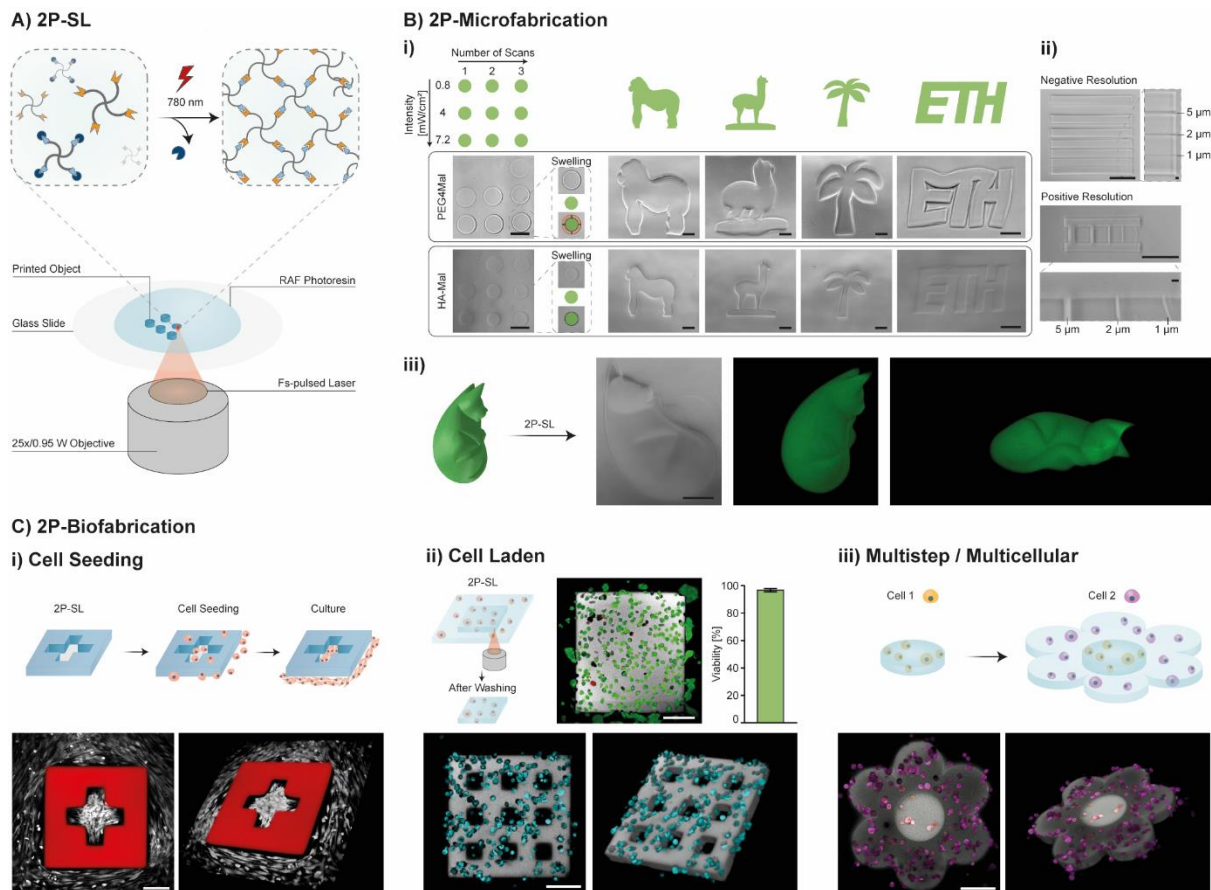
Riccardo Rizzo, Nika Petelinsek, Angela Bonato and Marcy Zenobi-Wong

Tissue Engineering and Biofabrication, D-HEST, ETH Zurich

In the past decades, the development of novel photo-crosslinking strategies and photosensitive materials has promoted a widespread use of light-mediated biofabrication methods.^{1,2} However, despite the great progress towards faster and more biocompatible photochemical strategies, current photoresins still rely on the presence of photoinitiators (PIs) generating radical-initiating species to trigger the so called free-radical crosslinking. The presence of radicals raises concerns of potential cytotoxicity in the context of bioprinting. In this work, we present a universal radical-free (RAF, Fig. A) photocrosslinking strategy to be used for light-based biofabrication techniques. The RAF strategy presented in this work relies on the caging of thiol groups with water coumarin-based photocage and base-catalysed thiol-ene crosslinking. Upon one photon (365/405 nm) or two photon (2P, 780 nm) light exposure, the cage is removed, therefore triggering the crosslinking of synthetic (PEG based) or natural-derived (hyaluronic acid) polymers (Fig. B). Gene expression and toxicity analysis showed a higher biocompatibility when compared to systems containing gold-standard photoinitiator LAP. Finally, we have demonstrated the possibility to perform high resolution 2P-biofabrication using the proposed RAF chemical design (Fig. C).

[1] M. Lee et al., Chem. Rev. 120, 10950–11027 (2020).

[2] R. Rizzo, et al., Adv. Mater. 33, 2102900 (2021).



A) 2P illustration. B) 2P-microfabrication (Scale bars: 100 μm(i, iii), 50 μm (ii) and 5 μm (ii, close-up)). C) 2P-biofabrication (Scale bars: 100 μm).

A Novel Vascularization Model of the Human Dental Pulp and Periodontium

Sara Svanberg, Elisabeth Hirth and Petra S. Dittrich

Bioanalytics, D-BSSE, ETH Zurich

Confidential

Anomalous Thermal Expansion of FeBYMo Bulk Metallic Glasses

Alexander Firlus[1], Mihai Stoica[1], Stefan Michalik[2], Robin E. Schäublin[1] and Jörg F. Löffler[1]

[1] Metal Physics and Technology, D-MATL, ETH Zurich

[2] Diamond Light Source Ltd., Harwell Science and Innovation Campus, Didcot, Oxfordshire OX11 0DE, UK

(Fe_{73.2}B₂₂Y_{4.8})₉₅Mo₅ is a well-known bulk metallic glass (BMG) with excellent glass-forming ability [1]. Moreover, it exhibits an anomalously small coefficient of thermal expansion in its ferromagnetic state. At the Curie temperature it increases by a factor of 3. This effect is known as Invar effect and observed rarely in crystalline materials. However, it was recently found that the Invar effect is universal to Fe-based BMGs [2]. Due to the lack of any long-range order in BMGs, the origin of this effect can only be understood at the atomic level. FeBYMo BMG is a useful model system because it includes only one (ferro)magnetic element (Fe).

In this work, we studied FeBYMo BMGs by in-situ high-energy X-ray diffraction. The analysis of the diffraction pattern allows to measure the average atomic distances as a function of temperature. Moreover, the large size difference of the atomic species allows to deconvolute the pair distribution function to specific atomic pairs. It appears that Fe-Fe pairs can even show negative thermal expansion below the alloy's Curie temperature. In addition, full atomic shells, which contain all atomic species,

show an abrupt increase in their thermal expansion at the Curie temperature. This proves that the Invar effect is not just a macroscopic effect but has clear origins at the atomic scale [3].

[1] Z. Han, et. al., *Intermetallics* 15, 1447-1452 (2007)

[2] Q. Hu, et. al., *Intermetallics* 93, 318-322 (2010)

[3] A. Firlus, et. al., *Nat Commun* 13, 1082 (2022)

Giant Shape-Memory Effect in Twisted Ferroic Nanocomposites

Donghoon Kim, Minsoo Kim, Xiangzhong Chen and Salvador Pané

Materials for Robotics, D-MAVT, ETH Zurich

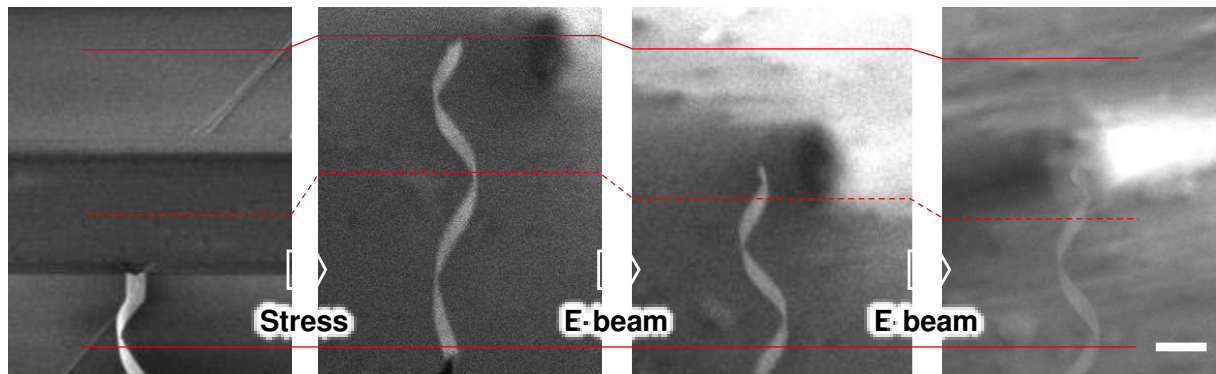
The shape recovery ability of shape-memory alloys vanishes below a critical size (~50nm) [1,2], which prevents their practical applications at the nanoscale. In contrast, ferroic materials, even when scaled down to dimensions of a few nanometers, exhibit actuation strain through domain switching, though the generated strain is modest (~1%) [3,4]. Here, we develop free-standing twisted architectures of nanoscale ferroic oxides showing shape-memory effect with a giant recoverable strain (>10%). The twisted geometrical design amplifies the strain generated during ferroelectric domain switching, which cannot be achieved in bulk ceramics or substrate-bonded thin films. The twisted ferroic nanocomposites allow us to overcome the size limitations in traditional shape-memory alloys and opens new avenues in engineering large-stroke shape-memory materials for small-scale actuating devices such as nanorobots and artificial muscle fibrils.

[1] J.F. Gomez-Cortes, et. al., *Nature Nanotechnology*. 12, 790 (2017).

[2] X. Wang, A. Ludwig. *Shape Memory and Superelasticity*, 6, 287 (2017).

[3] J. Zhang, et. al., *Nature Communications*, 4, 2768 (2013).

[4] J. X. Zhang, et. al., *Nature Nanotechnology*, 6, 98 (2011).



Deformation under tensile loading and shape-memory effect under electron beam irradiation in BaTiO₃/CoFe₂O₄ twisted nanocomposite

POSTER PRESENTATIONS

| Poster No. | Name | Poster Title | Affiliation |
|------------|---------------------------|---|---|
| 1 | Wohlwend, Jelena | Mapping of Plasmonic Modes in Self-Assembled Disordered Two-Phase Metamaterial Networks | Nanometallurgy, D-MATL |
| 2 | Del Campo Fonseca, Alexia | Real Time Imaging and Navigation of Acoustic Microrobots Inside Ex-Vivo Blood Vessels | Acoustic Robotics for Life Science and Healthcare, D-MAVT |
| 3 | Kavas, Baris | Multi-Sensor Evaluation of the Effect of Preheat in Melt-pool Characteristics in Laser Powder Bed Fusion | Advanced Manufacturing, D-MAVT |
| 4 | Breitfeld, Maximilian | High-Throughput Deposition of Picoliter Droplet Reactors on Plates for Chemical Analysis and Synthesis | Bioanalytics, D-BSSE |
| 5 | Fernandez-Rico, Carla | Arrested Spinodal Decomposition in Elastic Matrices for Structural Color Applications | Soft and Living Materials, D-MATL |
| 6 | Castellano, Miguel | Slip Phase Transition at the Origin of Local Frictional Instabilities | Computational Mechanics of Building Materials, D-BAUG |
| 7 | Feng, Yanxia | Controlling Phase Separation in Crosslinked Poly(ethylene Glycol) Diacrylate (PEGDA) Gel | Soft and Living Materials, D-MATL |
| 8 | Klein Cerrejon, David | Boosting Buccal Drug Absorption with a Simple Bioinspired Stretching Device Fabricated by 3D Printing | Drug Formulation and Delivery, D-CHAB |
| 9 | Van Kesteren, Steven | Self-Replicating Colloidal Microstructures | Soft Materials and Interfaces, D-MATL |
| 10 | Furcas, Fabio Enrico | Electrodissolution of Steel in the Presence of Aqueous Carbonates | Durability of Engineering Materials, D-BAUG |
| 11 | Efe, Ipek | In-Situ Tracking of the Polarization Dynamics During the Growth of Layered Ferroelectric Aurivillius Thin Films | Multifunctional Ferroic Materials, D-MATL |
| 12 | Jin, Tonghui | Amyloid Fibril-Based Membranes for PFAS Removal from Water | Food and Soft Materials, D-HEST |
| 13 | Guichard, Xavier | Interdependence of Structural and Compositional Parameters on Up-Converting Hafnia Nanoparticles | Multifunctional Materials, D-MATL |
| 14 | Bovone, Giovanni | Supramolecular Reinforcement of Polymer–Nanoparticle Hydrogels for Modular Materials Design | Macromolecular Engineering, D-MAVT |

| Poster No. | Name | Poster Title | Affiliation |
|------------|--------------------|---|---|
| 15 | Diona, Pietro | Modeling and Characterization of Racetrack Memories with VCMA Synchronization | Magnetism and Interface Physics, D-MATL |
| 16 | Menétrey, Maxence | Electrostatically Assisted Nanoscale Printing | Nanometallurgy, D-MATL |
| 17 | Senol Gungor, Ayca | Capacity-Limiting Factors of Solid-state S/Li ₂ S Conversion in Microporous Carbon-based Lithium-Sulfur Batteries | Materials and Device Engineering, D-ITET |
| 18 | Esswein, Tobias | Ferroelectric, Quantum Paraelectric or Paraelectric? Calculating the Evolution from BaTiO ₃ to SrTiO ₃ to KTaO ₃ Using a Single-Particle Quantum-Mechanical Description of the Ions | Materials Theory, D-MATL |
| 19 | Stanko, Štefan | Structural and Thermal Characterisation of a AuGe Alloy via Electron Microscopy and Fast Differential Scanning Calorimetry | Metal Physics and Technology, D-MATL |
| 20 | Kuo, Hsin-Hung | Rational Design of Luminescent Au(III) Complexes for High-Performance Organic Light-Emitting Diodes | Nanomaterials Engineering, D-CHAB |
| 21 | Crimmann, Juri | Towards Strain-Controlled WSe ₂ Single-Photon Emitters | Optical Materials Engineering, D-MAVT |
| 22 | Böddeker, Thomas | Non-Specific Adhesive Forces Reorganize the Cytoskeleton Around Membraneless | Soft and Living Materials, D-MATL |
| 23 | Talts, Ulle-Linda | Bottom-up Fabricated Nonlinear Barium Titanate 2D Photonic Crystals and L3 Cavities | Optical Nanomaterials, D-PHYS |
| 24 | Meijs, Zazo | Patterning of Defects in Nematic/Smectic-A Liquid Crystals by Colloidal Arrays | Soft Materials and Interfaces, D-MATL |
| 25 | Lauener, Carmen | Micro-Shear of Silicon: Elastic Strain Analysis Using Digital Image Correlation | Nanometallurgy, D-MATL |
| 26 | Lee, Seunghun S. | 3D-Printed LEGO®-inspired Titanium Scaffolds for Patient-Specific Regenerative Medicine | Orthopaedic Technology, D-HEST |
| 27 | Galata, Aikaterini | Globular Proteins and Where to Find Them Within a Polymer Brush – a Case Study | Polymer Physics, D-MATL |
| 28 | Khosla, Nathan | Micro-Scale Biomolecule Patterning on Nitrocellulose Substrates | Biochemical Engineering, D-CHAB |
| 29 | Kholina, Yevheniia | Tuning Local Structure in Prussian Blue Analogues (PBAs) | Multifunctional Ferroic Materials, D-MATL |

| Poster No. | Name | Poster Title | Affiliation |
|------------|-------------------------|--|---|
| 30 | Norris, Graham | Reproducible 3D-Integrated Superconducting Circuits Through Polymer Spacers | Quantum Device, D-PHYS |
| 31 | Notter, Daniel | Computational Screening and Experimental Validation of Binary and Ternary Metal Nitrides for the Solar-Driven Thermochemical Production of Green Ammonia | Renewable Energy Carriers, D-MAVT |
| 32 | Lehéricy, Pierre | Probing Plastic Rearrangements in Colloidal Gels | Soft Materials, D-MATL |
| 33 | Deng, Zhikang | Performance of Glass to Iron-based Shape Memory Alloy Adhesively Bonded Shear Joints | Steel and Composite Structures, D-BAUG |
| 34 | Dillinger, Cornel | Ultrasound-driven Particle Manipulation Inspired by Starfish-Larva | Acoustic Robotics for Life Science and Healthcare, D-MAVT |
| 35 | Born, Friederike-Leonie | Microfluidic Hollow Fiber Model to Visualize and Quantify Bacterial Response to Dynamic Drug Treatments | Bioanalytics, D-BSSE |
| 36 | Gerber, Dominic | Cryosuction Induced Freezing Damage | Soft and Living Materials, D-MATL |
| 37 | Bernero, Margherita | The Role of Matrix Viscoelasticity in 3D Osteocyte Morphogenesis | Bone Biomechanics, D-HEST |
| 38 | Ocana Pujol, Jose Luis | Thermal Instability of Ag/a-Si Planar Hyperbolic Metamaterials | Nanometallurgy, D-MATL |
| 39 | Menasce, Stefano | 3D Printing of Autonomous Self-Healing Elastomers for Soft Robotics | Complex Materials, D-MATL |
| 40 | Koureas, Ioannis | Understanding the Stick-Slip Governed Failure of Topologically Interlocked Structures | Computational Mechanics of Building Materials, D-BAUG |
| 41 | Yuts, Yulia | Digital Light Processing 3D Printing of Biodegradable Elastomers for Biomedical Applications | Drug Formulation and Delivery, D-CHAB |
| 42 | Bernhard, Stéphane | Supramolecular interactions in the design of polymer–nanoparticle hydrogels | Macromolecular Engineering, D-MAVT |
| 43 | Hoffmann, Marco | Spin-orbit Torque Switching of Elliptical Three-Terminal Magnetic Tunnel Junctions | Magnetism and Interface Physics, D-MATL |
| 44 | Niggel, Vincent | Insights in Dense Suspensions by Visualizing Silica Particles with Tunable Surfaces | Soft Materials and Interfaces, D-MATL |
| 45 | Sun, Qiyao | Thermo-Responsive Nanocellulose Hydrogels as a Universal Drug Release Platform | Food Process Engineering, D-HEST |

| Poster No. | Name | Poster Title | Affiliation |
|------------|-----------------------------|--|---|
| 46 | Vogel, Alexander | Impact of Oxygen Vacancies on Improper Ferroelectricity at YMnO ₃ Thin Film Interfaces | Multifunctional Ferroic Materials, D-MATL |
| 47 | Wenzler, Nils | Operando X-Ray Diffraction and Tomography to Track Morphological Changes in LiNi _{0.8} Mn _{0.1} Co _{0.1} O ₂ (NMC 811) Cathode Particles | Materials and Device Engineering, D-ITET |
| 48 | Verbeek, Xanthe | Interfaces of Oxides with Different Magneto-Electric Responses | Materials Theory, D-MATL |
| 49 | Fellner, Madeleine | Synthesis of Morphology Controlled Cesium Hafnium Halide Double Perovskites and Lutetium Hydroxy Halide Luminescent Nano and Micro-Particles | Multifunctional Materials, D-MATL |
| 50 | Porenta, Nikolaus | Additively Manufactured Nano-Porous Micro-Scale Ag Structures for SERS Sensing | Nanometallurgy, D-MATL |
| 51 | Li, Tianchi | Multiscale Modelling of Size Effects in the Fracture of Soft Solids | Soft and Living Materials, D-MATL |
| 52 | Hernandez Oendra, Alexander | Synthesis of Metal-Organic Chalcogenide Semiconductor Nanoparticles | Optical Materials Engineering, D-MAVT |
| 53 | Souza Plath, André | Poly(ϵ -caprolactone)/Zein Blends Increase Bovine Chondrocytes Cytocompatibility | Orthopaedic Technology, D-HEST |
| 54 | Parkatzidis; Kostas | Transformer-Induced Metamorphosis of Polymeric Nanoparticle Shape at Room Temperature | Polymeric Materials, D-MATL |
| 55 | Pagani, Gabriele | No Yield Stress "Yield-Stress" Material | Soft Materials, D-MATL |
| 56 | Boev, Dimitar | Micro-scale Volumetric 3D Printing | Acoustic Robotics Systems, D-MAVT |
| 57 | Müller, Philip | Consistent Damage Transformation for Multiscale Simulations | Computational Mechanics of Building Materials, D-BAUG |
| 58 | Schwarz, Fabian | Studying the Front Propagation in Reactive Multilayers via MD Simulations: From Crystal Structure to Alloying | Nanometallurgy, D-MATL |
| 59 | Wied, Markus | Ionic Transport and Current Density Simulations in Composite LLZO-PEO Electrolytes | Materials and Device Engineering, D-ITET |
| 60 | Rolland, Manon | Shape-Controlled Nanoparticles from a Low-Energy Nanoemulsion | Polymeric Materials, D-MATL |

| Poster No. | Name | Poster Title | Affiliation |
|-------------------|----------------------|--|---|
| 61 | Shen, Xueting | Printing on Particles: Combining Two-Photon Nanolithography and Capillary Assembly to Fabricate Multi-Material Microstructures | Soft Materials and Interfaces, D-MATL |
| 62 | Zauchner, Doris | Ultrafast Volumetric Bioprinting of Perfusible 3D Bone Tissue Models | Bone Biomechanics, D-HEST |
| 63 | Zhao, Yaqi | A Pseudo Flocculation Method for Poly-Dispersed Colloidal Systems | Computational Mechanics of Building Materials, D-BAUG |
| 64 | Yang, Chia-Jung | Probing Crystal Electric Field States in a Dense Kondo-Lattice Antiferromagnet Using Terahertz Time-Domain Spectroscopy | Multifunctional Ferroic Materials, D-MATL |
| 65 | Chen, Jialu | Tailoring PEEK Crystallinity for Hemocompatible, Durable, and Affordable Cardiovascular Devices | Composite Materials and Adaptive Structures, D-MAVT |
| 66 | Toncich, Nensi | Controlling the Reaction Propagation in Ni-Al Multilayers with Premixed Interlayers | Nanometallurgy, D-MATL |
| 67 | De Rosa, Valentina | Shrinking Micropatterns with 3D Hydrogel Templates | Optical Materials Engineering, D-MAVT |
| 68 | Torzynski, Alexandre | Surface-Initiated Polymerisation from Lipid Membranes: Mechanism, Curvature, and Thermoresponsivity | Soft and Living Materials, D-MATL |
| 69 | Marin, Luca | DFT Simulations of atomic, solid and liquid Xenon for Dark Matter Direct Detection | Materials Theory, D-MATL |

ABSTRACTS OF POSTERS

1. Mapping of Plasmonic Modes in Self-Assembled Disordered Two-Phase Metamaterial Networks

Jelena Wohlwend[1], Georg Haberfehlner[2], Ralph Spolenak[1] and Henning Galinski[1]

[1] *Nanometallurgy, D-MATL, ETH Zurich*

[2] *Institut für Elektronenmikroskopie und Nanoanalytik, TU Graz*

Confidential

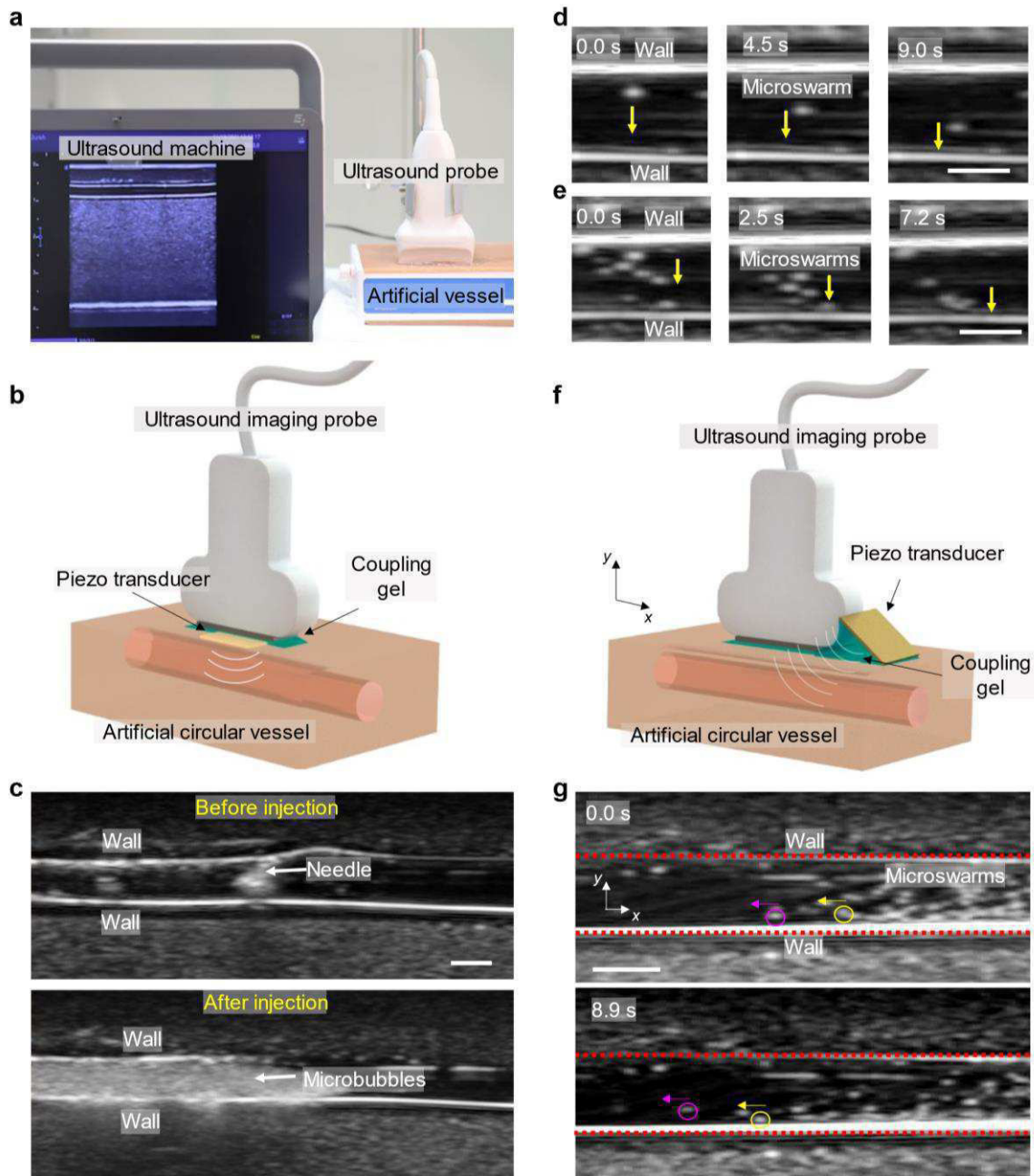
2. Real Time Imaging and Navigation of Acoustic Microrobots Inside Ex-Vivo Blood Vessels

Alexia D.C Fonseca, Anna Heinle, Tirza Heinle and Daniel Ahmed

Acoustic Robotics for Life Science and Healthcare, D-MAVT, ETH Zurich

Combined navigation and imaging of microrobots in living vasculatures is essential in realizing targeted drug delivery. However, in the present there are still few microrobots which can show both functionalities simultaneously when implemented inside a physiologically relevant environment. We developed a dual acoustic control and imaging of “swarmbots”, in which we can track in real time microrobot navigation inside microfluidic vessels and also inside ex-vivo vessels. Microrobot manipulation is based in fundamental acoustic radiation forces; and we already proved in previous research that this technique can navigate microbubble-based swarms (microrobots) in physiological conditions.[1] Here, we incorporate ultrasound imaging for microrobot visualization, providing an essential feedback needed for MB based-microrobot control inside microchannels. Furthermore, we additionally show how to exploit Power Doppler imaging to identify microrobotic movement when the traditional ultrasound imaging does not provide enough contrast. Doppler image acquisition serves as imaging assistance by detecting MB oscillations and velocities.

[1] A. D. C. Fonseca, T. Kohler, and D. Ahmed, “Navigation of Ultrasound-controlled Swarmbots under Physiological Flow Conditions.” *bioRxiv*, p. 2022.02.11.480088, Feb. 14, 2022. doi: 10.1101/2022.02.11.480088



Ultrasound imaging of microbots. a). Imaging setup. An ultrasound-imaging probe is acoustically coupled to an artificial tissue phantom for real-time visualization. b). Schematic illustrating positions of the imaging probe, piezo transducer, coupling gel, and artificial vessel with circular cross-section. c). Images before and after microbubble injection into the artificial vessel using a needle syringe. This setup was used to move microswarms towards the wall. Images showing real-time migration of d). one and e). multiple microswarms towards the bottom wall of the vasculature. f). Schematic illustrating positions of the imaging probe, piezo transducer, coupling gel, and artificial vessel with circular cross-section. This setup was used to navigate microswarms along the wall. g). Images showing real-time migration of several microswarms along the wall and away from the piezo transducer (placed at top right of channel). Scale bars, 3 mm.

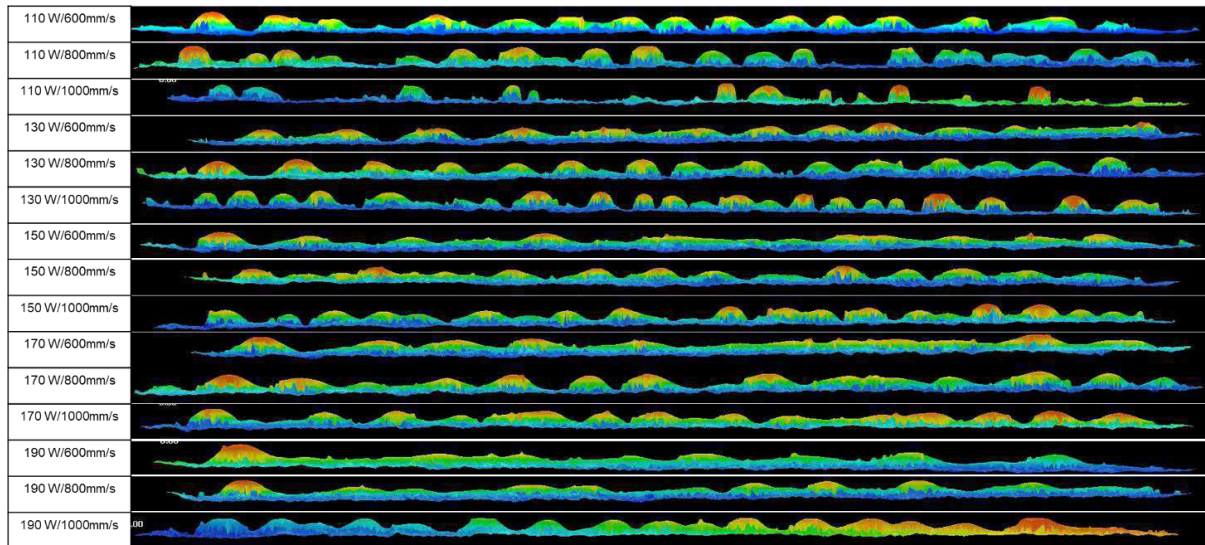
3. Multi-Sensor Evaluation of the Effect of Preheat in Meltpool Characteristics in Laser Powder Bed Fusion

Baris Kavas, Michael Tucker and Markus Bambach

Advanced Manufacturing, D-MAVT, ETH Zurich

In state-of-the-art applications of selective laser melting process, process parameters are optimized by design of experiment studies and fixed to be globally applied throughout the manufactured part. However, during the process there are variations in local and global thermal conditions that significantly

alter the applicable process window. Among these changes, pre-heat temperature is arguably the most important for obtaining a stable melt pool and solidification geometry through the printed part. Due to the geometry of the parts, process noise, and local heat accumulation, pre-heat temperature has been shown to vary within and between layers. Understanding the effects of pre-heat temperature is imperative for closed-loop control applications based on in-situ monitoring systems. This paper aims to experimentally isolate the effects of pre-heat temperature on single track and single layer laser exposure patterns with various laser power and laser scan speed parameters. Furthermore, a process monitoring system with an in-line high-speed CMOS camera and a dual in-line pyrometer has been employed to monitor the single-track exposures and collected signals have been processed to correlate with the process conditions. The outcomes of this study enhance the state-of-the-art understanding of the signal dependencies and pre-heat temperature on melt pool geometry using two of the most commonly used in-situ process monitoring modalities.



4. High-Throughput Deposition of Picoliter Droplet Reactors on Plates for Chemical Analysis and Synthesis

Maximilian Breittfeld, Mario A. Saucedo-Espinosa and Petra S. Dittrich

Bioanalytics, D-BSSE, ETH Zurich

Confidential

5. Arrested Spinodal Decomposition in Elastic Matrices for Structural Color Applications

Carla Fernandez-Rico, Charlotta Lorenz, Sai Tianqi, Sanjay Schreiber, Robert W. Style and Eric R. Dufresne

Soft and Living Materials, D-MATL, ETH Zurich

Phase separation is a ubiquitous process and finds applications in a variety of biological, organic, and inorganic systems [1]. Nature has evolved the ability to control phase separation to both regulate cellular processes and make composite materials with outstanding mechanical and optical properties. Striking examples of the latter are the feathers of many bird species, which show fascinating structural colours and are thought to result from an exquisite control of their phase-separated microstructures [2]. By contrast, it is much harder for material scientists to arrest and control phase separation in synthetic materials with such a high level of precision and over large volumes [3]. In this work, we demonstrate the control over spinodal decomposition processes at the microscale by using elastic polymer matrices. Our simple yet robust phase separation method [4], consist of a silicone gel, which is immersed in a partially miscible oil, at high temperatures. Subsequent cooling results on the formation of bicontinuous structures at the microscale. We show that the length scale our arrested spinodal structures is tuneable

and controlled by the mechanical properties of the polymer network. We also show that the threshold for phase separation is not only suppressed by increasing elasticity, but that phase separation prefers to take place via spinodal decomposition over nucleation and growth for stiffer matrices. Finally, we unveil the composition of our structures and compare the resulting phase diagram with a physical model. These results open up a range of possibilities for both fundamental and applied research, including the development of polymer composites with engineered internal structure for structural colour and superior mechanical properties.

[1] Perry, S.L., et al., "Phase separation: Bridging Polymer Physics and Biology". *Current Opinion in Colloid and Interface Science*, (2019) [2] Dufresne, E., et al., "Self-assembly of amorphous biophotonic nanostructures by phase separation". *Soft Matter*, (2009). [3] Fernandez-Rico, C., et al., "Putting the Squeeze on Phase Separation". *JACS Au*, (2021). [4] Style, R., et al., "Liquid-Liquid Phase Separation in an Elastic Network", *PRX* (2018).

6. Slip Phase Transition at the Origin of Local Frictional Instabilities

Miguel Castellano and David S. Kammer

Computational Mechanics of Building Materials, D-BAUG, ETH Zurich

A system of two bodies in frictional contact, subject to shear loading, accumulates stress on the contact asperities that form the interface. Typically, when loaded over their strength limit, these asperities start weakening, releasing some of the accumulated stress inelastically through the nucleation of frictional slip. During this so-called cohesive slip phase, the frictional strength reduces continuously with slip. Eventually, the asperity breaks, reaching the residual slip phase, where friction is constant at a residual level. In literature, nucleation of frictional sliding is generally studied through the lens of two different theories. On the one hand, classical nucleation theory (CNT) is used in fracture mechanics to derive the critical nucleation length from the free energy of a slip patch in its residual phase — i.e., a crack — . This is known as the Griffith's criterion. On the other hand, a stress criterion, based on linear stability analysis (LSA), is used for slip patches in their cohesive phase — i.e., containing no fully broken asperities — . This leaves us with two different length-scales applicable to either situation. However, it remains unclear when and how these different situations apply as well as what happens when asperities change slip phase during nucleation and how this affects the stability of the nucleation process. Building up on the work by Albertini et al. [1] and Schär et al. [2], we focus on the study of highly heterogeneous interfaces, where both the strength and the toughness vary largely between asperities. This allows for weaker asperities to break before global instability is triggered, thereby exposing the transition from cohesive to residual nucleation. We find that, depending on the size and amplitude of heterogeneities, the nucleation process can locally migrate from one stable solution (LSA) to another (CNT), either quasi-statically or dynamically, generating localized dynamic slip events of different magnitude on its way.

[1] G. Albertini, et. al., *Journal of the Mechanics and Physics of Solids* 147 (2021)

[2] S. Schär, et. al., *International Journal of Solids and Structures* 225 (2021)

7. Controlling Phase Separation in Crosslinked Poly(ethylene Glycol) Diacrylate (PEGDA) Gel

Yanxia Feng, Eric R. Dufresne and Robert W. Style

Soft and Living Materials, D-MATL, ETH Zurich

Poly(ethylene glycol) diacrylate (PEGDA) hydrogel as one of the most popular hydrogels that has been extensively explored in biomedical fields, for example, drug delivery, tissue and cell scaffold and others. PEGDA hydrogels are simple and fast to be synthesized by curing a mixture of PEGDA, water and photoinitiator precursor under UV light source. PEGDA hydrogels are biocompatible and their mechanical properties can be easily controlled by varying the concentration or molecular weight of the PEGDA polymer[1]. While engineering and application of PEGDA hydrogel has been massively studied, however, deep understanding of the polymerization process is missing. We observed polymerization induced phase separation in PEGDA hydrogel and controlled the phase separation by varying temperature, solvent, and types of photoinitiators.

[1] W.S.Lim, et. al., *Biomaterials*. 165, 25-38 (2018).

8. Boosting Buccal Drug Absorption with a Simple Bioinspired Stretching Device Fabricated by 3D Printing

David Klein Cerrejon[†][1], Zhi Luo[†][1,2] Simon Römer[1], Nicole Zoratto[1] and Jean-Christophe Leroux[1]

[†] These authors contributed equally to this work.

[1] *Drug Formulation and Delivery, D-CHAB, ETH Zurich*

[2] *Biomedical Engineering, Southern University of Science and Technology, P.R. China*

Macromolecular drugs, such as peptides and proteins, have revolutionized the treatment of many diseases, from diabetes to cancer. However, their administration mostly relies on parenteral injections. Only a few of those drugs are marketed as oral formulations and their bioavailability is typically less than 1%, with large inter- and intra-patient variations. As a result, the delivery methods of such macromolecular drugs have been shifted towards complex technologies such as microneedle injections in the gastrointestinal tract. In contrast, we present a simple platform technology based on a 3D printed device that can boost diffusion of drugs through the buccal mucosa. Inspired by the unique structure of octopus suckers, we developed a self-applicable suction patch device for soft and wet tissue. The device was produced by 3D printing with a biodegradable polymer (poly(β -thioester) and characterized thoroughly. Moreover, the diffusion-enhancing properties of the device were carried out *ex-vivo* on porcine buccal mucosa. The suction patch was loaded with fluorescent drug surrogates and tested under various relevant mechanical and biochemical conditions. Semi-quantitative and immunohistological image analysis was used to compare the effect of investigated conditions. It was found that the suction patch achieves up to two orders of magnitude higher adhesion than current state-of-the-art mucoadhesives while showing high resistance to shear forces. Most importantly, we could boost the permeation of minimal permeable compounds by combining mechanical stretching and chemical permeation enhancers. Finally, we identified critical permeation enhancing parameters and could show macromolecule diffusion below the penetration barrier of the buccal mucosa. In conclusion, we present a novel and non-invasive route for administering biopharmaceuticals via a bioinspired device. The technology shows potential for clinical translation and provides new opportunities for drug delivery and development.

Funding: ETH Zurich Research Grant No. 33 20-1 & Postdoctoral Fellowship program No. 18-2 FEL-14, Southern University of Science and Technology Start-up grant No. Y01386119

9. Self-Replicating Colloidal Microstructures

Steven van Kesteren and Lucio Isa

Soft Materials and Interfaces, D-MATL, ETH Zurich

Self-replication is nature's preferred method to generate and multiply the complex micro- and nanostructures that are vital for life. Despite many efforts, building replicating microsystems in the lab remains elusive. Here we show our attempts at microscale replication which pushes beyond what was possible before [1]. We take micron-sized colloids coated with DNA and assemble these into well-defined microstructures using capillary assembly [2]. Then we add magnetic colloids coated with complementary DNA strands that duplicate the initial structure. Using magnetic fields and a UV-activated crosslinker these structures are fixed and separated from their parent structure by increased temperature. This rudimentary system demonstrates the basics of microscale self-replication and shows a clear path forward to future self-replicating building blocks for metamaterials, microrobots, electronic components.

[1] Leunissen, M. E., et al. *Soft Matter*, 5(12), 2422–2430.

[2] S. Ni, et al. *Science Advances*, 2(4), e1501779–e1501779 (2016)

10. Electrodeposition of Steel in the Presence of Aqueous Carbonates

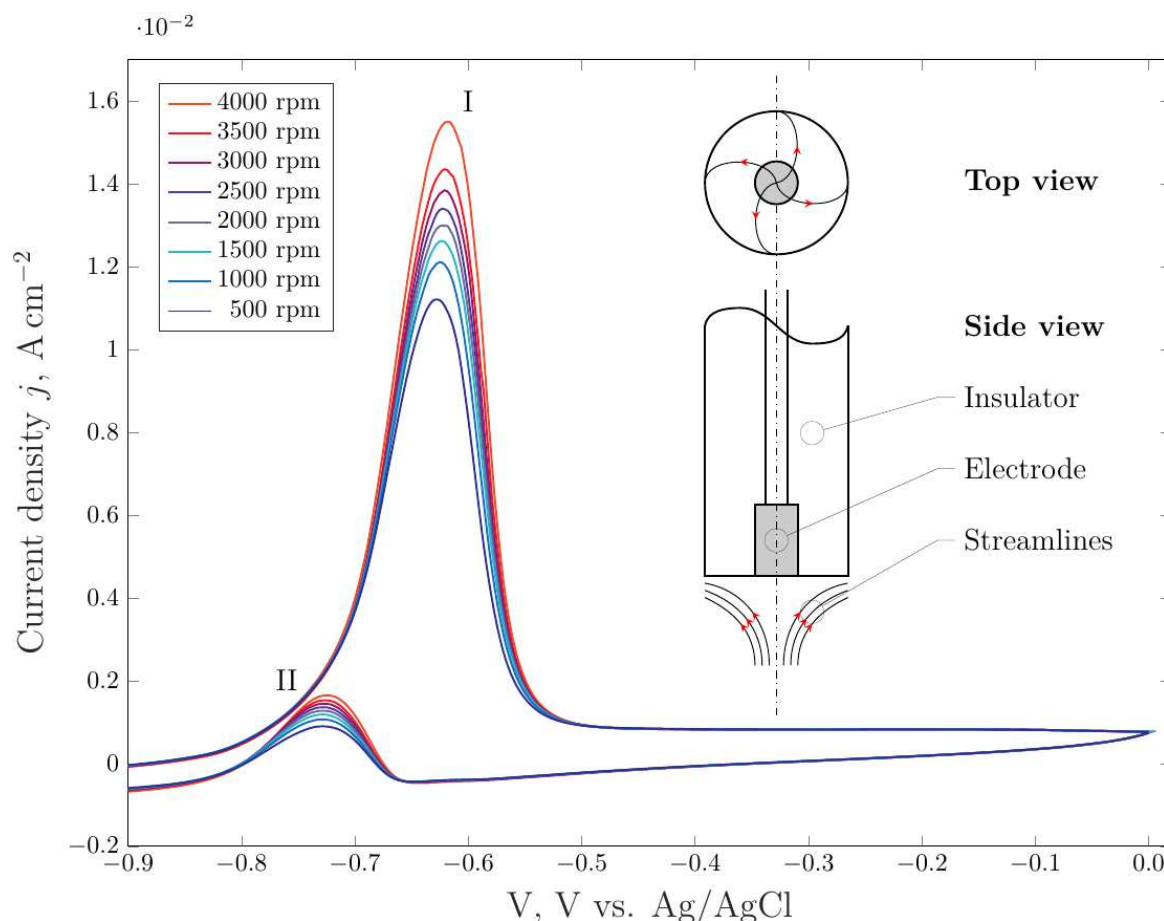
Fabio E. Furcas and Ueli Angst

Durability of Engineering Materials, D-BAUG, ETH Zurich

Whilst carbon steel is thermodynamically passive at alkaline pH, the ingress of CO_2 through the concrete cover may diminish its pH buffering capacity and thus promote corrosion. A number of publications support the hypothesis that aqueous carbonate species actively partake in the dissolution mechanism [1]. Sustained structural damage may hence be catalysed by a carbonation-induced kinetic mechanism, rather than a mere shift in the energetic feasibility from passive to actively corroding regimes.

Here, we present a detailed electrochemical investigation into the electron-transfer reactions of C50 carbon steel exposed to carbonate electrolytes by means of cyclic voltammetry and electrochemical impedance spectroscopy. It is found that two major, mass transfer- controlled reactions facilitate the electro-dissolution of steel within the potential range of -1.0 to 0.0 V vs. $\text{Ag}/\text{AgCl}_{\text{sat}}$. Their respective peak position on the voltammogram and the maximum current density depend on the total and relative HCO_3^- and CO_3^{2-} concentration and therefore, the pH. To further unravel the dissolution mechanism and investigate its effect on the durability of reinforced concrete, the study is being extended to electrolytes representative of the chemical environment characteristic to cementitious systems.

[1] E. Castro, J. Vilche, *Journal of Electroanalytical Chemistry*, 323 (1992) 231-246.



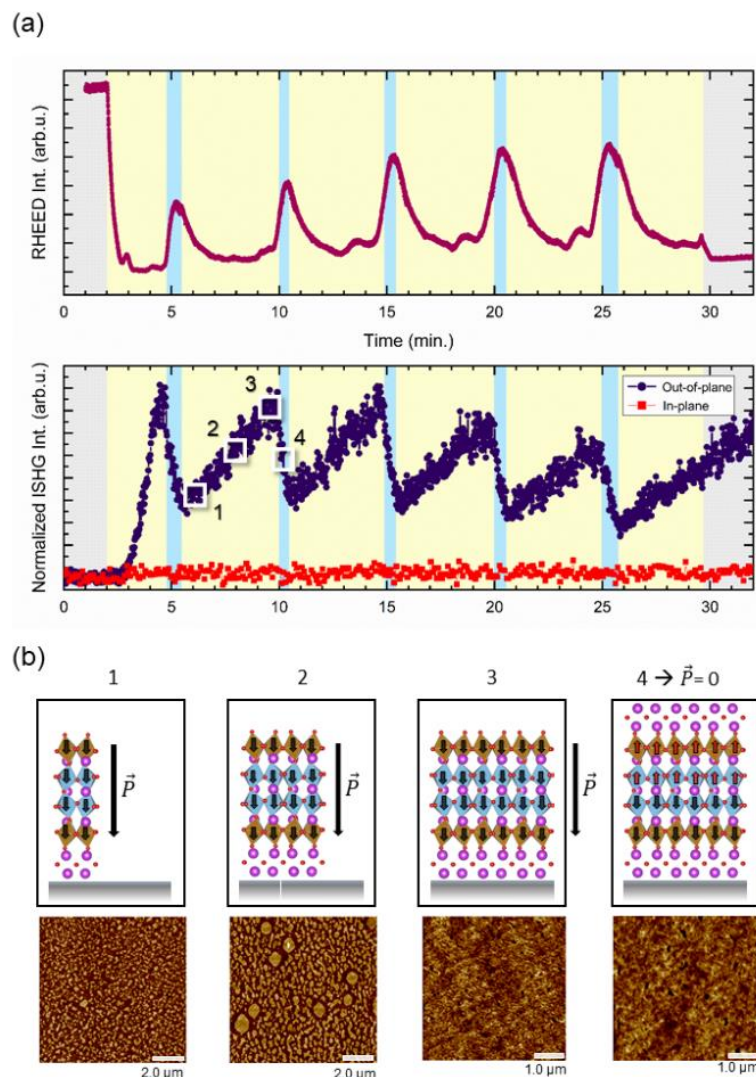
Cyclic voltammogram at $v = 0.025 \text{ V/s}$ in $0.50 \text{ M KHCO}_3(\text{s}) + 0.85 \text{ K}_2\text{CO}_3(\text{s})$, together with a schematic of the rotating disk electrode setup.

11. In-Situ Tracking of the Polarization Dynamics During the Growth of Layered Ferroelectric Aurivillius Thin Films

Ipek Efe, Elzbieta Gradauskaite, Manfred Fiebig and Morgan Trassin

Multifunctional Ferroic Materials, D-MATL, ETH Zurich

The highly anisotropic nature of layered oxides is key to exotic functionalities such as superconductivity, magnetoresistance, and ferroelectricity, which are promising for applications. However, their integration in epitaxial design is challenging due to the complexity of the unit-cell, which makes precise monitoring of the growth a necessity. Here, we directly access the polarization dynamics of the model system Aurivillius $\text{Bi}_5\text{FeTi}_3\text{O}_{15}$ films during the epitaxial growth using in-situ optical second harmonic generation (ISHG). We identify an oscillating intensity of the ISHG signal during two-dimensional layer-by-layer growth (Fig. a). We correlate these oscillations with the periodical evolution of the polarization of ferroelectric film dictated by the chemistry of the planes in the unit-cell, which consists of alternating positively charged fluorite-like $(\text{Bi}_2\text{O}_2)_2^+$ layer and negatively charged $(\text{Bi}_3\text{FeTi}_3\text{O}_{13})_2^-$ perovskite blocks. In combination with reflection high-energy electron diffraction, we show how polarization of the films consistently switches from an out-of-plane orientation during the perovskite blocks growth, to a fully in-plane orientation with the completion of the unit-cell termination and the $(\text{Bi}_2\text{O}_2)_2^+$ capping. Our findings reveal previously hidden polarization dynamics during the epitaxial design and bring new insights in the sub-unit cell control of layered oxide films properties for the development of energy efficient oxide electronics.



a) Recorded ISHG and RHEED oscillations during the growth of $\text{Bi}_5\text{FeTi}_3\text{O}_{15}$ films. b) Four steps of our mechanism describing the evolution of polarization controlled by the layer chemistry during the growth of $\text{Bi}_5\text{FeTi}_3\text{O}_{15}$ films and corresponding surface topography images.

12. Amyloid Fibril-Based Membranes for PFAS Removal from Water

Tonghui Jin[1], Mohammad Peydayesh[2], Hanna Joeress[3], Jiangtao Zhou[1], Sreenath Bolisetty[4] and Raffaele Mezzenga[1]

[1] Food and Soft Materials, D-HEST, ETH Zurich

[2] Helmholtz-Zentrum Hereon, Institute of Coastal Environmental Chemistry, Germany

[3] Institute of Inorganic and Applied Chemistry, Universität Hamburg, Germany

[4] BluAct Technologies GmbH, Dufaux-strasse 57, 8152 Zurich, Switzerland

We introduce a green and efficient approach for removing per- and polyfluoroalkyl substances (PFASs) based on the β -lactoglobulin amyloid fibril membrane. The membrane exhibits superior adsorption capability for long-chain PFASs. At low pH, the membrane efficiency improved significantly due to enhanced electrostatic interactions between positively charged fibrils and negatively charged PFASs. Furthermore, intermolecular adhesion force measurements confirm the hydrophobic–hydrophobic interaction at the nanoscale with PFOS and PFOA representing perfluoroalkyl sulfonic acids (PFSA) and perfluoroalkyl carboxylic acids (PFCAs), respectively. For real PFAS-contaminated water from the Xiaoqing River basin and under single-step filtration mode, the membrane exhibits high efficiency for removing both high ($> \mu\text{g L}^{-1}$) and trace (ng L^{-1}) levels of the compounds. To demonstrate the scalability and generality, a commercial amyloid–carbon-based hybrid membrane is applied for removal of a range of long-chain and short-chain PFASs as well as their replacement compounds, offering complete removal of PFASs with ≥ 4 perfluorinated carbon atoms in the molecular structure and a removal efficiency of low molecular weight PFBA (3 perfluorinated carbon atoms) exceeding 96%. Analysis of the sustainability footprint reveals the superiority of the amyloid–carbon hybrid membrane for PFAS removal. Altogether, these results demonstrate a high potential of amyloid fibril membrane technology for the sustainable removal of PFASs from water.

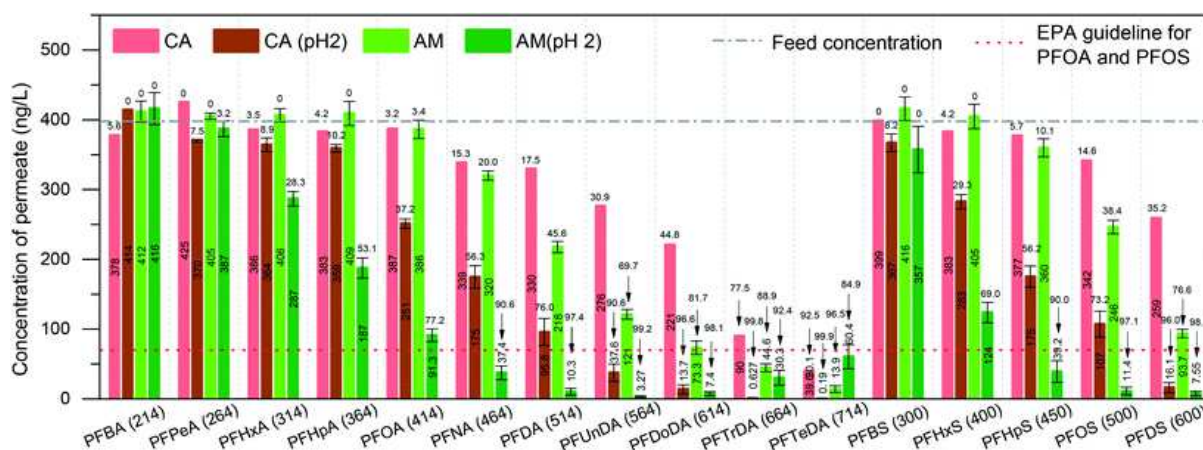


Fig. 1 Concentrations of PFCAs and PFSA in the permeate. The pH of the feed is around 7 unless otherwise stated. The number in the brackets is the MW of each compound. The red dashed line stands for EPA guideline for PFOA and PFOS regulation, which is 70 ng L⁻¹. The grey dashed line stands for the spike concentration of each PFAS, which is around 400 ng L⁻¹. The removal efficiencies (%) are shown above the permeate bars.

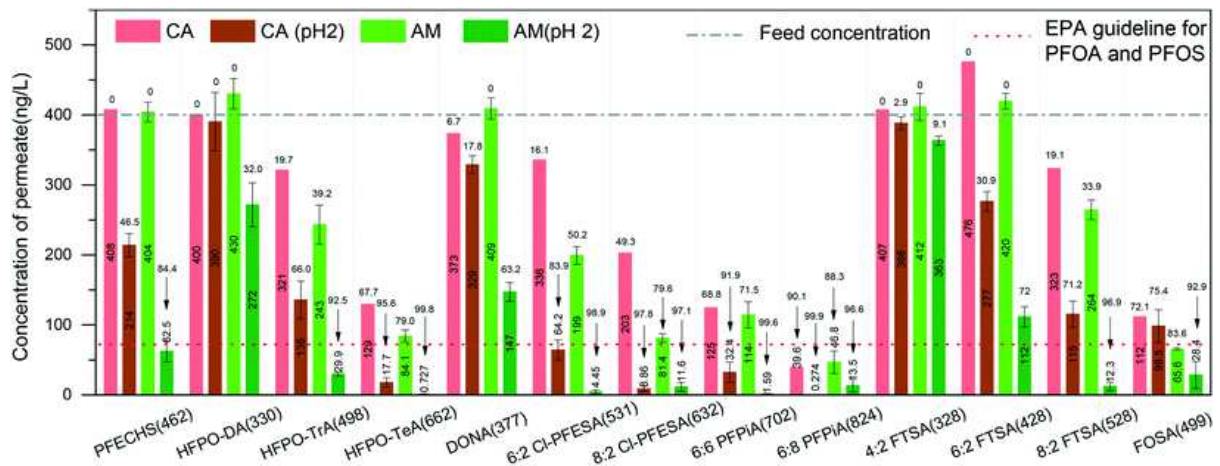


Fig. 2 Concentrations of replacement PFASs and overlooked PFASs in the permeate (PFAAs). The pH of the feed is around 7 unless otherwise stated. The number in the brackets is the MW of each compound. The red dashed line stands for the EPA guideline for PFOA and PFOS regulation, which is 70 ng L⁻¹. The grey dashed line stands for the spike concentration of each PFAS, which is around 400 ng L⁻¹. The removal efficiencies (%) are shown above the permeate bars.

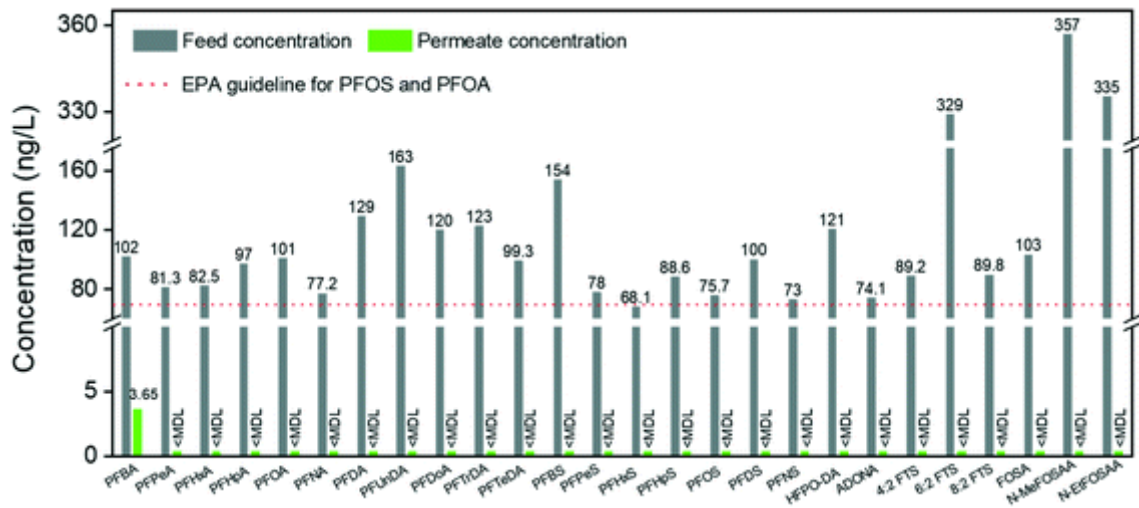


Fig. 3 PFAS treatment by the amyloid-carbon hybrid membrane.

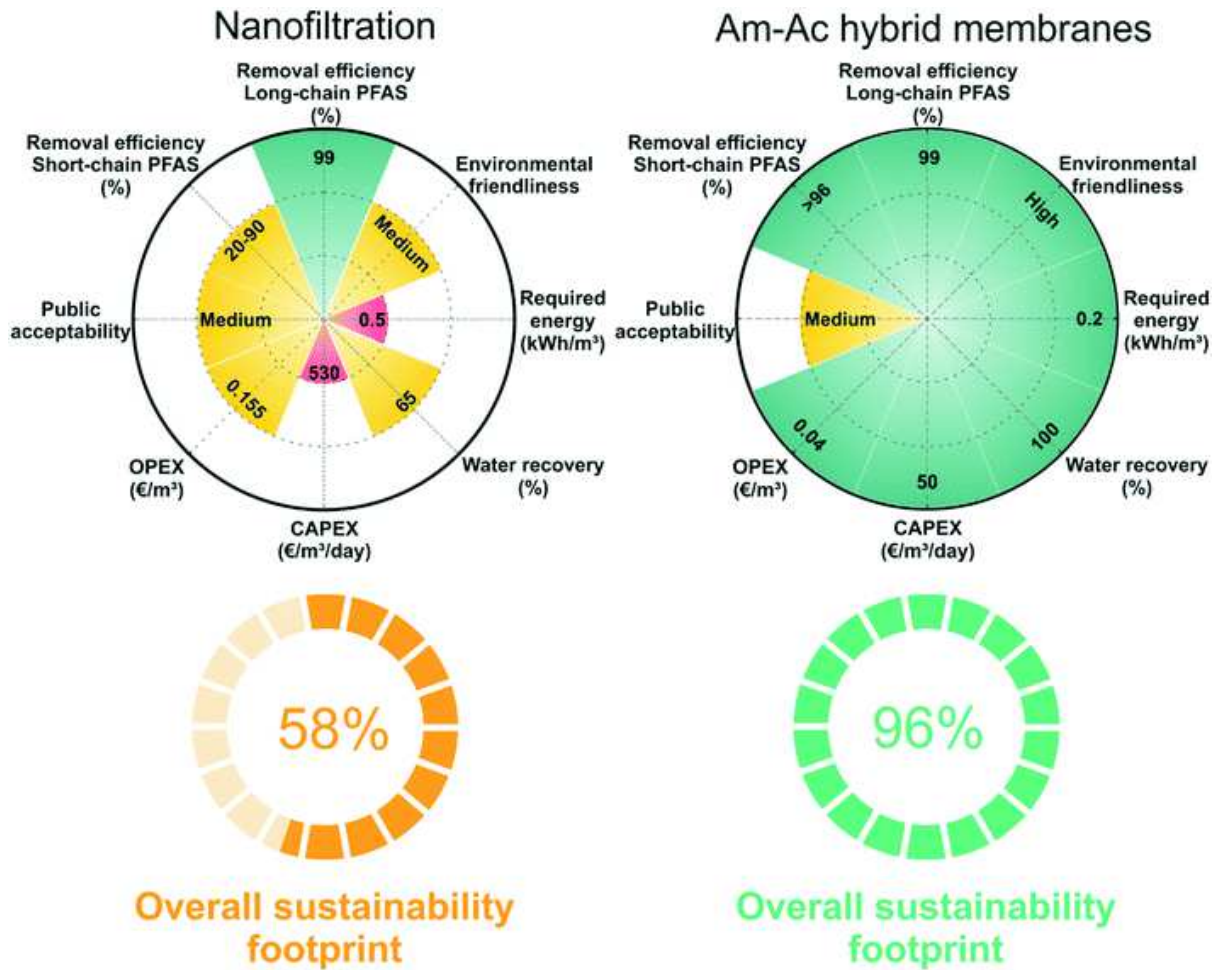


Fig. 4 Sustainability footprint comparison between nanofiltration and amyloid-carbon hybrid membrane. The aspects considered are long-chain PFAS removal efficiency, short-chain PFAS removal efficiency, public acceptability, OPEX, CAPEX, water recovery, required energy, and environmental friendliness. The performance of the technologies in each parameter is evaluated on a 3-rank basis of low (red), medium (yellow), and high (green) levels. The overall sustainability footprint of each technology is evaluated according to each aspect.

13. Interdependence of Structural and Compositional Parameters on Up-Converting Hafnia Nanoparticles

Xavier H. Guichard and Alessandro Lauria

Multifunctional Materials, D-MATL, ETH Zurich

NIR-Vis up-conversion (UC) plays a key role in many emerging applications such as theranostics, solar energy harvesting, sensing and others.^[1] While rare earth (RE) up-conversion luminescence in fluoride nanoparticles is extensively studied,^[2] HfO₂ nanocrystals seem to be a promising alternative due to their high stability and biocompatibility.^[3] Nevertheless, the polymorphism observed in hafnia when high RE doping levels are used, hinder a clear understanding of the parameters relevant for controlled and improved UC. Therefore, a finer control over doping levels and crystal structure is necessary to optimize the optical performance.

In this work, we studied the influence of structural and compositional modifications on the up-conversion luminescence (UCL) recorded in Er/Yb co-doped hafnia nanocrystals. The up-conversion characteristics of the materials were monitored in dependence of structural parameters such as crystal size and lattice symmetry originating from the multifunctional doping.^[4] We report that the cubic polymorph of hafnia expresses much higher up-conversion efficiency with respect to monoclinic nanoparticles. On the other hand, the elemental analysis carried out by TEM energy dispersive X-ray spectroscopy (EDS) allowed us to correlate the composition of Er/Yb/Lu:HfO₂ with the main UC features like efficiency and the ratio between green and red emission deriving from radiative recombination on Er³⁺ centres. Moreover, we possibly explain the inhomogeneity of doping in mixed polymorphs by analysing UCL profiles as probes of the local rare earth environment. These results give useful insights about the phenomena responsible for UCL features in hafnia nanocrystals, enabling their employment in various fields, thanks to improved UC intensities and control over the emission profile.

[1] B. Zhou, et al., *Nat. Nanotechnol.*, 10, 924, (2015).

[2] S. Wilhelm, *ACS Nano*, 11, 10644, (2017).

[3] I. Villa, et al., *Nanoscale*, 10, 7933, (2018).

[4] A. Lauria, et al., *ACS Nano*, 7, 7041, (2013).

14. Supramolecular Reinforcement of Polymer–Nanoparticle Hydrogels for Modular Materials Design

Giovanni Bovone*, Elia A. Guzzi*, Stéphane Bernhard*, Tim Weber, Dalia Dranseikiene, and Mark W. Tibbitt

* These authors contributed equally to this work

Macromolecular Engineering, D-MAVT, ETH Zurich

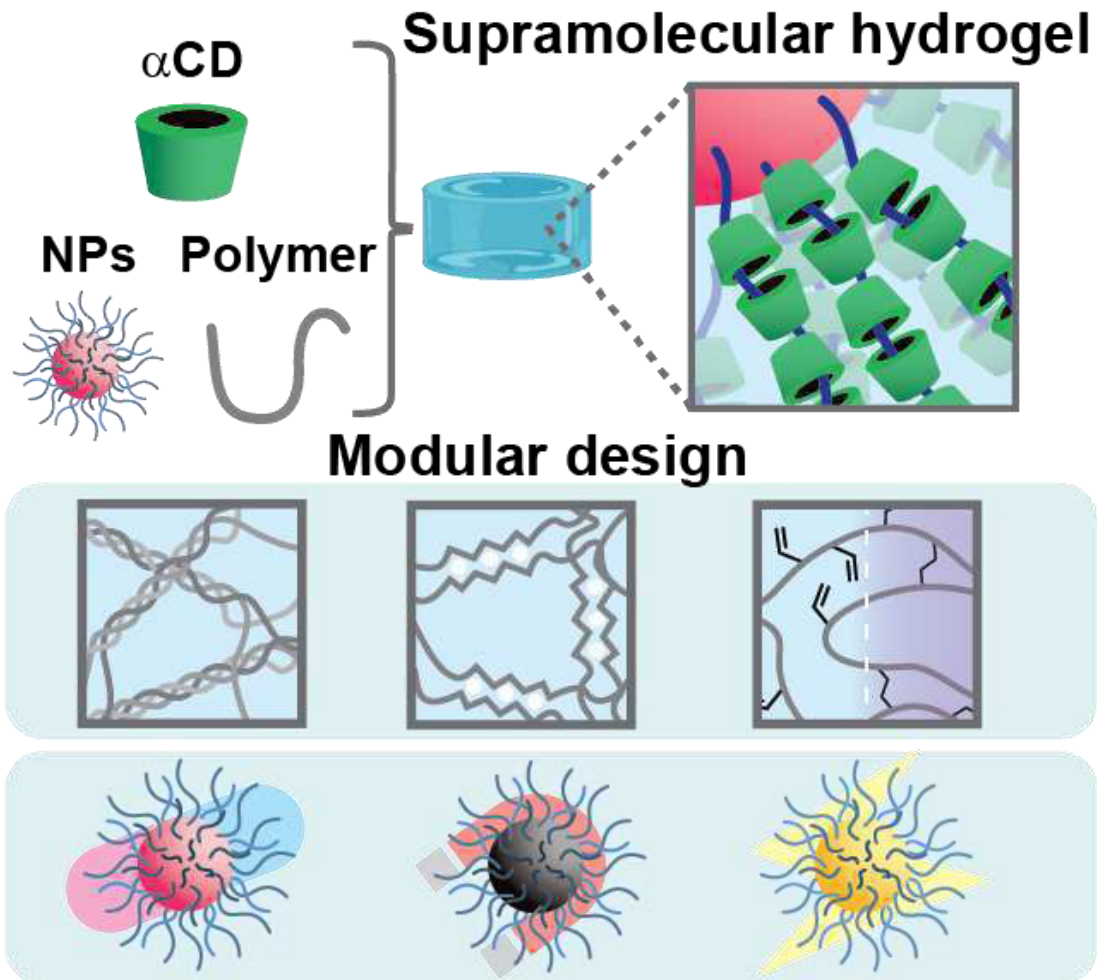
Shear-thinning and self-healing materials are increasingly used in biomedicine and industry. Polymer–nanoparticle (PNP) hydrogels are an emerging class of moldable biomaterials whose rheological properties arise from reversible intermolecular interactions between polymer chains and nanoparticles.^[1] Their application has been restricted because stable networks are formed exclusively between specific combinations of polymer chains and nanoparticles. PNP hydrogels have also limited mechanical properties.

We developed a simple strategy to reinforce PNP hydrogels which expanded the application spectrum of these materials.^[2] We hypothesized that α CD could enhance NP–NP interactions. The inclusion of α -cyclodextrin (α CD) into the formulation of CD–PNP hydrogels increased the storage modulus by several orders of magnitude. In CD–PNP hydrogels, we were able to exchange the structural polymers and nanoparticles on a modular manner and applied these hydrogels in 3D bioprinting, drug delivery, and other applications which required electroconductivity and magnetism.

Supramolecular reinforcement broadened the application spectrum of PNP hydrogels without the need to re-engineer the network.

[1] E.A. Appel, M.W. Tibbitt, et. al., *Nat. Commun.* 6, 6295 (2015).

[2] G. Bovone, E.A. Guzzi, S. Bernhard, et. al., *Adv. Mater.* 34, 2106941 (2022).



We hypothesized that, after adding α CD to the PNP formulation, α CD threaded onto PEG chains present on nanoparticles and formed polypseudorotaxane structures which improved nanoparticle–nanoparticle interactions within the hydrogel network. This reinforcement allowed us to exchange the hydrogel structural components with a library of different polymer chains (collagen, alginate, and methacrylated hyaluronic acid), and nanoparticles (block copolymer nanoparticles, magnetic iron nanoparticles, and electroconductive gold nanoparticles) to expand the application spectrum of this class of materials.

15. Modeling and Characterization of Racetrack Memories with VCMA Synchronization

Pietro Diona[1], Luca Gnoli[2] and Fabrizio Riente[2]

[1] *D-MATL, ETH Zurich*

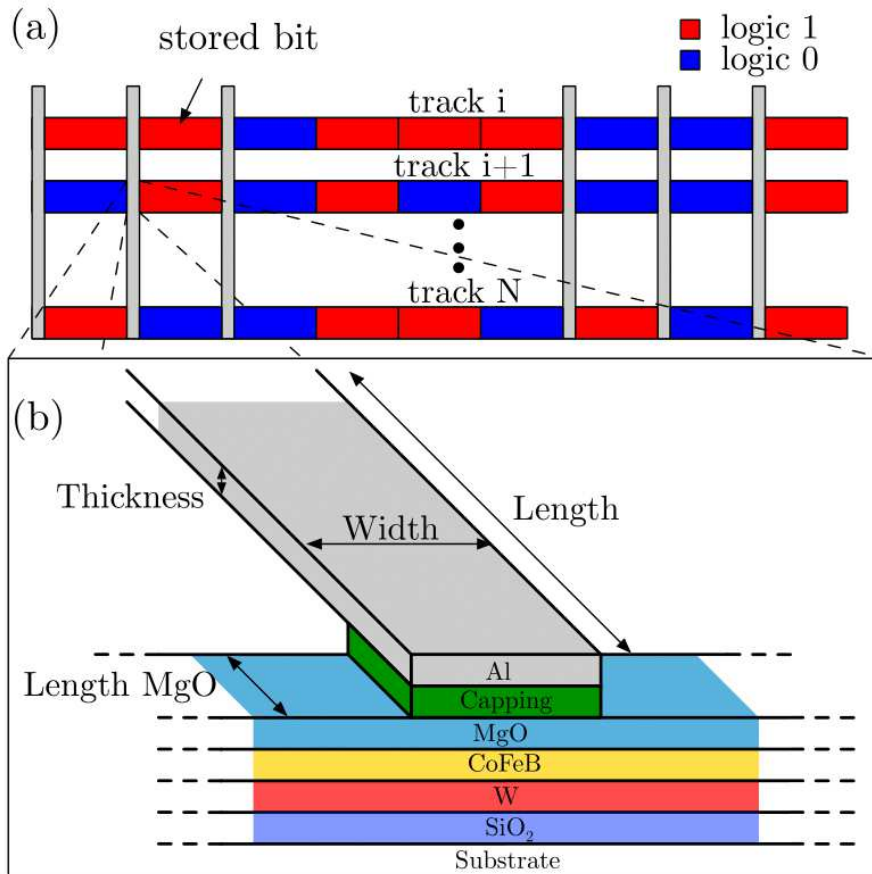
[2] *Politecnico di Torino, DET, PoliTO Turin*

The control of the motion of magnetic domains is of crucial interest for the development of spintronic applications, such as high-density racetrack memories and domain wall logic [1]. In these devices, the domain wall manipulation can be achieved via pulsed currents or applying an external field. However, real-world applications require accurate synchronization systems, keeping limited the power budget. The Voltage Controlled Magnetic Anisotropy (VCMA) effect appears a promising synchronization technique because it can effectively confine different magnetic textures, avoiding the need for strong depinning currents [2]. The anisotropy variation induced by the VCMA can create barriers or wells that can be used to limit the movement of domain walls and obtain an effective synchronization. In our study, we propose a system-level evaluation of the effectiveness of the proposed VCMA synchronization methods [3]. Starting from a two-coordinates model, the motion of domain walls and its performance are evaluated.

[1] R. Bläsing, et al., Proc. of the IEEE 108, 8, (2020).

[2] X. Li, et al., App. Ph. Lett. 107, 14, (2015).

[3] P. Diona, et al., IEEE Transactions on Electron Devices, (2022).



(a) System-level representation of the racetrack memory, organized in tracks where the bit of information is defined between two VCMA gates. (b) Schematic of the VCMA gate.

16. Electrostatically Assisted Nanoscale Printing

Maxence Men  trety[1], Luk  s Zezulka[1], Fabian Schmid[2], Pascal Fandr  [1] and Ralph Spolenak[1]

[1] *Nanometallurgy, D-MATL, ETH Zurich*

[2] *Multifunctional Materials, D-MATL, ETH Zurich*

While macro-scale additive manufacturing readily established itself as a suitable process for rapid prototyping and industrial production, its micro/nano-scale counterpart currently emerges as a versatile manufacturing route with application in different fields, from photonics to sensing and microelectronics. In this evolving field, electrohydrodynamic redox 3D printing (EHD-RP) positions itself as a toolbox combining high-resolution, fast deposition rate and multi-metal capabilities [1].

Here, we demonstrate how external electrodes can be employed as an alternative to mechanical stages as a mean to precisely control the landing point of the charged droplets, meaning the deposition location of a voxel (3D equivalent of a pixel). We study how the amplitude of the deflection is linked to the electrode potential and other factors. On the one hand, the possibility to vary the field strength quasi instantaneously allows faster lateral movement in comparison to a mechanical stage, thereby opening the possibility to utilize the EHD process in other ejection modes—such as the Taylor cone—which would enhance the deposition rate by orders of magnitude. On the other hand, the presented strategy to manipulate droplet trajectories indirectly reveals their physical nature. In that regards, we show how the comparison to a simple finite element model allows to determine a possible range for the size and the number of charge inside the droplet.

Overall, this work unlocks various opportunities, from fundamental understanding of the EHD-RP process, to future development of the technique as an ultra-fast micro-scale additive manufacturing technique.

[1] A. Reiser, et. al., Nat. Commun. 10, 1853 (2019).

17. Capacity-Limiting Factors of Solid-state S/Li₂S Conversion in Microporous Carbon-based Lithium-Sulfur Batteries

Ayca Senol Gungor, Vanessa Wood and Christian Prehal

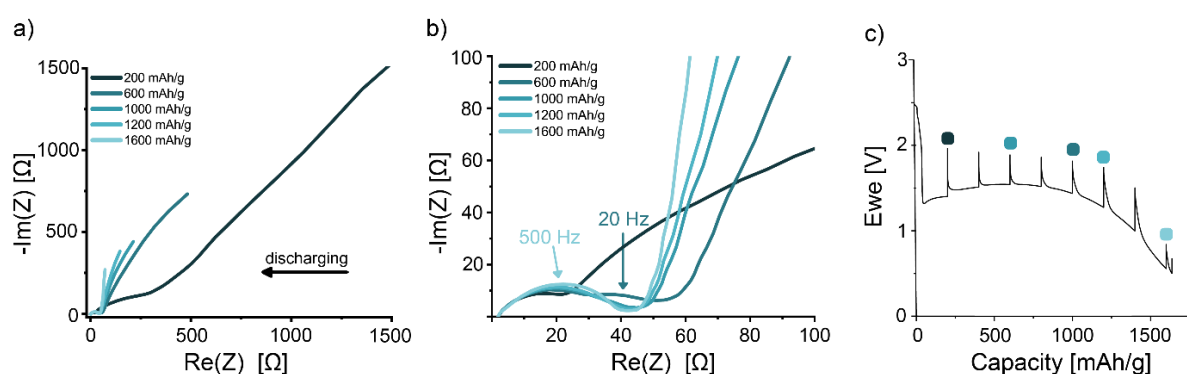
Materials and Device Engineering, D-ITET, ETH Zurich

Lithium-sulfur (Li-S) batteries promise extraordinary theoretical capacities, low cost and sustainability due to the sulfur abundance[1]. The solid-liquid-solid conversion from sulfur(S) to Lithium sulfide(Li₂S) in common ether-based electrolytes results in problems caused by the soluble polysulfides: active material loss, poor cycle life and self-discharge. Solid-state S/Li₂S conversion using carbonate electrolytes and microporous carbons (pores<2 nm) could circumvent these issues[2]. A cathode-electrolyte interface (CEI) layer prevents polysulfide dissolution and ensures solid-state conversion with high cycle life. However, major progress in understanding the capacity and rate-limiting processes is necessary to improve S loadings, S utilization and rate capabilities.

In this work we investigate the physicochemical mechanism of S/Li₂S solid-state conversion in microporous carbon-sulfur cathodes using various electrochemical/materials characterization methods with a focus on electrochemical impedance spectroscopy (EIS). We systematically vary parameters such as the carbon pore size, the temperature, the sulfur loading in the cathodes and the charging rate. In-situ EIS with the galvanostatic intermittent titration technique (GITT) monitors CEI formation, Li ion transport and interface charge transfer during cycling. The study demonstrates that next to Li ion diffusion into the porous carbon particles, charge transfer across the S/Li₂S-C interface, is the rate/capacity limiting factor. Our results indicate that solid-state S/Li₂S conversion with carbonate electrolytes is also possible in carbons with pores beyond 2 nm, a strategy that could significantly increase S loadings in the future.

[1] Manthiram, A., et. al., Chemical reviews, 114(23), 11751-11787 (2014).

[2] Kensy, C., et. al., Batteries & Supercaps, 4(4), 612-622 (2021).



a) EIS spectra during the first discharge, b) magnification of the high and middle frequency region of EIS spectra, c) GITT curve during the first discharge, dots represent the EIS measurement points with their colors matching the spectra.

18. Ferroelectric, Quantum Paraelectric or Paraelectric?

Calculating the Evolution from BaTiO₃ to SrTiO₃ to KTaO₃ Using a Single-Particle Quantum-Mechanical Description of the Ions

Tobias Esswein and Nicola A. Spaldin

Materials Theory, D-MATL, ETH Zurich

We present an inexpensive first-principles approach for describing quantum paraelectricity that combines density functional theory (DFT) treatment of the electronic subsystem with quantum-mechanical treatment of the ions through solution of the single-particle Schrödinger equation with the DFT-calculated potential. Using BaTiO₃, SrTiO₃ and KTaO₃ as model systems, we show that the approach can straightforwardly distinguish between ferroelectric, paraelectric and quantum paraelectric materials, based on simple quantities extracted from standard density functional and density functional perturbation theories. We calculate the influence of isotope substitution and strain on quantum paraelectric behavior and find that experimentally accessible strains can induce large changes, while

complete replacement of oxygen-16 by oxygen-18 has a surprisingly small effect. Finally, we collect the various choices for the phonon mass that have been introduced in the literature and identify those that are most physically meaningful by comparing them with our results that avoid such a choice through the use of mass-weighted coordinates.

[1] T. Esswein, N.A. Spaldin, <https://doi.org/10.48550/arXiv.2112.11284>

19. Structural and Thermal Characterisation of a AuGe Alloy via Electron Microscopy and Fast Differential Scanning Calorimetry

Štefan Stanko[1], Jürgen E.K. Schawe[1,2] and Jörg F. Löffler[1]

[1] *Metal Physics and Technology, D-MATL, ETH Zurich*

[2] *Mettler-Toledo GmbH, Analytical, 8606 Nänikon, Switzerland*

A device combining scanning electron microscopy (SEM) and fast differential scanning calorimetry (FDSC) was developed to perform *in situ* characterisation of metastable phase transformations. The potential of this device is demonstrated on the example of a AuGe eutectic alloy. Upon rapid cooling, the alloy forms the metastable crystalline phases β and γ and an amorphous phase.

A thin lamella for transmission electron microscopy (TEM) was produced from a sample prepared in FDSC to further characterise the microstructure of the alloy beyond the capabilities of the *in situ* device. *Ex situ* FDSC experiments were performed using cooling and heating rates of several 1000 K/s to characterise the thermal behaviour of the β and γ phase. The transformation kinetics of the metastable phases was investigated. Finally, we show that we can prepare the glassy phase in FDSC and determine its thermophysical properties.

20. Rational Design of Luminescent Au(III) Complexes for High-Performance Organic Light-Emitting Diodes

Hsin-Hung Kuo, Sudhir Kumar and Chih-Jen Shih

Interface and Surface Engineering of Nanomaterials, D-CHAB, ETH Zurich

Organic light-emitting diodes (OLEDs) have outperformed the conventional display technologies, for which the advent of phosphorescent materials plays an indispensable role. Nowadays, luminescent cyclometalated Ir(III) complexes have been successfully utilized in cutting-edge OLED displays. However, the scarcity of iridium limited their chances to produce cost-effective OLED products in the future. Recently, Au(III) complexes are emerging as a strong contender for the conventional Ir(III) complexes because of the higher abundance of gold on the earth. Herein, we rationally design a series of Au(III) complexes employing asymmetrical bis-cyclometalated ligands and heterocyclic mono-dental donor. Photophysical, electrochemical, and thermal characteristics of Au(III) complexes are carefully studied, and further substantiated with time-dependent density functional theory (TD-DFT) computations. The doped film of Au(III) complex exhibits an excited-state lifetime, 10.4 μs , and a high photoluminescence quantum yield, $\sim 76\%$, due to the efficient intersystem crossing from the excited states to the ground state. These emitters also demonstrated exceptionally preferred horizontal orientation of emission transition dipole moment upto 88%. The Au(III) complexes possess excellent processing feasibility with both spin-coating and thermal evaporation because of their excellent solubility in common organic solvents and low sublimation temperature with high thermal stability. Our preliminary OLED devices show a maximum external quantum efficiency (η_{ext}) of over 26% and current efficiency (η_{CE}) of 110 cd A^{-1} in dry-process, while $\sim 22\%$ and $\sim 90 \text{ cd A}^{-1}$ in wet-process emissive layers. With further device optimization with our Au(III) complexes, we believe the electroluminescent performance can be further boosted. Moreover, the device shows nearly non-roll-off η_{ext} between 100 and 5000 cd m^{-2} and a high operational lifetime of 800 hours at an initial driving current density of 5 mA cm^{-2} . Our Au(III) emitters pave the way to energy-efficient and long-lasting OLED displays and lighting applications.

21. Towards Strain-Controlled WSe₂ Single-Photon Emitters

Juri G. Crimmann[1], Nolan Lassaline[1], Ario Cocina[1], Deepankur Thureja[1,2], Yannik Glauser[1], Valentina De Rosa[1], Gabriel Nagamine[1], Daniel Petter[1] and David J. Norris[1]

[1] *Optical Materials Engineering, D-MAVT, ETH Zurich*

[2] *Quantum Photonics, D-PHYS, ETH Zurich*

Two-dimensional (2D) materials are an emerging platform for the next generation of atomically thin optical and electronic devices[1]. To engineer device functionality, it is necessary to manipulate the flow of electrons by tailoring their environment through strain or electrostatic gating[2]. This has the fascinating consequence that the electronic band structure in transition-metal dichalcogenides (TMDs) is no longer an intrinsic material property provided by nature, but rather one that can be engineered to produce enhanced optical and electronic properties. A prominent example of what can be achieved with this approach is the engineering of quantum-emitter arrays obtained by placing TMD monolayers such as WSe₂ on a non-planar substrate containing an array of nanoscale pillars. At the positions of the pillars, strain induces high photoluminescence intensities and single-photon emission from the TMD[3, 4]. However, despite these findings, full control over the emission wavelength and the strain profile has not yet been achieved due to the almost random strain profiles generated by simple pillar geometries. To address this issue, we utilize thermal scanning-probe lithography to freeform pattern the SiO₂ substrate beneath the WSe₂ flake. By doing so, we can produce single-photon emitters by precisely engineering strain in WSe₂. Simultaneously, we aim to find the origin of the single-photon emission to fully control this phenomenon.

[1] K. S. Novoselov, et. al., *Science* 353, aac9439 (2016).

[2] A. Castellanos-Gomez, et. al., *Nano Lett.* 13, 5361 - 5366 (2013).

[3] A. Branny, et. al., *Nat. Commun.* 8, 15053 (2017).

[4] C. Palacios-Berraquero, et. al., *Nat. Commun.* 8, 15093 (2017).

22. Non-Specific Adhesive Forces Reorganize the Cytoskeleton Around Membraneless

Thomas J. Bøddeker, Kathryn A. Rosowski and Eric R. Dufresne

Soft and Living Materials, D-MATL, ETH Zurich

Phase-separation of biomolecules in cells takes place in a complex environment crossed by multiple filaments of the cytoskeleton or chromatin. To understand the potential coupling between emerging droplets and the surrounding network, we study the interactions of stress granules, a phase-separated protein-RNA droplet in the cytosol, with the microtubule network. Statistical tools similar to the radial distribution function enable us to quantify long-ranged enhancement in filament density in the vicinity of stress granules. When microtubules are depolymerized, the molecular subunits partition to the surface of the droplet. We interpret the data using a thermodynamic model, revealing a weak non-specific affinity of the subunits to the surface of about 0.1 kT. As filaments polymerize, the affinity is amplified leading to significant adhesion of filaments to the granule surface. This adhesion leads to reorganization of filaments around the granule and makes microtubule rich regions of the cell energetically favorable for stress granules. We find that the liquid nature of membraneless organelles leads to non-specific adhesion of larger particles to their surface due to the surface tension of these protein droplets, reminiscent of Pickering emulsions [1].

[1] T.J. Bøddeker, et. al. *Nature Physics* 18, 571 (2022)

23. Bottom-up Fabricated Nonlinear Barium Titanate 2D Photonic Crystals and L3 Cavities

Ülle-Linda Talts[1], Viola V. Vogler-Neuling[1], David Pohl[1], Helena C. Weigand[1], Joel Winiger[2], Juerg Leuthold[2] and Rachel Grange[1]

[1] *Optical Nanomaterials, D-PHYS, ETH Zurich*

[2] *Institute of Electromagnetic Fields, D-ITET, ETH Zurich*

Non-centrosymmetric metal-oxides such as barium titanate (BTO) are well-known for their advantageous physical properties of high stability, broad transparency window as well as large optical nonlinear coefficient.[1] While the two latter characteristics provide motivation for producing high-speed communication modulators as well as various quantum devices, the chemical inertness results in inherent difficulty of efficient top-down fabrication of BTO-based photonic devices. Solution-processed nanoparticles have been previously combined with cost-effective self-assembling colloidal solutions or imprint lithography to produce photonic crystals [2]. However, the tetragonal crystal phase, responsible for the nonlinear properties in barium titanate, is known to be present in crystals with domain sizes above 30 nm which limits the critical dimensions of densely filled structures from nanoparticles to several hundred nanometers range. Here, we demonstrate a method that enables fabrication of high quality BTO photonic crystals with up to 60 nm critical dimensions with aspect ratios of 10 and refractive index of 2.0 at 600 nm using combination of solution processed BTO sol-gel [3] with soft- nanoimprint lithography (SNIL).

Standard SNIL protocol was followed to imprint nanostructures into a thin film of spin-coated BTO sol-gel. As an example of a challenging structure to fabricate using conventional top-down processing, BTO 2D photonic crystal structures with a L3 cavity were fabricated using SNIL with optimized design based on FDTD simulations. The devices were characterized to showcase the potential of this technique for scalable production of variety of BTO metastructures for improved refractive index modulation efficiencies as well as active nonlinear photonic crystal devices.

[1] A. Karvounis, et. al. *Adv. Opt. Mater.* 2001249 (2020)

[2] V. V. Vogler-Neuling, et. al *Phys. Status Solidi B* 2070024 (2020)

[3] B. I. Edmondson, et al, *J. Am. Ceram. Soc.* 103:1209–1218 (2019)

24. Patterning of Defects in Nematic/Smectic-A Liquid Crystals by Colloidal Arrays

Zazo C. Meijs[1], Yun, Hee Seong[2], Fu, Yutong[1], Park, Geonhyeong[2], Yoon, Dong Ki[2]* and Lucio Isa[1]*

[1] *Soft Materials and Interfaces, D-MATL, ETH Zurich*

[2] *KAIST; Korea Advanced Institute of Science and Technology*

Although substantial effort has been historically made to find ways to minimize the formation and influence of defects in the orientation of liquid-crystalline films [1], recent work has shown that creating local defects both enables studying their fundamental properties and potentially leads to new applications relying on defect engineering [2].

To this end, here, we use capillarity-assisted particle assembly (CAPA) to create microscopic patterns of silica colloids [3]. Our arrays contain 4 μm particles at varying separation, which are transferred and sintered onto a microscope glass surface. Both the glass and the particle surfaces induce specific local direction in the ordered LC-phases. The geometrical shapes gives rises to controlled localized defects. Fig. 1 shows a typical POM image of a square lattice of the colloids and the connected defects they induce.

In the future, by varying the surface chemistry of the colloids, the type of LCs, and the overall geometry of the patterns, we envisage obtaining precise control over the defects for a broad range of conditions and in turn enabling new routes to studying their fundamental properties towards novel defect-based applications.

[1] BC. Jiang, et al., *Journal of Production Research*, **43**, 67 (2005).

[2] MJ. Kim, et al., *Nature communications*, **8**, 1 (2017).

[3] S. Ni, et al., *Faraday Discussions*, **181**, 225 (2015).

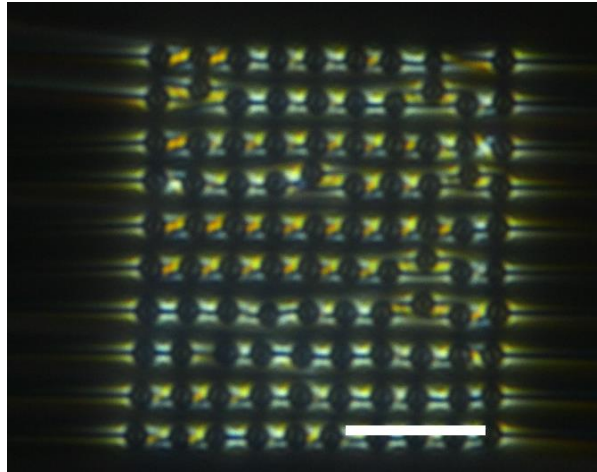


Fig. 1. POM image (x40 magnification), with crossed polarizer-analyzer, showing connected defects, induced by 4 μm colloids with a 3 μm separation and at a temperature of 33.5 $^{\circ}\text{C}$, i.e., in the smectic-A phase of 8CB. Scale bar is 25 μm .

25. Micro-Shear of Silicon: Elastic Strain Analysis Using Digital Image Correlation

Carmen Lauener[1], Fabian Schwarz[1], Laszlo Pethö[2], Jeffrey M. Wheeler[1], Johann Michler[2] and Ralph Spolenak[1]

[1] Nanometallurgy, D-MATL, ETH Zurich

[2] Mechanics of Materials and Nanostructures, Advanced Materials & Surfaces, Empa Thun

Confidential

26. 3D-Printed LEGO®-inspired Titanium Scaffolds for Patient-Specific Regenerative Medicine

Seunghun S. Lee[1], Xiaoyu Du[1], Thijs Smit[1], Elisa G. Bissacco[1], Daniel Seiler[2], Michael de Wild[2] and Stephen J. Ferguson[1]

[1] Orthopaedic Technology, D-HEST, ETH Zurich

[2] Institute for Medical Engineering and Medical Informatics IM2, FHNW, Switzerland.

Despite the recent advances in 3D-printing, it is often difficult to fabricate implants that optimally fit a defect size or shape. There are some approaches to resolve this issue, such as patient-specific implant/scaffold designs based on CT images of the patients, however, this process is labor-intensive and costly. Especially in developing countries, affordable treatment options are required, while still not excluding these patient groups from potential material and manufacturing advances. Here, a selective laser melting (SLM) 3D-printing strategy was used to fabricate a hierarchical, LEGO®-inspired Assemblable Titanium Scaffold (ATS) system, which can be manually assembled in any shape or size with ease. A surgeon can quickly create a scaffold that would fit to the defect right before the implantation during the surgery. Additionally, the direct inclusion of micro- and macroporous structures via 3D-printing, as well as a double acid-etched surface treatment (ST) in the ATS, ensure biocompatibility, sufficient nutrient flow, cell migration and enhanced osteogenesis. Three different structures were designed (non-porous:NP, semi-porous:SP, ultra-porous:UP), 3D-printed with the SLM technique and then surface treated for the ST groups. After analyzing characteristics of the ATS such as surface roughness and interconnected porosity, mechanical testing and FEA demonstrated that individual and stacked ATS have sufficient mechanical properties to withstand loading in a physiological system. All ATS showed high cell viability, and the SP and UP groups demonstrated enhanced cell proliferation rates compared to the NP group. Furthermore, we also verified that cells were well-attached and spread on the porous structures and successful cell migration between the ATS units was seen in the case of assemblies. The UP and SP groups exhibited higher calcium deposition and RT-qPCR proved higher osteogenic gene expression compared to NP group. Finally, we demonstrate a number of possible medical applications that reveal the potential of the ATS through assembly.

27. Globular Proteins and Where to Find Them Within a Polymer Brush – a Case Study

Aikaterini A. Galata and M. Kröger

Polymer Physics, D-MATL, ETH Zurich

Confidential

28. Micro-Scale Biomolecule Patterning on Nitrocellulose Substrates

Nathan Khosla, Daniel A. Richards and Andrew J. DeMello

Microfluidics and Nanoscale Science, D-CHAB, ETH Zurich

Confidential

29. Tuning Local Structure in Prussian Blue Analogues (PBAs)

Yevheniia Kholina and Arkadiy Simonov

Disordered Materials, D-MATL, ETH Zurich

Prussian Blue analogues, $M[M'(CN)_6]_{1-x} \cdot n \cdot H_2O$, which we abbreviate here as $M[M']$ (M and M' =transition metal ions), is a diverse family of cyanide materials, which is intensely investigated for its potential application for hydrogen storage, as catalysts and as electrode materials. Applications that require efficient mass transport utilize the ability of the structure to accommodate a large number of $M'(CN)_6$ vacancies, which create a highly connected porous network. It was theoretically shown that the connectivity and the accessible volume of such a network depend on the local structure[1]. Therefore, to optimize mass transport properties not only the number of vacancies but also their distribution must be precisely controlled. In this work we show how to tune the local structure of Mn[Co] Prussian Blue analogues grown in gel by varying the crystallization parameters: the type of gel, the crystallization temperature, the concentration of reactants, and the concentration of chelating agents. We probe the defect distribution by single-crystal x-ray diffuse scattering, which allows quantitative characterization of the local structure. All of the above-mentioned parameters allow smooth continuous control of diffuse scattering and thus of the local order in Mn[Co] crystals.

[1] A. Simonov, et. al., Nature 578.7794, 256-260 (2020).

30. Reproducible 3D-Integrated Superconducting Circuits Through Polymer Spacers

Graham J. Norris, Laurent Michaud, Jean-Claude Besse, Christopher Eichler and Andreas Wallraff

Quantum Device Lab, D-PHYS, ETH Zurich

Creating devices with hundreds of superconducting qubits is difficult on single-layer devices due to the large number of intra-die connections and impractical with multi-layer wiring processes due to their use of potentially lossy dielectrics. Instead, indium flip-chip bonding, a type of 3D-integration, can be used to join several single-layer superconducting dies, providing extra signal routing planes while avoiding deposited dielectrics. Although indium bump bonding of superconducting circuits has been successfully demonstrated [1,2], precisely controlling the vertical chip spacing, which strongly affects circuit parameters such as resonator frequencies and qubit anharmonicities, without degrading the substrate surface remains a challenge [2]. Here we present a polymer hard-stop spacer fabrication process that provides deterministic inter-chip separation and benchmark the frequency reproducibility and internal loss rates of coplanar waveguide resonators. Since the flip-chip bonded die can significantly alter the electrical properties of circuit elements, we also characterize resonators with varying dimensions and discuss the implications of our results for large-scale devices.

[1] Rosenberg et al., IEEE Microw. Mag. 21, 72 (2020)

[2] Gold et al., npj Quantum Inf. 7, 142 (2021)

31. Computational Screening and Experimental Validation of Binary and Ternary Metal Nitrides for the Solar-Driven Thermochemical Production of Green Ammonia

Daniel Notter[1], María-Elena Gálvez[2], Brendan Bulfin[1], and Aldo Steinfeld[1]

[1] *Renewable Energy Carriers, D-MAVT, ETH Zurich*

[2] *Institute Jean le Rond d'Alembert, CNRS, Sorbonne Université*

The current conventional production of ammonia relies on the well-known Haber-Bosch process, involving a catalytic high-pressure reaction between H₂ and N₂. Due to the production of H₂ and N₂ based on highly energy-intensive processes using fossil fuels, the worldwide ammonia production is responsible for 1.2% of the anthropogenic global greenhouse gas emissions. Furthermore, the high pressures needed to increase the yield and the large recycle flows of the unreacted H₂ and N₂ impose demanding requirements on the equipment, increasing the cost and complexity of the process and favouring large, centralized plants. Multi-step thermochemical cycles based on metal nitrides stand as a promising alternative to this process, since they can substantially mitigate or even eliminate the concomitant CO₂ emissions linked to ammonia production. In such cycles, concentrated solar energy is used to supply the high-temperature heat required in the endothermic reaction steps. Previous studies have proven successful synthesis of ammonia at much lower pressures – even around ambient conditions. Nevertheless, the availability of literature and experimental data on the metal nitrides involved in these cycles is scarce. In an effort to investigate a broader range of candidates, this work presents the results of a screening of different metal nitride compounds using DFT (Density Function Theory) calculations from open-access databases. The probable reaction pathways encompassing either the hydrogenation (H₂) or the hydrolysis (H₂O) of such nitrides, as well as their re-nitridation to recycle the pristine metal nitride were identified through a Gibbs free energy minimization algorithm. The experimental validation of the selected candidates was conducted both through dynamic thermogravimetric analysis (TGA) and in a high-pressure reactor. Finally, the different fresh and spent materials were submitted to physicochemical characterization, to evaluate the chemical, structural and morphological changes inferred through hydrogenation/hydrolysis/re-nitridation and aiming to assess their performance under cyclic operation.

32. Probing Plastic Rearrangements in Colloidal Gels

Pierre Lehericé[1], Laura Stricker[1], Lucio Isa[2] and Jan Vermant[1]

[1] *Soft Materials, D-MATL, ETH Zurich*

[2] *Soft Materials and Interfaces, D-MATL, ETH Zurich*

Gelation of colloids lead to the formation of a percolated network of particles spanning through the material. The structure of the network is closely linked to the mechanical properties of the resulting gel, especially the emergence of a yield stress. A mechanistic understanding of yielding of colloidal gels is of both fundamental and practical interest, especially in view of the widespread use of these materials. However, rheo-confocal studies monitoring the evolution of the microstructure of the gel under shear could not provide a complete image of yielding because of their limited spatio-temporal resolution. Especially, plastic rearrangement between particles before yielding, already evidenced by rheo-DLS experiments as precursors of yielding [1], still need to be directly observed.

We mechanically sollicitate model depletion gels of PMMA-g-PHSA colloids while imaging their microstructure of the gels thanks to a homemade ultrafast rheo-confocal setup [2]. Image processing methods and particle tracking are used to determine the local strain field in the material. We study the dynamics of the plastic events from the variations of this local strain field and link them to the ultimate yielding of the material.

[1] S. Aime, et. al., *PNAS* 115, 3587-3592 (2018)

[2] G. Colombo, *Korea-Aust. Rheol. J.* 31, 229–240 (2019)

33. Performance of Glass to Iron-based Shape Memory Alloy Adhesively Bonded Shear Joints

Zhikang Deng[1], Vlad-Alexandru Silvestru[1], Julien Michels[2], Lingzhen Li[1,3], Elyas Ghafoori[1,3] and Andreas Taras[1]

[1] *Steel and Composite Structures, D-BAUG, ETH Zurich*

[2] *re-fer AG*

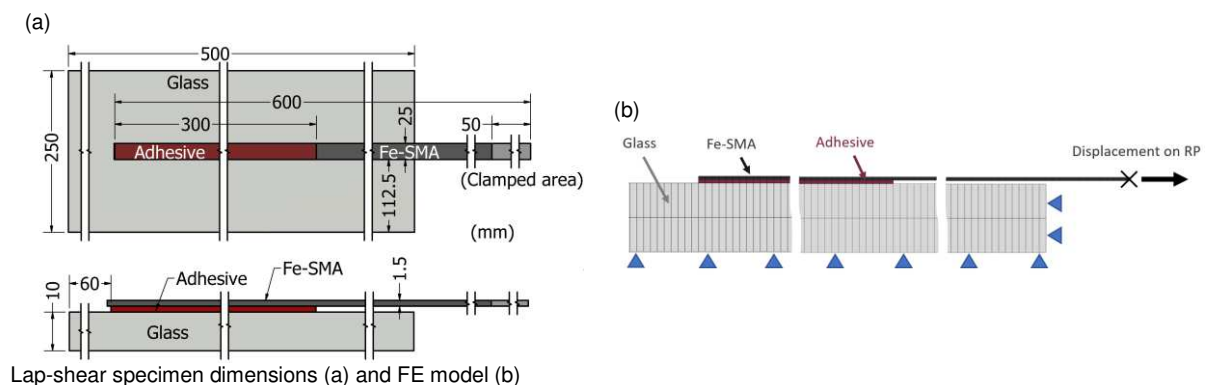
[3] *Sustainable Metallic Structures, Structural Engineering Lab, Empa*

The structural performance of glass beams can be improved by reinforcing them with external prestressed reinforcement (such as stainless steel or fiber-reinforced plastic). Compared with glass beams without any reinforcement, the post-tensioned glass beams have better performance in terms of initial and post-fracture load-bearing capacity. However, prestressing of stainless steel or FRP is complex and expensive, because it often requires special setups, such as hydraulic jacks. Iron-based shape memory alloys (Fe-SMAs) have outstanding performance as post-tensioning materials due to their efficient prestressing procedure (heating the Fe-SMA to a specific temperature followed by cooling down naturally to ambient temperature). This contribution aims to study the feasibility of strengthening glass elements with adhesively bonded Fe-SMA strips. It focuses on the bond behaviour of glass-to-Fe-SMA lap-shear joints based on both experimental and numerical investigations. The effective bond length was identified, the effect of adhesive thickness, Fe-SMA strip thickness and bond length on the structural behavior of glass to Fe-SMA lap-shear joints were evaluated.

[1] Wang, W, et. al., Eng. Fract. Mech. 244 (2021).

[2] Deng, Z, et. al., Challenging Glass 8, submitted

[3] Silvestru, V.A, et. al., Glass Struct. Eng. (2022), in press



34. Ultrasound-Driven Particle Manipulation Inspired by Starfish-Larva

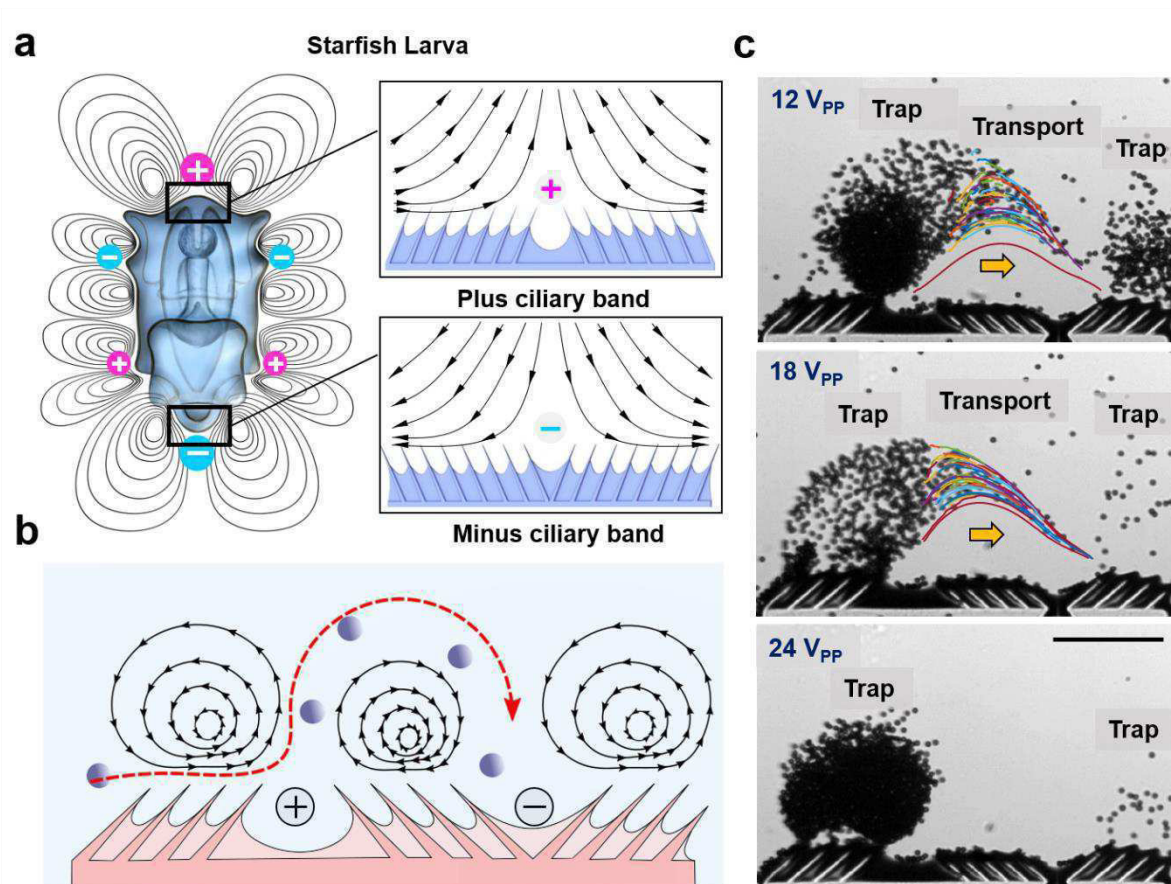
Cornel Dillinger[1], Nitesh Nama[2] and Daniel Ahmed[1]

[1] *Acoustic Robotics for Life Science and Healthcare, D-MAVT, ETH Zurich*

[2] *Nama Lab, Mechanical Engineering, University of Nebraska-Lincoln*

Biomimetic artificial cilia have become attractive since they can effectively address various functional tasks in the viscosity-dominated microfluidic domain. Artificial cilia enable microfluidic pumps, particle transport and trapping, fluid mixing, and sensing capabilities like their biological counterpart. Here, we introduce an ultrasound-driven microparticle trapping and transport strategy inspired by the feeding mechanism of starfish larvae [1]. Our system leverages nonlinear acoustics at microscales to drive bulk fluid motion via acoustically actuated small-amplitude oscillations of synthetic cilia [2]. Briefly, this mechanism is characterized by the juxtaposition of reversely arranged polymeric ciliary arrays, generating a flow field that facilitates the trapping and transport of particles along the ciliated surface. Ciliary arrays angled toward each other (/// \\) push fluid away, analogous to a source. In contrast, when cilia are angled away from each other (\\ \\ ///), fluid is forced in toward the band (analogous to a sink). We envision the combination of such ciliary bands to enable custom-engineered microfluidic flow fields that allow, not only for trapping and transport, but for various lab-on-a-chip and healthcare applications.

[1] W. Gilpin, et al., Nature Phys. 13, 380–386 (2017)
 [2] N. Nama, et al., Lab on a Chip 14.15 (2014).



Starfish larva-inspired ultrasound ciliary band designs. **a**. A starfish larva exhibits a complex flow profile of counter-rotating vortices generated by series of + and – ciliary bands arranged on its body protuberances. **b**. Schematic of a bioinspired trapping and transport mechanism consisting of a + ciliary band adjacent to a – ciliary band. **c**. Acoustic power-dependent transport and trapping of 10 μm particles with maximum transport efficiencies at 12 and 18 V_{PP} . At 24 V_{PP} the trapping mode became dominant. Scale bar, 200 μm .

35. Microfluidic Hollow Fiber Model to Visualize and Quantify Bacterial Response to Dynamic Drug Treatments

Friederike-Leonie Born and Petra S. Dittrich

Bioanalytics, D-BSSE, ETH Zurich

Heterogeneity of bacterial populations is considered an important factor in developing antibiotic resistance and persistence. Static assays, routinely used in clinics to identify potential resistance, do not sufficiently address the intercellular heterogeneity. Moreover, mimicking *in vivo* conditions, where bacterial cells are temporarily exposed to different antibiotic concentrations is only possible with dynamic models. The available dynamic *in vitro* models, e.g., the Hollow Fiber Infection Model (HFIM), require vast amounts of drugs and cells per experiment. Further, the drug effects are evaluated after the invasive sampling and only represent a finite moment in time. Inspired by the HFIM, we developed a dynamic, microfluidic *in vitro* model to investigate the antibiotic treatment effects over time, with single-cell resolution, requiring only a fraction of volumes necessary for the HFIM. To simulate the bacterial culture in tissue like environments (without shear stress) the bacterial cells are confined in fibrin hydrogel. In the model the bacterial cells are gradually exposed to antibiotic drugs with a pump ratio-based gradient generator and monitored using time-lapse microscopy for up to 15 hours. The developed model is characterized using *Escherichia coli* ATCC 25922, exposed to single drugs and drug combinations (Doxycycline, Amoxicillin). Preliminary results generated using different concentrations of Amoxicillin indicate that cells gradually exposed to an antibiotic drug show a reduced mortality rate and

a different regrowth behavior, but greater morphological changes than cells constantly exposed to the same drug. In the future, we will further focus on comparing constant versus gradient shaped dosing and we will extend our study to clinically relevant pathogen.

36. Cryosuction Induced Freezing Damage

Dominic Gerber, Eric R. Dufresne and Robert W. Style

Soft and Living Materials, D-MATL, ETH Zurich

Confidential

37. The Role of Matrix Viscoelasticity in 3D Osteocyte Morphogenesis

Margherita Bernero, Ralph Müller and Xiao-Hua Qin

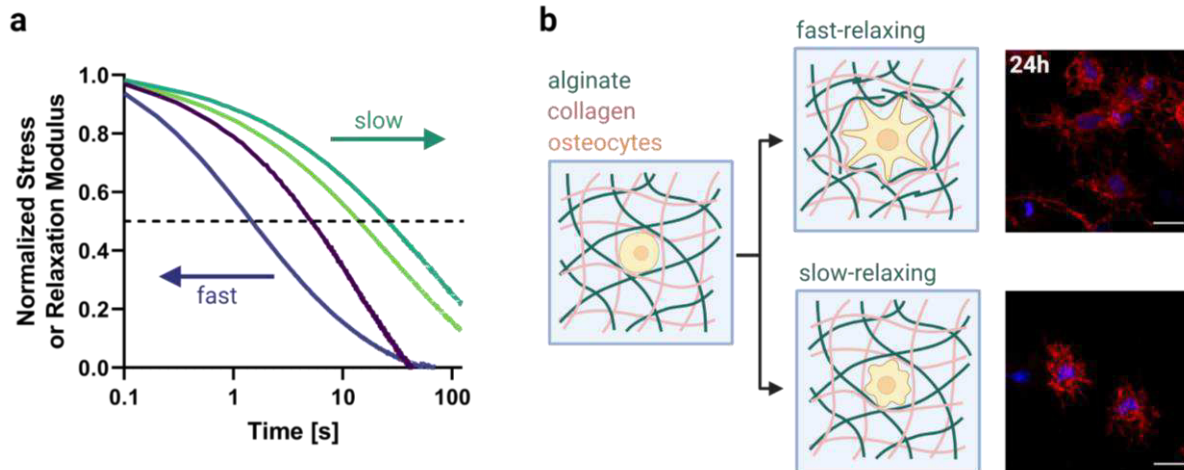
Bone Biomechanics, D-HEST, ETH Zurich

During bone formation, osteocytes are embedded in the osteoid and form an extensive 3D dendritic network within the mineralizing bone matrix. This location has made the study of their biology *in vivo* challenging. Despite immense efforts, a functional 3D interconnected osteocyte network has not been achieved *in vitro* so far.¹ Since the native osteoid tissue is a viscoelastic material that exhibits stress-relaxation properties,² we set out to investigate the role of this property in 3D osteocyte morphogenesis *in vitro*.

Here, we report a new 3D culture of osteocyte-like IDG-SW3 cells embedded in soft alginate-collagen hydrogels with varying stress-relaxation times ($t_{1/2}$, 1.5-14.4s) but comparable stiffnesses (4.4-4.7 kPa). Collagen was included to promote adhesion and cell-matrix remodeling. Cells remained highly viable following 7 days of embedding. After 24h, the fast-relaxing gels showed the largest cell area and longest dendrites. However, a significantly larger increase of osteogenic markers as well as intercellular connections via gap junctions were seen in slower-relaxing hydrogels after two weeks. These findings may further advance the development of 3D *in vivo*-like osteocyte models to better understand bone mechanobiology.

[1] Zhang et al., *Curr Osteoporos Rep* 17, 207-216 (2019).

[2] Chaudhuri et al., *Nature* 584, 535-546 (2020).



a Hydrogel compositions of varying stress-relaxation speeds were developed, and their mechanical properties determined by unconfined compression testing.

b Left: Schematic of the spreading osteocyte cells embedded in fast- and slow-relaxing alginate-collagen hydrogels. Right: Fluorescence microscopy images of actin (red) and nuclei (blue) stained IDG-SW3 osteocytes embedded in hydrogels of varying stress-relaxation speeds after 24h of culture in 3D. Scale bars = 20 μ m.

38. Thermal Instability of Ag/a-Si Planar Hyperbolic Metamaterials

Jose L. Ocana-Pujol[1], Lea Forster[2], Henning Galinski[1] and Ralph Spolenak[1]

[1] *Nanometallurgy, D-MATL, ETH Zurich*

[2] *Multifunctional Ferroic Materials, D-MATL, ETH Zurich*

Hyperbolic Metamaterials (HMMs) are structured optical nanomaterials that exhibit, due to their intrinsic anisotropy, optical topological transitions (OTTs)[1], leading to exceptional optical behaviour such as an unbounded density of optical states or to super collimation. This has been demonstrated in applications like improved efficiency in solar energy, which require high-temperature stability.

In recent years, there has been a growing interest in the stability of multilayered HMMs under high-temperature conditions. However, most of these studies have focused on refractory metal-dielectric pairs with applications in the near-IR, while the stability of the metal-semiconductor HMMs showing OTTs in the visible has gathered little attention. In our work, we examine the evolution of Ag-Si layered HMMs as function of thermal treatments. Silver was chosen over other commonly used metals in plasmonics (eg. Au or Al) because thermodynamic considerations point out at higher thermal stability. The samples were produced by magnetron sputtering and annealed in ultra-high vacuum at temperatures ranging from 200 to 800C. The optical characterization involved Reflectometry measurements with polarized and unpolarized light and was assisted by transfer matrix calculations and finite element modelling. The structural and chemical characterization was carried out by FIB-SEM, XRD and RBS.

We demonstrate that thermal annealing of the HMM induces a multilayer instability. In a first regime, the expected HMM behaviour is observed, with broadband low reflectivity in agreement with our calculations. This optical regime persists even at 300C and although structural degradation can already be measured at that temperature. This initial degradation can be understood as enhanced roughness, and the measured lower reflectance is in agreement with previous numerical studies [3]. At higher temperatures, a second regime involving an order-disorder transition is found. Silver agglomerates inducing phase separation, and optically the system becomes an effective reflector. Finally, in the third regime, the Ag-to-Si ratio starts changing due to silver evaporation. We examine the different regimes of the multilayer instability and the different phenomena that may influence it.

Furthermore, we show that changing the stacking order in unit cell of the HMM directly impacts the onset and pathway of the instability, as well as the transition to the third regime. This behaviour has been found to hold for systems that differ in the bilayer thickness, composition and number of stacked layers, opening the door to enhance the stability of HMMs for applications in harsh environments.

[1] Krishnamoorthy et al. *Science* 336, 205–209 (2012).

[2] Baranov et al. *Nat. Mater.* 18, 920–930 (2019).

[3] Andryieuski et al. *Opt. Express*, OE 22, 14975–14980 (2014).

39. 3D Printing of Autonomous Self-Healing Elastomers for Soft Robotics

Stefano Menasce, Rafael Libanori, Fergal Coulter and André R. Studart

Complex Materials, D-MATL, ETH Zurich

Confidential

40. Understanding the Stick-Slip Governed Failure of Topologically Interlocked Structures

Ioannis Koureas, Mohit Pundir, Shai Feldfogel and David S. Kammer

Computational Mechanics of Building Materials, D-BAUG, ETH Zurich

Confidential

41. Digital Light Processing 3D Printing of Biodegradable Elastomers for Biomedical Applications

Yulia Yuts and Jean-Christophe Leroux

Drug Formulation and Delivery, D-CHAB, ETH Zurich

Three-dimensional (3D) printing via vat photopolymerization is a high resolution technology that enabled to achieve unprecedented results with regards to soft robotics, tissue engineering and implants.¹⁻³ To date, only a few commercial inks for digital light processing (DLP) 3D printing can produce elastic structures with good biocompatibility and biodegradability at the same time.⁴⁻⁶ We have overcome this challenge by developing pH-sensitive resins based on photocrosslinkable poly(β -aminoesters). A library of linear diacrylates was synthesized *via* aza-Michael addition and combined with *N*-vinyl pyrrolidone (NVP) to 3D print objects with heat-assisted DLP 3D printer. We obtained soft objects with tunable elongation at break (56-762%), stress at failure (0.2-8.3 MPa) and degradation rate at pH 7.4 that varied from minutes to months. For selected materials, when changing the pH to 6.8 the hydrolysis rate was significantly increased. The strongest 3D printed elastomer exhibited stress at break of 8.3 ± 1.1 MPa and maximum elongation of $762 \pm 65\%$. Its nonlinear stress-strain curve resembles rubberlike materials with strain hardening effect upon deformation. It degraded in 9.5 hours at 37 °C and was cytocompatible with Caco-2 cell line. These results demonstrate the potential of a new class of 3D-printable elastic biomaterials with controllable mechanical properties and degradation rate.

[1] Karakurt, I., et al. *Curr. Opin. Chem. Eng.* 28, 134–143 (2020).

[2] Ligon, S. C., et al. *Chem. Rev.* 117, 10212–10290 (2017).

[3] Rus, D., et al. *Nature* 521, 467–475 (2015).

[4] Bao, Y., et al. *Adv. Funct. Mater.* 2109864, (2022).

[5] Paunović, N. et al. *Sci. Adv.* 7, 1–13 (2021).

[6] Gil, N. et al. *Angew. Chemie* 202117700, (2022).

[7] Chen, J. Y. et al. *Polymers.* 10, 1263 (2018).

42. Supramolecular Interactions in the Design of Polymer–Nanoparticle Hydrogels

Stéphane Bernhard, Giovanni Bovone, Elia A. Guzzi, Marco Müller, Nika Petelinsek, Wenqing Guo and Mark W. Tibbitt

Macromolecular Engineering, D-MAVT, ETH Zurich

Injectable hydrogels are increasingly used in the biomedical field for their shear-thinning and self-healing properties. Polymer–nanoparticle (PNP) hydrogels are a class of injectable nanocomposites based on physical interactions between polymers and nanoparticles (NP). (1) Such hydrogels have been used as drug delivery platforms or bioinks for additive manufacturing. (2-3) Current design of PNP hydrogels is mainly based on hydrophobic polymer–nanoparticle interactions. Improved design of PNP hydrogels would be enabled by engineered supramolecular interactions of the constituents, enabling tailored rheological properties for biomedical application.

In this work three supramolecular motifs were used for the design of PNP systems. In a first design, alpha-cyclodextrin (α CD) was added to cellulose and PEG-*b*-PLA PNP hydrogels to enhance the mechanical properties via polypseudorotaxane formation. The rheological behavior of the material was controlled by α CD concentration. This approach enabled the modular design of PNP hydrogels from a variety of polymers and PEGylated NPs. Secondly, hyaluronic acid (HA) was functionalized with beta-cyclodextrin (β CD) and combined with adamantane functionalized PEG-*b*-PLA NPs to induce formation of β CD–adamantane host–guest complexes. PNP hydrogels with varying host:guest ratios were prepared. Gel formation was limited to specific ratios of host to guest. Finally, Histidine functionalized PEG-*b*-PLA nanoparticles were employed in the presence of metal salt and HPMC for the formation of metal–ligand-based PNP hydrogels. Here, hydrogel formation was driven by the formation of host–guest complexes. PNP hydrogels with varying host:guest ratios were prepared. Gel formation was limited to specific ratios of host to guest.

The designed hydrogels were employed as model systems to investigate the relationship between interactions of the building blocks, notably NP–NP and polymer–NP interactions, and the rheological behavior of the materials.

[1] E. Appel, M. W. Tibbitt et al. (2015) Nature Communications, 6:6295.
[2] G. Bovone, G. Guzzi, S. Bernhard et al. (2021) Advanced Materials, 2106941.

43. Spin-orbit Torque Switching of Elliptical Three-Terminal Magnetic Tunnel Junctions

Marco Hoffmann[1], Viola Krizakova[1], Giacomo Sala[1], Kevin Garello[2], Sebastien Couet[2] and Pietro Gambardella[1]

[1] *Magnetism and Interface Physics, D-MATL, ETH Zurich;*

[2] *imec, Kapledreef 75, 3001 Leuven, Belgium*

Confidential

44. Insights in Dense Suspensions by Visualizing Silica Particles with Tunable Surfaces

Vincent Niggel and Lucio Isa

Soft Materials and Interfaces, D-MATL, ETH Zurich

In complex particulate flows, the surfaces of flowing particles undergo both relative translation and rotation. While measuring the (relative) displacements of colloids is quite common, the measurement of their rotation is much less frequent. However, such information is quite important to provide a more complete picture of the details of interparticle contacts under flow or to investigate if rotational and translational degrees of freedom exhibit different dependencies on volume fraction when suspensions approach the glass transition. In our work, we have explored different synthesis paths to create several types of fluorescent silica colloids with tunable roughness and heterogeneous fluorescence, which allow us to track their individual motion (translation or rotation) in dense suspensions. Moreover, we have developed a method that enables us to track the 3D rotation of our particles based on 2D images in a fixed plane, greatly simplifying the acquisition of high-frame-rate videos. Finally, our goal is to image sheared dense suspensions, i.e. with a confocal microscopy in proximity of the zero-velocity plane of a counter-rotating shear cell, in order to directly characterize the interactions between the particles under flow conditions.

45. Thermo-Responsive Nanocellulose Hydrogels as a Universal Drug Release Platform

Qiyao Sun[1], Garam Han[1], Gilberto Siqueira[2], Luca Müller[2], Pascal Bertsch[3] and Peter Fischer[1]

[1] *Food Process Engineering, D-HEST, ETH Zurich*

[2] *Cellulose and Wood Materials Laboratory, Empa*

[3] *Radboud University Medical Center, Department of Dentistry-Regenerative Biomaterials, Radboud Institute for Molecular Life Sciences.*

Hydrogels are a particularly appealing type of drug delivery system and have been used in many branches of medicines and tissues. The mechanical property is the key to its ability to maintain the structure and avoid fracture during use and after placing *in vivo*. To fulfill the requirements for various applications, a toolbox of biocompatible thermoresponsive hydrogel with tunable mechanical strength is established, from a liquid injectable hydrogel to a solid hydrogel. Thermo-responsive polymer PNIPAM (Poly(N-isopropylacrylamide)) was cross-linked at different degrees and reinforced by cellulose nanocrystals (CNCs) and cellulose nanofibrils (CNFs) to obtain different mechanical properties. Model therapeutic agents with different physicochemical properties were explored for *in-vitro* locally targeted sustained drug release in the liquid injectable hydrogel. The different release patterns are attributed to drug size, hydrophilicity and specific drug-cellulose interactions. Antimicrobial agents were included in solid form hydrogels for the purpose of a wound dressing patch. Interactions between the hydrogel and antimicrobial agents were thoroughly studied to obtain stable complex. Broad-spectrum anti-microbial activity is confirmed against Gram-negative and Gram-positive bacteria as well as fungus. This work

expands the application of cellulose in the biomedical field by enabling well-defined hybrid biomaterials with control over hydrogel mechanical property and drug release behavior.

[1] Li, J et al., Nature Reviews Materials, 1(12), 1-17.

[2] Bertsch, P et al., ACS applied materials & interfaces, 11(42), 38578-38585.

[3] Weishaupt, R et al., ACS applied materials & interfaces, 10(23), 20170-20181.



46. Impact of Oxygen Vacancies on Improper Ferroelectricity at YMnO_3 Thin Film Interfaces

Alexander Vogel[1,2], Alicia Ruiz Caridad[1], Morgan Trassin[2] and Marta D. Rossell[1]

[1] Electron Microscopy Center, Advanced Materials & Surfaces, Empa

[2] Multifunctional Ferroic Materials, D-MATL, ETH Zurich

Confidential

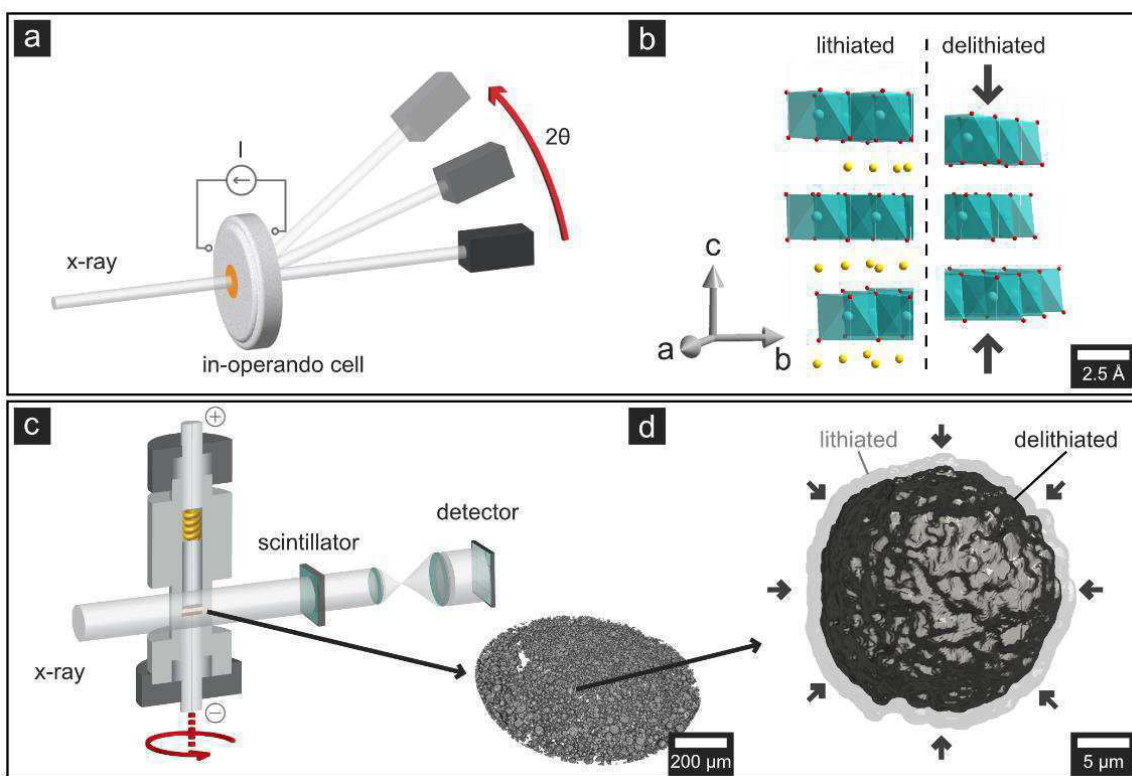
47. Operando X-Ray Diffraction and Tomography to Track Morphological Changes in $\text{LiNi}_{0.8}\text{Mn}_{0.1}\text{Co}_{0.1}\text{O}_2$ (NMC 811) Cathode Particles

Nils Wenzler[1], Federica Marone[2], Marco Stampanoni[2] and Vanessa Wood[1]

[1] Materials and Device Engineering, D-ITET, ETH Zurich

[2] X-Ray Tomography Group, PSI

High nickel content $\text{Li}(\text{Ni},\text{Mn},\text{Co})\text{O}_2$ cathode materials allow energy density to be increased while reducing the use of cobalt. However, these materials often have lifetime issues, which are partly due to mechanical changes in the material that occur during cycling, particularly during deep delithiation (i.e., high voltage operation). Direct observation of these morphological changes is challenging. Here, we demonstrate that it is possible to gain quantitative insight into the morphological changes occurring during cycling and their electrochemical origins by comparing the volume change of the unit cells measured using operando XRD to the volume change of the secondary particle measured using operando x-ray tomography. Specifically, we show that while the primary particles reversibly expand and contract, the secondary particles do not reversibly contract following the expansion of the primary particles along the c-axis.



We studied the volume dynamics of NMC811 cathodes during the first cycle on two different Length scales. Using in-operando x-ray diffraction spectroscopy (a) we measured the dynamics of the lattice (b) and used this to calculate the evolution of the unit cell volume. High resolution in-operando x-ray tomography (c) allowed us to track the volume dynamics of individual secondary particles, which consist of densely packed primary particles (d). Comparing the two we found that the secondary particle likely undergoes morphological changes and that its volume evolution is a complicated function of the crystal lattice change and mechanical interactions of the primary particles.

48. Interfaces of Oxides with Different Magneto-Electric Responses

Xanthe H. Verbeek, Mayan Si and Nicola A. Spaldin

Materials Theory, D-MATL, ETH Zurich

Confidential

49. Synthesis of Morphology Controlled Cesium Hafnium Halide Double Perovskites and Lutetium Hydroxy Halide Luminescent Nano and Micro-Particles

Madeleine Fellner and Alessandro Lauria

Multifunctional Materials, D-MATL, ETH Zurich

Luminescent particles can be applied in many areas such as lighting, display, or scintillator technologies, provided their efficiency is sufficiently high. Here, we present our efforts to expand the synthetic toolbox towards high density caesium hafnium halide double perovskites and lutetium hydroxy chlorides. For generating Cs_2HfF_6 (CHF), Cs_2HfCl_6 (CHC), and $\text{Lu}(\text{OH})_2\text{Cl}$ (LHC) particles, three different synthetic approaches were chosen: a heating-up synthesis in high boiling organic solvents, an emulsion synthesis, and a microwave assisted solvothermal synthesis, respectively. A heating-up approach was suitable to generate CHF nanocrystals [1]. The obtained nanopowder shows no intrinsic, visible band to band recombination due to its large bandgap of Cs_2HfF_6 . However, a defect-related emission is observed in CHF particles, which is enhanced by incorporating dopants such as Mn(II) and Eu(III) ions. Secondly, Cs_2HfCl_6 is an intrinsically fluorescent and radioluminescent material. A water in oil microemulsion synthesis was chosen to generate CHC with sizes scaled down to the microscale [1]. The microparticles produced by this method show the same absorption and emission profiles as reported bulk samples [2]. Lastly, $\text{Lu}(\text{OH})_2\text{Cl}$ microparticles were obtained *via* a microwave assisted

solvothermal synthesis with sizes ranging from 200 nm to 10 μm depending on the parameters chosen. Eu-doped samples show typical europium emission profiles [3]. All products were analysed by X-ray diffraction (XRD), scanning electron microscopy (SEM) and photoluminescence spectroscopy (PL). We discuss how various high-density materials can be obtained as nano- or micropowders using a range of synthetic techniques. Based on these results, the appropriate synthetic route can be selected to ensure suitable properties like luminescence, dispersibility, morphology, or size, depending on specific applications.

[1] M. Fellner, A. Lauria, *J. Mater. Chem. C*, 10, 4383-4392, (2022).

[2] R. Král, *et. al.*, *J. Phys. Chem. C*, 121, 12375–12382, (2017).

[3] M. Fellner, A. Soppelsa and A. Lauria, *Crystals*, 11, 992, (2021).

50. Additively Manufactured Nano-Porous Micro-Scale Ag Structures for SERS Sensing

Nikolaus Porenta and Ralph Spolenak

Nanometallurgy, D-MATL, ETH Zurich

Most current SERS active substrates rely on wet-chemical syntheses of nanoparticles or classical thin film production such as physical vapour deposition, often combined with pre-patterned substrates or post-deposition annealing. Both these techniques have drawbacks, e.g. use of toxic chemicals or limited geometrical freedom. To circumvent these issues, additive manufacturing of sub-micron scale SERS active substrate has received more interest in recent years [1].

One AM technique able to fabricate 3D metal structures with sub-micron feature sizes is EHD-RP [2]. This AM technique enables the production of high quality metallic structures with precise geometrical control and feature sizes of 100nm. It furthermore enables the fabrication of multiple different metals, as well as alloys. In this contribution we would like to present how we utilised the precise geometrical and chemical control of EHD-RP to produce SERS active micron-scale substrates. Using metal salt solutions with different ratios of silver to a less noble metal and subsequent selective dealloying of the less noble metal, we were able to produce micron-sized three dimensional silver structures with controlled nano-porosity. Different geometric structures and arrays, such as pillars, walls and pads were fabricated and tested for their SERS activity. To this end, differently concentrated rhodamine6G solutions in ethanol were dropcast onto the substrates and dried before Raman measurements were conducted. To further show the plasmonic activity of our substrates 4-NBT was used as a probe molecule. 4-NBT has been shown to undergo plasmonically catalysed dimerisation to DMAB. Measuring a sequence of multiple Raman spectra in short time intervals the progress of the dimerisation reaction could be monitored. With these findings we want to show that, using EHD-RP as a high chemical control AM technique, enabled the production of micron-scale SERS active structures.

[1] *Opt. Mater. Express* **2016**, 6, 1587–1593

[2] *Nat. Commun.* **2019**, 10, 1853

51. Multiscale Modelling of Size Effects in the Fracture of Soft Solids

Tianchi Li[1], Stefanie Heyden[1], Martin Kröger[2] and Eric R. Dufresne[1]

[1] Soft and Living Materials, D-MATL, ETH Zurich

[2] Polymer Physics, D-MATL, ETH Zurich

Confidential

52. Synthesis of Metal-Organic Chalcogenide Semiconductor Nanoparticles

Alexander C. Hernandez Oendra, Maximilian A. Aspect, Julia L. Jaeggi, Carin R. Lightner, Andrew B. Pun and David J. Norris

Optical Materials Engineering, D-MAVT, ETH Zurich

Metal-organic chalcogenide (MOC) particles are an emerging class of crystalline materials. In particular, silver benzeneselenolate, with the chemical formula $[\text{AgSePh}]_{\infty}$, which forms a two-dimensional

multiple-quantum-well structure, has sparked interest recently.^{1,2} The layered system exhibits strong quantum confinement with properties similar to two-dimensional materials like transition metal dichalcogenides or layered perovskites, while still exhibiting high material stability under ambient conditions.³ This makes silver benzeneselenolate a suitable candidate for applications such as excitonic lasers or light-emitting diodes. To facilitate the integration of MOCs into such optoelectronic device architectures, a need exists for simple and efficient fabrication methods.

Here, we present a method to synthesize silver benzeneselenolate crystals.⁴ The method is broadly tunable, and we can synthesize crystals with lateral sizes ranging from tens of micrometers to < 50 nm. These smallest particles are colloidally stable in polar solutions. The modularity of the material system also allows the fabrication of different variants of MOCHAs, with different chalcogenides and organic ligands.

Based on these demonstrations, we envision that our novel fabrication approach can also enable the fabrication of new semiconductor materials and facilitate their incorporation into optoelectronic devices.

[1] E. Schriber, et. al., ACS Appl. Nano Mater. 1, 3498–3508 (2018).

[2] B. Trang, et. al., J. Am. Chem. Soc. 140, 13892-13903 (2018).

[3] K. Yao, et. al., ACS Nano 15, 4085-4092 (2021).

[4] A. C. Hernandez Oendra, et. al., in preparation.

53. Poly(ϵ -caprolactone)/Zein Blends Increase Bovine Chondrocytes Cytocompatibility

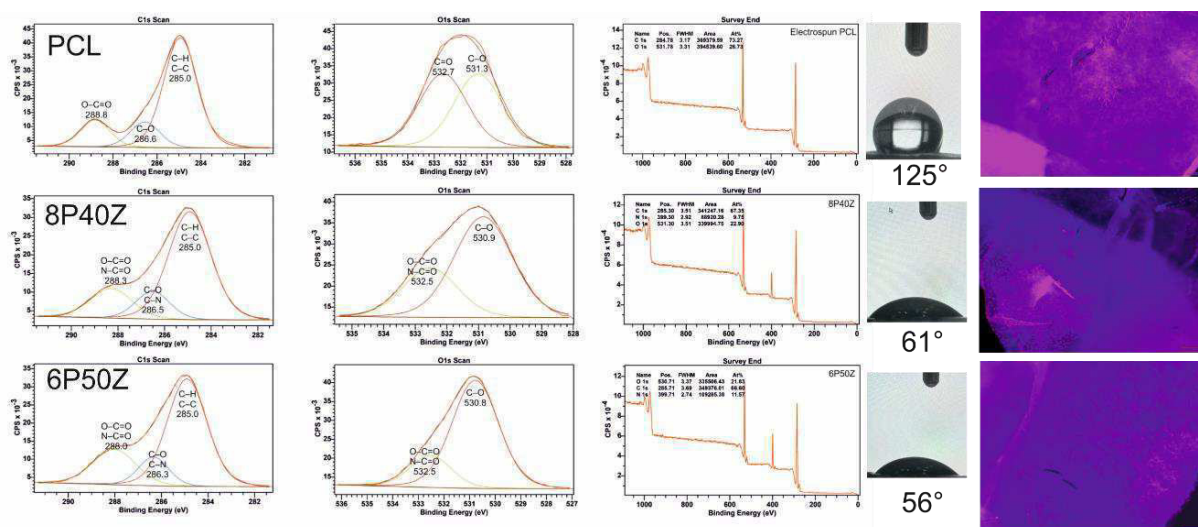
Andre Mathias Souza Plath[1], Helen Greuter[1], Daniel Abbott[2], Minghan Hu[3], Victor Mougel[2], Lucio Isa[3] and Stephen J. Ferguson[1]

[1] Institute for Biomechanics, D-HEST, ETH Zurich

[2] Bioinspired Molecules and Materials, D-CHAB, ETH Zurich

[3] Soft Materials and Interfaces, D-MATL, ETH Zurich

Osteoarthritis (OA) is a debilitating global disease with limited treatment options. Matrix-assisted chondrocyte implantation (MACI) delivers progenitor or primary cells and restores tissue homeostasis delaying the need for a metal prosthesis. This work aimed to investigate electrospun membranes based on PCL-blends as MACI alternatives to treat OA. For this, poly(caprolactone) (PCL) blends were electrospun. We optimized nanofibers for the smallest diameter. We studied surface chemistry using X-ray photoelectron spectroscopy (XPS) and static water contact angles. Bovine chondrocytes were cultured on the surfaces for up to 14 days. The XPS results show significant surface chemistry changes in the blends compared to pure PCL. The charged groups from the protein increased surface charges and interactions with water. In all groups, cells were confluent at day 14 and 5000 cell/cm² density. However, the cell cultures show an increase in f-actin polymerization in the zein blends. These results showcase the potential of PCL-zein blends for MACI applications in cartilage tissue engineering.



54. Transformer-Induced Metamorphosis of Polymeric Nanoparticle Shape at Room Temperature

Kostas Parkatzidis, Nghia P. Truong and Athina Anastasaki

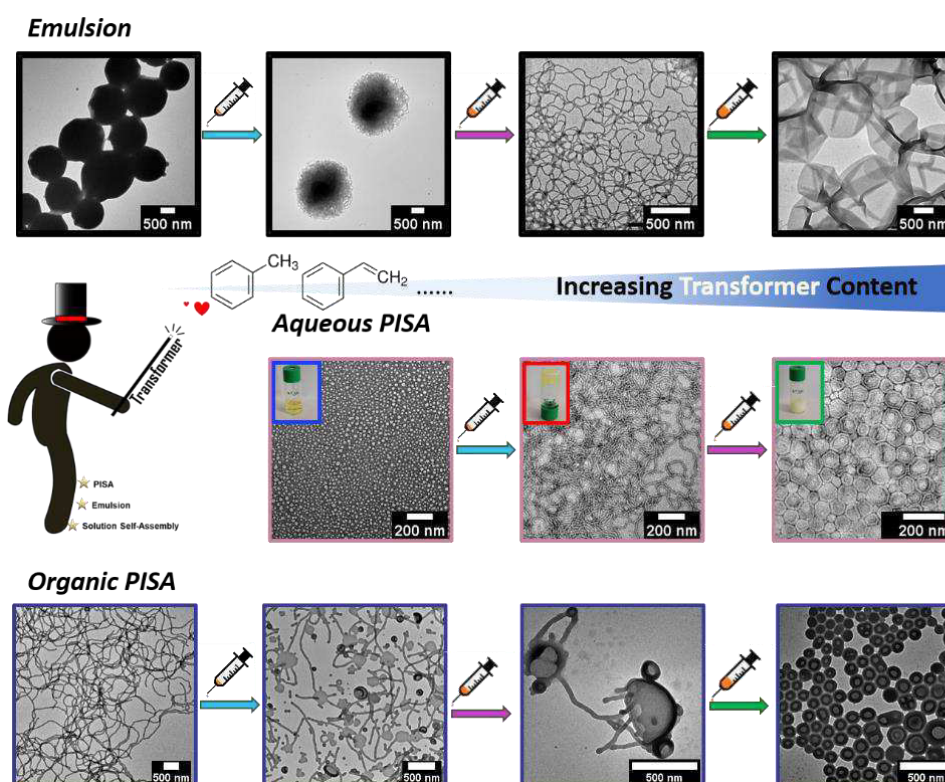
Polymeric Materials, D-MATL, ETH Zurich

Controlled polymerizations have enabled the synthesis of a wide range of amphiphilic block copolymers which can form nanostructured materials with different shapes exhibiting distinct properties and performance.¹ Despite the importance of shape, current strategies that allow for the efficient morphological transformation are limited in polymer scope, often alter the chemical structure, operate at high temperatures, and can be fairly tedious and time-consuming. Herein we present a rapid and versatile morphological transformation strategy which operates at ambient temperature and without impairing the chemical structure of the resulting morphologies. By simply adding a small amount of a molecular transformer (i.e. small organic molecule) in an aqueous solution of polymeric nanoparticles, a rapid evolution to the next high-ordered morphology was observed within seconds, yielding a range of nanoparticles morphology from the same starting material. Significantly, this approach can be applied to nanoparticles produced by disparate block copolymers (i.e. with different cores and corona) obtained by various synthesis techniques, including emulsion polymerization, polymerization-induced self-assembly and traditional solution self-assembly.^{2,3}

[1] K. Parkatzidis, H. S. Wang, N. P. Truong and A. Anastasaki, *Chem*, **2020**, 6, 1575–1588.

[2] M. Rolland, N. P. Truong, K. Parkatzidis, E. H. Pilkington, A. L. Torzynski, R. W. Style, E. R. Dufresne, and Athina Anastasaki, *JACS Au*, **2021**, 1, 11, 1975–1986.

[3] K. Parkatzidis, N. P. Truong, M. Rolland, V. Lutz-Bueno, E. H. Pilkington, R. Mezzenga and A. Anastasaki, *Angew. Chem. Int. Ed.*, **2022**, e202113424.



Transformer-Induced Metamorphosis of Polymeric Nanoparticle Shape at Room Temperature: application in nanoparticles obtained via emulsion polymerization, aqueous PISA and organic PISA

55. No Yield Stress “Yield-Stress” Material

Gabriele Pagani, Theo Tervoort and Jan Vermant

Soft Materials, D-MATL, ETH Zurich

Confidential

56. Micro-Scale Volumetric 3D Printing

Prajwal Agrawal, Dimitar Boev and Daniel Ahmed

Acoustic Robotics for Life Science and Healthcare, D-MAVT, ETH Zurich

Confidential

57. Consistent Damage Transformation for Multiscale Simulations

Philip P. Müller[1], Falk K. Wittel[2] and David S. Kammer[1]

[1] Computational Mechanics of Building Materials, D-BAUG, ETH Zurich

[2] Complex Systems and Materials, D-BAUG, ETH Zurich

The fracture process of heterogeneous microstructured materials, such as concrete, is strongly influenced by its microstructure. However, to accurately simulate the fracture process of such materials full-scale simulations are needed. Domain decomposition methods, a family of multiscale methods, split the computational domain into disjoint regions. Inside each region a different computational method can be applied. For instances in a region where fracture will appear, a high resolution method can be used. The different regions are then coupled together at their junctions, resulting in one large system. This allows to lower the overall computational burden, since full-scale resolution is only used where it is needed. In case the decomposition is not known in advance, adaptive schemes, which allow to dynamically refine certain regions on demand, have been proposed. Their main challenge is, that the refined domain has to be initialised. Since, the coarse representation, that was previously active, has already accumulated damage, its mechanical behaviour will be different from its undamaged state. Instead, damage has to be artificially introduced into the fine representation, and matches the damage from the coarse representation. Here, we propose a method for initialising these fine scale representations. The proposed method employs FEM for the coarse and a network composed of Bernoulli beams on the fine scale, the different regions will be coupled together through the Arlequin method. On the FEM level a continuum damage model (CDM) is employed to model the degradation of the material and to trigger the refinement operation, which will replace it with the discrete representation. These discrete representations, will be initialised based on the accumulated damage on the coarse level, which was monitored by the CDM, to match the degraded state of the continuum scale.

58. Studying the Front Propagation in Reactive Multilayers via MD Simulations: From Crystal Structure to Alloying

Fabian Schwarz and Ralph Spolenak

Nanometallurgy, D-MATL, ETH Zurich

Molecular Dynamics (MD) simulations can be used as a tool to study the front propagation in reactive multilayers. So far, key characteristics of reactive multilayers, such as the crystal structure of the layers or the existence of a premixed interlayer at the interface have not been considered in MD simulations of reactive multilayers. The poster will show the influence of the crystal structure [1] as well as the influence of a premixed interlayer [2] on the front propagation speed in Al-Ni reactive multilayers. Furthermore, the premixed interlayer can also be used as a tool to control the front propagation velocity. Finally, alloying with Al, Ni and Co is shown as an architecture independent approach to control the front propagation velocity.

[1] Fabian Schwarz and Ralph Spolenak, "Molecular dynamics study of the influence of microstructure on reaction front propagation in Al-Ni multilayers", Appl. Phys. Lett. 119, 133901 (2021)

[2] Fabian Schwarz and Ralph Spolenak, "The influence of premixed interlayers on the reaction propagation in Al-Ni multilayers —An MD approach", Journal of Applied Physics 131, 075107 (2022)

59. Ionic Transport and Current Density Simulations in Composite LLZO-PEO Electrolytes

Markus Wied[1], Anne Bonnin[2] and Vanessa Wood[1]

[1] *Materials and Device Engineering, D-ITET, ETH Zurich*

[2] *X-Ray Tomography Group, PSI*

All-solid-state-batteries (ASSBs) are needed as a next generation battery technology to increase the energy density and safety of battery electric vehicles. This is a major milestone to decarbonize our emissions. [1] In ASSBs the electrolyte that facilitates Lithium-ion transport can be made from ceramics, polymers or a composite of both. [2] Composite solid electrolytes (CSEs) aim at combining the high ionic conductivity and stability of ceramic materials with the flexibility and good interfacial contact of polymers. [2] Key performance factors are the ionic transport across the ceramic-polymer interface and the 3D current density distribution within the CSE. [3] Therefore, this study systematically evaluates and quantifies ionic transport by performing simulations on real 3D CSE structures obtained by x-ray tomography. [4] We fabricate LLZO-PEO CSEs of different LLZO particle size and loading. Within those structures, Lithium-ions encounter a different number of LLZO-PEO interfaces and different path lengths between crossings. We quantify the influence of the specific contact resistivity between LLZO and PEO and how it affects the contribution of each phase to the overall charge transport. Further, we show that this relation is temperature dependent and changes in a different manner for low LLZO particle densities and high LLZO particle densities. Also, our simulations visualize current density distributions and hot spots that could increase degradation. Overall, we are able to predict the relative importance of each phase in LLZO-PEO CSEs under different operation conditions. Additionally, we highlight the importance to minimize the specific contact resistivity to maximize material synergies for high conductivity and improved current density uniformity.

[1] K.J. Kim, et. al., *Adv. Energy Mater.* 11, 2002689 (2021)

[2] J. Popovic, et. al., *J.Mater. Chem. A.* 9, 6050 (2021)

[3] X.C. Chen, et. al., *ACS Energy Lett.* 4, 1080-1085 (2019)

[4] V.C. Wood, *Nat. Rev. Mater.* 3, 293-295 (2018)

60. Shape-Controlled Nanoparticles from a Low-Energy Nanoemulsion

Manon Rolland[1], Nghia P. Truong[1,2], Kostas Parkatzidis[1], Emily H. Pilkington[2], Alexandre L. Torzynski[3], Robert W. Style[3], Eric R. Dufresne[3] and Athina Anastasaki[1] *

[1] *Polymeric Materials, D-MATL, ETH Zürich*

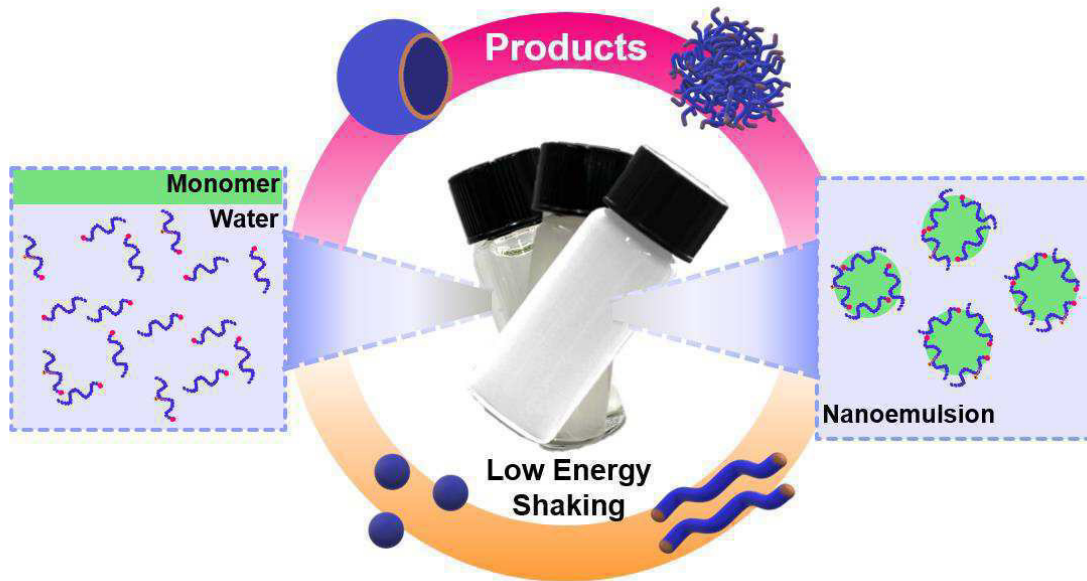
[2] *Monash Institute of Pharmaceutical Sciences, Monash University*

[3] *Soft and Living Materials, D-MATL, ETH Zürich*

Nanoemulsion technology enables the production of uniform nanoparticles for a wide range of applications. However, existing nanoemulsion strategies are limited to the production of spherical nanoparticles. Here, we describe a low-energy nanoemulsion method to produce nanoparticles with various morphologies. By selecting a macroRAFT agent (poly(di(ethylene glycol) ethyl ether methacrylate-co-N-(2-hydroxypropyl) methacrylamide) (P(DEGMA-co-HPMA))) that dramatically lowers the interfacial tension between monomer droplets and water, we can easily produce nanoemulsions at room temperature by manual shaking for a few seconds.[1] With the addition of a common ionic surfactant (SDS), these nanoscale droplets are robustly stabilized at both the formation and elevated temperatures. Upon polymerization, we produce well-defined block copolymers forming nanoparticles with a wide range of controlled morphologies, including spheres, worm balls, worms, and vesicles.[2] Our nanoemulsion polymerization is robust and well-controlled even without stirring or external deoxygenation. This method significantly expands the toolbox and availability of nanoemulsions and their tailor-made polymeric nanomaterials.

[1] M. Rolland, N.P. Truong, K. Parkatzidis, E.H. Pilkington, A.L. Torzynski, R.W. Style, E.R. Dufresne, A. Anastasaki, Shape-Controlled Nanoparticles from a Low-Energy Nanoemulsion, *JACS Au* 1(11) (2021) 1975-1986.

[2] K. Parkatzidis, N.P. Truong, M. Rolland, V. Lutz-Bueno, E.H. Pilkington, R. Mezzenga, A. Anastasaki, Transformer-Induced Metamorphosis of Polymeric Nanoparticle Shape at Room Temperature, *Angew. Chem. Int. Ed.* (2022) e202113424.



61. Printing on Particles: Combining Two-Photon Nanolithography and Capillary Assembly to Fabricate Multi-Material Microstructures

Steven van Kesteren*[1], Xueting Shen*[1], Michele Aldeghi[2] and Lucio Isa[1]

[1] *Soft Materials and Interfaces, D-MATL, ETH Zurich*

[2] *IBM Research, Zürich*

Increasing complex colloidal structures are being developed to be building blocks for new materials. Additive manufacturing at micron- and nanoscale have seen an increased use to suite the demand for more elaborate colloidal structures. However, the fabrication routes demonstrated in previous works has limitations in the choice of material and the fabrication of micron-scale composite structures remains as a challenge. Here, we combine the directed assembly of colloidal particles with sequential capillarity-assisted particle assembly (sCAPA) and two-photon direct laser writing (DLW). We use DLW fabricate the novel 3D micro-templates for the capillary assembly of differently-sized colloids. Furthermore, we use DLW to link well-defined arrangements of polystyrene or silica particles made with sCAPA. We demonstrate novel approaches to fabricating multi-material lines, waves, lattices and various shapes of micro-structures in large quantities. The patterned particles are selectively linked together in arbitrary shapes with a commercial photo-resist (IP-L or IP-PDMS) and dispersed in water. The flexibility of our method allows the combination and patterning of a wide range of materials enabling the fabrication of complex configurations on the sub-micron scale.

62. Ultrafast Volumetric Bioprinting of Perfusable 3D Bone Tissue Models

Doris Zauchner, Leana Bissig, Nicole Jucker, Wanwan Qiu, Margherita Bernero, Ralph Müller and Xiao-Hua Qin

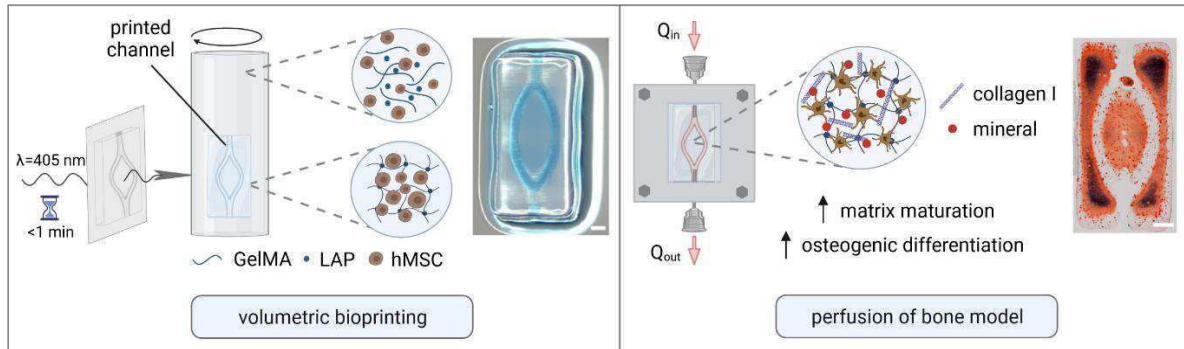
Bone Biomechanics, D-HEST, ETH Zurich

Volumetric bioprinting (VBP) is a novel technique that enables layerless photofabrication of cell-laden hydrogels within seconds. [1] We recently developed a soft bioresin of gelatin methacryloyl (GelMA) for VBP of in vitro bone models. [2] Yet, after 42 days of static culture, matrix mineralization was limited. Here, we leverage the advantages of VBP and dynamic culture to fabricate centimeter-scale bone models with enhanced functionality. This platform enables us to study the effect of perfusion on human mesenchymal stem cells and flow-enhanced matrix maturation. After optimization of GelMA bioresins, we integrate cell-laden hydrogel constructs with a custom-made millifluidic chip for dynamic perfusion culture.

After 3 weeks, more pronounced matrix mineralization is observed in the dynamic group compared to a static control while maintaining high cell viability. Immunostaining and qPCR assays evidence

increased secretion of collagen type I and enhanced expression of osteogenic protein markers in the dynamic group. Altogether, this work presents the first platform that combines VBP with dynamic cell culture for a physiologically relevant *in vitro* bone model, opening avenues for disease modeling without using animal models.

- [1] P. N. Bernal, et al., *Adv. Mater.*, 31, 42 (2019)
 [2] J. Gehlen, et al., *Acta Biomaterialia*, in press (2022)



Volumetric bioprinting of perfusable bone models from gelatin methacryloyl (GelMA), the photoinitiator LAP (lithium phenyl-2,4,6-trimethylbenzoylphosphine) and human mesenchymal stem cells. Perfusion of these bone models enhances matrix maturation and osteogenic differentiation after 21 days.

63.A Pseudo Flocculation Method for Poly-Dispersed Colloidal Systems

Yaqi Zhao and David S. Kammer

Computational Mechanics of Building Materials, D-BAUG, ETH Zurich

The very early stage of the cement hardening process is characterized by flocculation of cement particles, which eventually leads to a percolated particle-network providing initial stiffness to the cement paste. While flocculation has been widely studied, this is a particularly complex system. In fact, cement is highly polydisperse, where the size ratio of the largest particle to the smallest exceeds two orders of magnitude. This poses not only fundamental questions but also technical ones.

Modeling this flocculation process with a discrete-element approach is particularly challenging. A common approach consists of two steps. First, one creates a system with randomly distributed particles, and subsequently, it is solved for the flocculated equilibrium state. Solving this system, however, is far from trivial. If an explicit time-stepping approach is applied, the simulation becomes prohibitively long due to very small timesteps, which are required for such a highly poly-dispersed system. Nevertheless, using a static solver, is prone to fail as it requires initial conditions close to the equilibrium solution.

Here, we propose a geometric method that has the potential of overcoming these limitations for highly poly-dispersed colloidal systems. The key concept is to construct the system step-wise and to solve for the local potential energy minimum on small sub-systems. We will show that this approach leads to flocculated microstructures with statistically equivalent properties to those of fully equilibrated configurations, while being computationally considerably faster.

64. Probing Crystal Electric Field States in a Dense Kondo-Lattice Antiferromagnet Using Terahertz Time-Domain Spectroscopy

Chia-Jung Yang[1], Payel Shee[2], Arumugam Thamizhavel[3], Manfred Fiebig[1] and Shovon Pal[2]

[1] *Multifunctional Ferroic Materials, D-MATL, ETH Zurich*

[2] *TeraDynamics Group, School of Physical Sciences, National Institute of Science Education and Research, HBNI, Jatni, Odisha, India*

[3] *Crystal Growth Lab, Department of Condensed Matter Physics and Material Science, Tata Institute of Fundamental Research, Mumbai, India*

In some Ce-based intermetallic compounds, two interactions compete with each other – the Ruderman-Kittel-Kasuya-Yosida interaction and the Kondo interaction. This competition leads to numerous

interesting properties such as pressure-induced superconductivity in CeRh₂Si₂, non-Fermi-liquid state in CeCu_{6-x}Au_x system, etc. As most of these collective excitations lie within a few meV, terahertz (THz) light is a favorable tool to study the mechanisms behind these phenomena. In particular, THz time-domain spectroscopy (THz-TDS) has recently been used to study the dynamics of quasiparticles and the role of different temperature scales in the evolution of Fermi volume^[1-2] that were otherwise not accessible. In this contribution, we present our latest results on the investigation of crystal electric field (CEF) states of a dense Kondo-lattice antiferromagnet, CeAg₂Ge₂ (CAG).

CAG has been intensively studied by various techniques as antiferromagnets below $T_N = 4.6$ K or as Kondo material below Kondo temperature $T_K = 3$ K^[3-5]. However, there are no direct experimental observations for the CEF states. The complex behavior posed by the competing nature of the two temperature scales requires rather direct access to the CEF states that eventually dictates the microscopy of the Kondo spin-flip scattering processes. Here, we perform temperature-dependent THz-TDS measurements. We collect the reflected THz transients from a single crystal CAG facing perpendicular to the crystallographic c-axis. We then obtain the spectra by Fourier transforming the time transients. We find two CEF excitations at frequencies of 0.5 THz and 2.1 THz that display distinct temperature dependence. We note that our results differ from previous simulations based on the magnetic susceptibility and neutron diffraction measurements^[3,5]. Our result marks the direct experimental evidence of CEF states in such Kondo lattice antiferromagnets.

[1] S. Pal, et. al., Phys. Rev. Lett. 122, 096401 (2019).

[2] C.-J. Yang, et. al., Phys. Rev. Research 2, 033296 (2020).

[3] S. Banik, et. al., RSC Adv. 10, 24343 (2020).

[4] A. Thamizhavel, et. al, Phys. Rev. B 75, 144426 (2007).

[5] A. Loidl, et. al., Phys. Rev. B 46, 9341 (1992).

65. Tailoring PEEK Crystallinity for Hemocompatible, Durable, and Affordable Cardiovascular Devices

Mary Jialu Chen[1], Georgios A. Pappas[1], Daniele Massella[1], Arthur Schlothauer[1], Sarah Motta[2], Volkmar Falk[3,4,5], Nikola Cesarovic[3,4] and Paolo Ermanni[1]

[1] *Composite Materials and Adaptive Structures, D-MAVT, ETH Zurich*

[2] *Institute for Regenerative Medicine, University of Zürich*

[3] *Translational Cardiovascular Technologies, ETH Zurich*

[4] *Klinik für Herz-, Thorax- und Gefäßchirurgie, Deutsches Herzzentrum Berlin*

[5] *Klinik für Kardiovaskuläre Chirurgie, Charité Universitätsmedizin Berlin*

Confidential

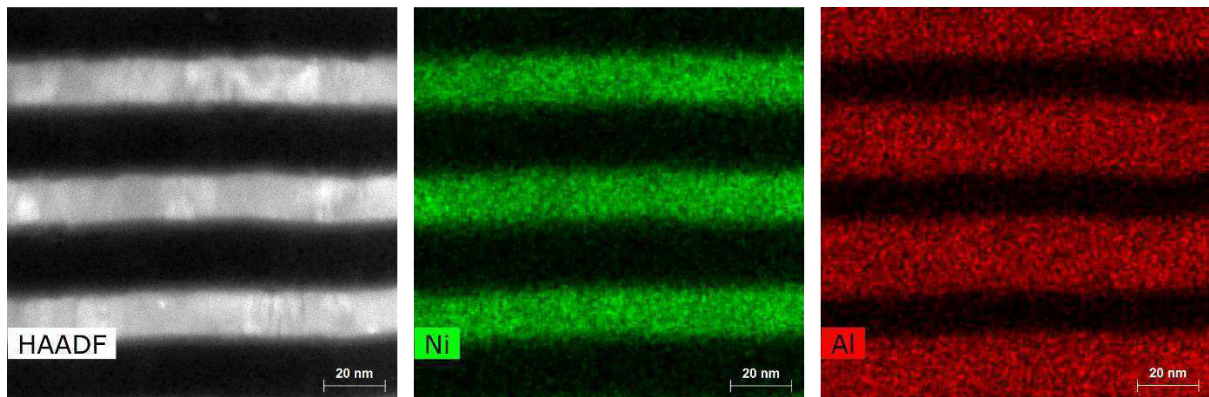
66. Controlling the Reaction Propagation in Ni-Al Multilayers with Premixed Interlayers

Nensi Toncich and Ralph Spolenak

D-MATL, ETH Zurich

The presence of the premixed layers represents a physical barrier to interdiffusion and atomic mixing between the Ni and Al layers. Molecular dynamics simulations of the solid-state combustion in Ni/Al multilayers have shown a direct correlation between the premixed layer thickness and the front propagation velocity of the Ni/Al reactive multilayers [1]. In this study, a premixed interlayer was used to control the heat propagation speed in Ni/Al reactive multilayers. The Ni and Al layers were deposited with a commercial magnetron sputtering system on Si wafers coated with a photoresist layer providing thermal insulation between the layers and the wafer. A premixed layer was introduced between each layer by co-sputtering Ni and Al. The bilayer height, including the premixed layers, was kept constant at 40 nm with a 30-fold repetition. An 1:1 atomic ratio between the Ni and Al elements was used to adjust the thicknesses of the Ni, Al and premixed layers.

[1] F. Schwarz and R. Spolenak, J. Appl. Phys. 131, 075107 (2022).



Cross-section of alternating Ni and Al layers which bilayer thickness is 40 nm. STEM images show a clear presence of an intermixed layer at each interface.

67. Shrinking Micropatterns with 3D Hydrogel Templates

Valentina G. De Rosa[1], Juri G. Crimmann[1], Nolan Lassaline[1], Bruno Marco-Dufort[2], Deepankur Thureja[1,3], Daniel Petter[1], Yannik Glauser[1], David Seda[1], Gabriel Nagamine[1], Mark W. Tibbitt[2] and David J. Norris[1]

[1] *Optical Materials Engineering, D-MAVT, ETH Zurich*

[2] *Macromolecular Engineering, D-MAVT, ETH Zurich*

[3] *Quantum Photonics, D-PHYS, ETH Zurich*

Hydrogels are a unique class of materials that can go through significant volume changes by absorbing large amounts of a solvent and swell without losing their original structure. This effect is reversible, meaning that hydrogels can be shrunk back to their initial state through dehydration[1]. Here, we propose using the shrinkable property of hydrogels as a degree of freedom to manipulate the size of precisely fabricated microstructures. We explore the efficacy of this approach by shrinking the wavelength of Fourier surfaces[2] fabricated by thermal scanning-probe lithography (tSPL). Lassaline et al. recently demonstrated that tSPL can create sinusoidal patterns (recently-termed Fourier surfaces) with nanometer features[2]. In this project, we transfer Fourier surfaces with micrometer features to an acrylamide hydrogel using a templating process from a silicon master. The hydrogel is then shrunk in a controlled environment by means of dehydration. As a consequence, the patterns on its surface shrink. The dried and shrunken hydrogel is then used as a template to produce replica of the pattern on a thin gold layer. The latter is achieved by evaporating gold onto the hydrogel. To assess the overall success of this method, the topography of all the resulting patterns (on the silicon substrate, on the dried hydrogel, and on the gold surface) are examined using atomic force microscopy (AFM). The ability to shrink Fourier surfaces, and more broadly, patterned micro- and nanostructures, offers new opportunities for optical and electronic devices.

[1] D. Oran, et al., *Science* 362.6420, 1281-1285 (2018).

[2] N. Lassaline, et al., *Nature* 582.7813, 506-510 (2020)

68. Surface-Initiated Polymerisation from Lipid Membranes: Mechanism, Curvature, and Thermoresponsivity

Alexandre L. Torzynski[1], Dominique Grimm[1], Matteo Romio[2], Bilal Qureshi[3], Edmondo M. Benetti[4] and Eric R. Dufresne[1]

[1] *Soft and Living Materials, D-MATL, ETH Zurich*

[2] *Biointerfaces Lab, Empa*

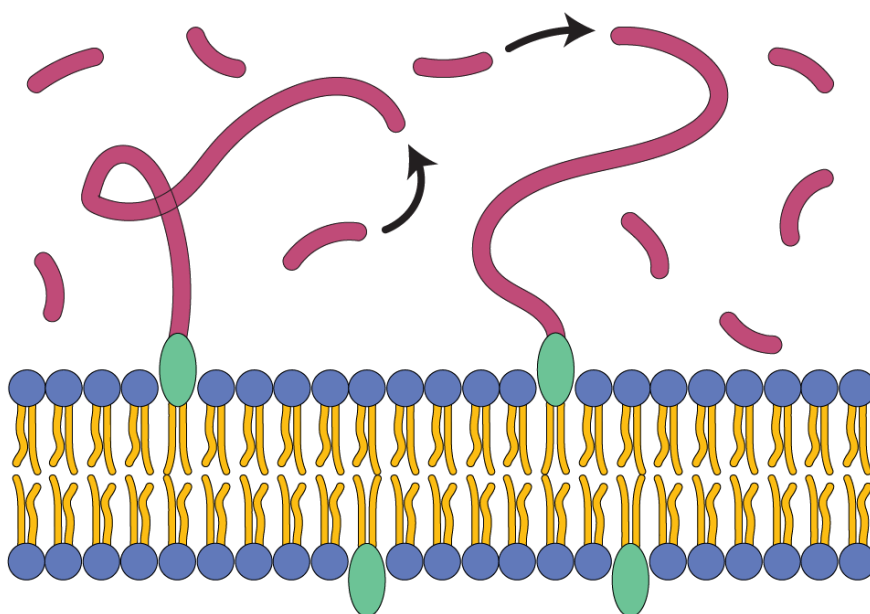
[3] *ScopeM, D-MATL, ETH Zurich*

[4] *Department of Chemical Sciences, University of Padua (Italy)*

In order to mimic the glycocalyx, a brush-like structure covering many cells, we aim to grow polymer brushes of controlled density and thickness from one side of a lipid membrane. To this end, we initiate the aqueous polymerization of N-isopropylacrylamide (NIPAM) from the surface of phospholipid bilayers

in two different systems: supported lipid bilayers (SLBs), adsorbed on a flat surface, and small unilamellar vesicles (SUVs), suspended in solution. Polymerisations from these lipid membranes are monitored with quartz-crystal microbalance with dissipation monitoring (QCM-D) and dynamic light scattering (DLS) respectively. In both systems, the growth of a polymer layer is observed, whose thickness strongly correlates with the bilayer's surface concentration of initiator. SUV-initiated polymerizations run for longer and yield thicker brushes than their SLB counterparts, which we attribute to the difference in membrane curvature between these systems. Non-monotonic variations of the brush thickness suggest degrafting at high surface densities. Reversible collapse of the poly(NIPAM) brushes is observed when the temperature is cycled around the polymer's lower critical solution temperature (LCST). Once applied to micrometer-sized vesicles, this technique will yield an experimental model system allowing membrane deformations and a direct comparison to the glycocalyx. [1]

[1] C.R. Shurer, et al., Cell 177, 1757–1770 (2019).



Schematic of a surface-initiated polymerization yielding a brush on one side of a phospholipid bilayer.

69. DFT Simulations of atomic, solid and liquid Xenon for Dark Matter Direct Detection

Luca Marin, Marek Matas and Nicola A. Spaldin

Materials Theory, D-MATL, ETH Zurich

Some of the most sensitive detectors for the direct detection of dark-matter (DM) use xenon to search for scattering events between a DM and an ordinary matter particle [1]. Within the light DM scenario, the electrons of a given material become the dominant target [2, 3].

We exploit DFT to reproduce electronic and structural experimental data of xenon. We include corrections to the exchange-correlation (XC) functional to account for the non-local van der Waals interactions, spin-orbit interaction and corrections to the self-interaction effects in the localized 4d states of Xe.

We then compute the electronic wavefunctions and energy levels of the isolated atom and the electronic band structure and density of states of the solid phase. Finally, we perform preliminary calculations of the energy levels of the liquid phase, using Monte Carlo simulations to model the atomic positions.

Our results provide fertile ground to predict the DM-induced electronic excitation rate for xenon detectors.

[1] R. Essig, J. Mardon, and T. Volansky. Direct Detection of Sub-GeV Dark Matter. Phys. Rev., D85:076007, 2012

[2] R. Catena, T. Emken, N. A. Spaldin, and W. Tarantino. Atomic responses to general dark matter-electron interactions. Phys. Rev. Res., 2(3):033195, 2020.

[3] R. Catena, T. Emken, M. Matas, N. A. Spaldin, and E. Urdshals. Crystal responses to general dark matter-electron interactions. Phys. Rev. Research, 3:033149, Aug 2021.

LIST OF PARTICIPANTS

- ABANDO, Nerea, Nanometallurgy, D-MATL,
nerea.abando@mat.ethz.ch
- AGRAWAL, Prajwal, Acoustic Robotics for Life
Sciences & Healthcare, D-MAVT, pprajwal@ethz.ch
- AHMED, Daniel, Prof., Acoustic Robotics for Life
Science and Healthcare, D-MAVT, dahmed@ethz.ch
- ALAGU UTHAYA KUMAR, Guru Aathavan, Acoustic
Robotics for Life Sciences & Healthcare, D-MAVT,
galagu@student.ethz.ch
- ALFARANO, Serena, Dr., Food & Soft Materials,
D-HEST, serenarosa.alfarano@hest.ethz.ch
- ALMUKAMBETOVA, Madina, Food & Soft Materials,
D-HEST, madina.almukambetova@hest.ethz.ch
- ANGEHRN, Andrew, Materials & Device Engineering,
D-ITET, andrew.angehrn@ife.ee.ethz.ch
- ANGST, Ueli, Prof., Durability of Engineering Materials,
D-BAUG, ueli.angst@ifb.baug.ethz.ch
- ANTHIS, Alexandre, Dr., Nanoparticle Systems
Engineering, D-MAVT, ahcanthis@gmail.com
- BALCIUNAITE, Aiste, Soft Robotics, D-MAVT,
aiste.balcunaite@srl.ethz.ch
- BAO, Yinyin, Dr., Drug Formulation & Delivery,
D-CHAB, yinyin.bao@pharma.ethz.ch
- BARGARDI, Fabio, Dr., Complex Materials, D-MATL,
fabio.bargardi@mat.ethz.ch
- BERNERO, Margherita, Bone Biomechanics, D-HEST,
margherita.bernero@hest.ethz.ch
- BERNHARD, Stéphane, Macromolecular Engineering,
D-MAVT, sbernhard@ethz.ch
- BINELLI, Marco, Complex Materials, D-MATL,
marco.binelli@mat.ethz.ch
- BÖDDEKER, Thomas, Soft & Living Materials,
D-MATL, thomas.boeddeker@mat.ethz.ch
- BOEV, Dimitar, Acoustic Robotics for Life Sciences &
Healthcare, D-MAVT, diboev@ethz.ch
- BOGGON, Cameron, Soft Materials & Interfaces,
D-MATL, cboggon@ethz.ch
- BOOLAKEE, Oliver, Computational Mechanics,
D-MAVT, oboolakee@ethz.ch
- BOONS, Rani, Complex Materials, D-MATL,
Rani.boons@mat.ethz.ch
- BORN, Friederike-Leonie, Bioanalytics, D-BSSE,
friederike.born@bsse.ethz.ch
- BOVONE, Giovanni, Macromolecular Engineering,
D-MAVT, gbovone@ethz.ch
- BREITFELD, Maximilian, Bioanalytics, D-BSSE,
maximilian.breitfeld@bsse.ethz.ch
- BUCHER VAN LIGTEN, Simone, ETH Office of the
President, simone.bucher@sl.ethz.ch
- BURGERT, Ingo, Prof., Wood Materials Science,
D-BAUG, iburgert@ethz.ch
- CASTELLANO, Miguel, Computational Mechanics of
Building Materials, D-BAUG,
miguel.castellano@ifb.baug.ethz.ch
- CHEIBAS, Ina, Architecture & Digital Fabrication,
D-ARCH, icheibas@ethz.ch
- CHEN, Jialu, Composite Materials & Adaptive
Structures, D-MAVT, jichen@ethz.ch
- CHEN, Xiulin, Durability of Engineering Materials,
D-BAUG, D-HEST, xiulchen@student.ethz.ch
- CIPOLATO, Oscar, Nanoparticle Systems Engineering,
D-MAVT, ocipolato@ethz.ch
- CRIMMANN, Juri, Optical Materials Engineering,
D-MAVT, jcrimmann@ethz.ch
- CUI, Yifan, Macromolecular Engineering, D-MAVT,
cuiy@ethz.ch
- DANUN, Aschraf, Product Development, D-MAVT,
aschrafdanun@ethz.ch
- DE ROSA, Valentina, Optical Materials Engineering,
D-MAVT, vaderosa@ethz.ch
- DEILLON, Léa, Dr., Advanced Manufacturing, D-MAVT,
Ideillon@ethz.ch
- DEL CAMPO FONSECA, Alexia, Acoustic Robotics for
Life Sciences & Healthcare, D-MAVT,
afonseca@ethz.ch
- DEMIRÖRS, Ahmet, Dr., Complex Materials, D-MATL,
ahmet.demiroers@mat.ethz.ch
- DENG, Zhikang, Steel & Composite Structures,
D-BAUG, zhideng@ethz.ch
- DESHMUKH, Dhananjay, Macromolecular Engineering,
D-MAVT, desh Mukd@ethz.ch
- DILLINGER, Cornel, Acoustic Robotics for Life
Sciences & Healthcare, D-MAVT, corneld@ethz.ch
- DIONA, Pietro, Magnetism & Interface Physics,
D-MATL, pietro.diona@mat.ethz.ch
- DITTRICH, Petra, Prof., Bioanalytics, D-BSSE,
petra.dittrich@bsse.ethz.ch
- DONG, Zhou, Food & Soft Materials, D-HEST,
dongzhouplf@163.com
- DUTTO, Alessandro, Complex Materials, D-MATL,
alessandro.dutto@mat.ethz.ch
- EFE, Ipek, Multifunctional Ferroic Materials, D-MATL,
ipek.efe@mat.ethz.ch
- ELIASSON, Henrik, Multifunctional Ferroic Materials,
D-MATL, henrik.eliasson@empa.ch

EMIROGLU, Börte, Macromolecular Engineering, D-MAVT, boerte.emiroglu@chem.ethz.ch

ESSWEIN, Tobias, Materials Theory, D-MATL, tobias.esswein@mat.ethz.ch

FAGNONI, Francesco, Laboratory for Nuclear Materials, PSI / D-MATL, francesco.fagnoni@psi.ch

FARK, Giacumin, Acoustic Robotics for Life Sciences & Healthcare, D-MAVT, farkg@student.ethz.ch

FELLNER, Madeleine, Multifunctional Materials, D-MATL, madeleine.fellner@mat.ethz.ch

FENG, Yanxia, Soft & Living Materials, D-MATL, yanxia.feng@mat.ethz.ch

FERGUSON, Stephen, Prof., Orthopaedic Technology, D-HEST, sferguson@ethz.ch

FERNANDEZ-RICO, Carla, Dr., Soft & Living Materials, D-MATL, carla.fernandezrico@mat.ethz.ch

FIRLUS, Alexander, Metal Physics & Technology, D-MATL, alexander.firlus@mat.ethz.ch

FORSTER, Lea, Multifunctional Ferroic Materials, D-MATL, lea.forster@mat.ethz.ch

FURCAS, Fabio Enrico, Durability of Engineering Materials, D-BAUG, ffurcas@ethz.ch

GALATA, Aikaterini, Polymer Physics, D-MATL, aikaterini.galata@mat.ethz.ch

GAMBARDELLA, Pietro, Prof., Magnetism & Interface Physics, D-MATL, pietro.gambardella@mat.ethz.ch

GANZEBOOM, Sophia, Structural Mechanics & Monitoring, D-BAUG, sophia.ganzeboom@ibk.baug.ethz.ch

GEHRE, Christian, Bone Biomechanics, D-HEST, cgehre@ethz.ch

GERBER, Dominic, Soft & Living Materials, D-MATL, dominic.gerber@mat.ethz.ch

GERLT, Michael, Dr., Biochemical Engineering, D-CHAB, michael.gerlt@chem.ethz.ch

GHOULI, Saeid, Computational Mechanics, D-MAVT, sghouli@ethz.ch

GIOVANOLI, Diego, Complex Materials, D-MATL, diego.giovanoli@mat.ethz.ch

GIRALDO, Marcela, Multifunctional Ferroic Materials, D-MATL, marcela.giraldom@mat.ethz.ch

GIRARD, Arthur, Computational Modelling of Materials in Manufacturing, D-MAVT, agirard@ethz.ch

GLAUSER, Yannik, Optical Materials Engineering, D-MAVT, yglaiser@ethz.ch

GORA, Michal, Advanced Fibers, Empa / D-MATL, michal.gora@empa.ch

GRABER, Pascal, Acoustic Robotics for Life Sciences & Healthcare, D-MAVT, graberp@student.ethz.ch

GRADAUSKAITE, Elzbieta, Multifunctional Ferroic Materials, D-MATL, elzbieta.gradauskaite@mat.ethz.ch

GRAY, Natascha, Complex Materials, D-MATL, natascha.gray@mat.ethz.ch

GUICHARD, Xavier, Multifunctional Ferroic Materials, D-MATL, xavier.guichard@mat.ethz.ch

GÜNTHER, Roman, Multifunctional Materials, D-MATL, IMPE, roman.guenther@mat.ethz.ch

HABERMANN, Sebastian, Nanoparticle Systems Engineering, D-MAVT, shabermann@student.ethz.ch

HERNANDEZ OENDRA, Alexander, Optical Materials Engineering, D-MAVT, hernanda@student.ethz.ch

HOFFMANN, Marco, Magnetism & Interface Physics, D-MATL, mhoffma@ethz.ch

HONG, Chul Gi, Electrochemical Energy Systems, D-MAVT, chhong@ethz.ch

HU, Minghan, Dr., Soft Materials & Interfaces, D-MATL, minghu@ethz.ch

INDERGAND, Roman, Mechanics & Materials, D-MAVT, iroman@mavt.ethz.ch

ISA, Lucio, Prof., Soft Materials & Interfaces, D-MATL, lucio.isa@mat.ethz.ch

JESSERNIG, Alexander, Nanoparticle Systems Engineering, D-HEST, alexander.jessernig@hest.ethz.ch

JIN, Tonghui, Food & Soft Materials, D-HEST, tonjin@ethz.ch

JORDAN, Benoît, Artificial Intelligence in Mechanics & Manufacturing, D-MAVT, jordanb@ethz.ch

KAMMER, David, Prof., Computational Mechanics of Building Materials, D-BAUG, dkammer@ethz.ch

KANNAN, Vignesh, Dr., Mechanics & Materials, D-MAVT, kannanvi@ethz.ch

KAVAS, Baris, Advanced Manufacturing, D-MAVT, bkavas@ethz.ch

KHOLINA, Yevheniia, Multifunctional Ferroic Materials, D-MATL, yevheniia.kholina@mat.ethz.ch

KHOSLA, Nathan, Biochemical Engineering, D-CHAB, Nathan.khosla@chem.ethz.ch

KIM, Donghoon, Multi-Scale Robotics, D-MAVT, kimdon@ethz.ch

KINZELBACH, Sumei, Soft Materials & Interfaces, D-MATL, slpk3@cam.ac.uk

KIWIC, David, Multifunctional Materials, D-MATL, dkiwic@student.ethz.ch

KLEGER, Nicole, Dr., Complex Materials, D-MATL, nicole.kleger@mat.ethz.ch

KLEIN CERREJON, David, Drug Formulation & Delivery, D-CHAB, David.Klein@pharma.ethz.ch

KLÖSEL, Katrina, Micro & Nanosystems, D-MAVT, kloesek@ethz.ch

KOUREAS, Ioannis, Computational Mechanics of Building Materials, D-BAUG, ikoureas@ethz.ch

KRÜGER, Reto, D-MATL, kruegerr@student.ethz.ch

KUANG, Hekun, Multifunctional Materials, D-MATL, hkuang@student.ethz.ch

KUMAAR, Dhananjey, Chemistry & Materials Design, D-ITET, dvenkate@ethz.ch

KUMAR, Sudhir, Dr., Nanomaterials Engineering, D-CHAB, sudhir.kumar@chem.ethz.ch

KUO, Hsin-Hung, Nanomaterials Engineering, D-CHAB, hsin-hung.kuo@chem.ethz.ch

LAUENER, Carmen, Nanometallurgy, D-MATL, carmen.lauener@mat.ethz.ch

LAURENT, Julie, Complex Materials, D-MATL, julie.laurent@mat.ethz.ch

LAURIA, Alessandro, Dr., Multifunctional Materials, D-MATL, alessandro.lauria@mat.ethz.ch

LEE, Seunghun S., Orthopaedic Technology, D-HEST, seunglee@ethz.ch

LEHÉRICÉY, Pierre, Soft Materials, D-MATL, pierre.lehericey@mat.ethz.ch

LEVALLEY, Paige, Dr., Nanoparticle Systems Engineering, D-MAVT, plevalley@ethz.ch

LI, Jingwen, Multifunctional Ferroic Materials, D-MATL, jingwli@ethz.ch

LI, Mingqin, Dr., Food & Soft Materials, D-HEST, mingqin.mingqinli@hest.ethz.ch

LI, Tianchi, Soft & Living Materials, D-MATL, tianchi.li@mat.ethz.ch

LIBANORI, Rafael, Dr., Complex Materials, D-MATL, libanori@mat.ethz.ch

LO, Shao-Wei, Nanomaterials Engineering, D-CHAB, shao-wei.lo@chem.ethz.ch

LOTFY, Ahmed Samir, Multifunctional Ferroic Materials, D-MATL, samir.lotfy@mat.ethz.ch

MA, Zhongqi, Soft Materials & Interfaces, D-MATL, zhonma@ethz.ch

MAGRINI, Tommaso, Dr., Complex Materials, D-MATL, magrini@caltech.edu

MANAV, Manav, Dr., Computational Mechanics, D-MAVT, mmanav@ethz.ch

MARIN, Luca, Materials Theory, D-MATL, luca.marin@mat.ethz.ch

MATTICH, Iacopo, Complex Materials, D-MATL, iacopo.mattich@mat.ethz.ch

MEBOLDT, Mirko, Prof., Product Development, D-MAVT, meboldtm@ethz.ch

MEIJS, Zazo, Soft Materials & Interfaces, D-MATL, zmeijs@ethz.ch

MENASCE, Stefano, Complex Materials, D-MATL, stefano.menasce@mat.ethz.ch

MÉNÉTREY, Maxence, Nanometallurgy, D-MATL, maxence.menetrey@mat.ethz.ch

MERKEL, Maximilian, Materials Theory, D-MATL, maximilian.merkel@mat.ethz.ch

MICHEL, Luca, Computational Mechanics of Building Materials, D-BAUG, luca.michel@ifb.baug.ethz.ch

MICHEL, Veronica, Multifunctional Materials, D-MATL, veronica.michel@mat.ethz.ch

MONTI, Chiara, Advanced Manufacturing, D-MAVT, monti@inspire.ethz.ch

MOSER, Annina, Materials & Device Engineering, D-ITET, annmoser@ethz.ch

MÜLLER, Florence, Soft Materials, D-MATL, muellflo@ethz.ch

MÜLLER, Marvin, Multifunctional Ferroic Materials, D-MATL, marvin.mueller@mat.ethz.ch

MÜLLER, Philip, Computational Mechanics of Building Materials, D-BAUG, phimuell@ethz.ch

MYKOLENKO, Svitlana, Prof., Food & Soft Materials, D-HEST, svitlana.mykolenko@hest.ethz.ch

NEUER, Anna, Nanoparticle Systems Engineering, D-MAVT, aneuer@student.ethz.ch

NIGGEL, Vincent, Soft Materials & Interfaces, D-MATL, vincent.niggel@mat.ethz.ch

NORRIS, Graham, Quantum Device Lab, D-PHYS, graham.norris@phys.ethz.ch

NOTTER, Daniel, Renewable Energy Carriers, D-MAVT, danotter@ethz.ch

NUSSBAUM, Natalie, Food Process Engineering, D-HEST, natalie.nussbaum@hest.ethz.ch

NYDEGGER, Mirco, Nanometallurgy, D-MATL, mirco.nydegger@mat.ethz.ch

OCANA PUJOL, Jose Luis, Nanometallurgy, D-MATL, jose.ocana@mat.ethz.ch

PAGANI, Gabriele, Soft Materials, D-MATL, gabriele.pagani@mat.ethz.ch

PANZARASA, Guido, Dr., Wood Materials Science, D-BAUG, guidop@ethz.ch

PARKATZIDIS, Kostas, Polymeric Materials, D-MATL, kostas.parkatzidis@mat.ethz.ch

PAUNOVIĆ, Nevena, Drug Formulation & Delivery, D-CHAB, nevena.paunovic@pharma.ethz.ch

PEREIRA MARTENDAL, Caroline, Advanced Manufacturing, D-MAVT, pereirca@student.ethz.ch

PFÄNDLER, Patrick, Durability of Engineering Materials, D-BAUG, patrick.pfaendler@ifb.baug.ethz.ch

PORENTA, Nikolaus, Nanometallurgy, D-MATL, nikolaus.porenta@mat.ethz.ch

PUN, Andrew, Dr., Optical Materials Engineering, D-MAVT, andpun@ethz.ch

QIN, Xiao-Hua, Dr., Bone Biomechanics, D-HEST, qinx@ethz.ch

QIU, Wanwan, Bone Biomechanics, D-HEST, wanqiu@ethz.ch

RICHARDS, Daniel, Dr., Biochemical Engineering, D-CHAB, daniel.richards@chem.ethz.ch

RITTINER, Florian, Dr., ETH Collaborative Learning Platform, florian.rittiner@sl.ethz.ch

RIZZO, Riccardo, Tissue Engineering & Biofabrication, D-HEST, riccardo.rizzo@hest.ethz.ch

ROHNER, Adrian, Dr., ETH Office of Research, adrian.rohner@sl.ethz.ch

ROLLAND, Manon, Polymeric Materials, D-MATL, manon.rolland@mat.ethz.ch

SAKARIDIS, Emmanouil, Artificial Intelligence in Mechanics & Manufacturing, D-MAVT, esakaridis@ethz.ch

SCHRECK, Murielle, Dr., Multifunctional Ferroic Materials, D-MATL, murielle.schreck@mat.ethz.ch

SCHUTZIUS, Thomas, Prof., Multiphase Thermofluidics and Surface Nanoengineering, D-MAVT, thomschu@ethz.ch

SCHWARZ, Fabian, Nanometallurgy, D-MATL, fabian.schwarz@mat.ethz.ch

SCHWEGLER, Alain, Complex Materials, D-MATL, alainsc@student.ethz.ch

SECCHI, Eleonora, Dr., Groundwater & Hydromechanics, D-BAUG, secchi@ifu.baug.ethz.ch

SENOL GUNGOR, Ayca, Materials & Device Engineering, D-ITET, senola@ethz.ch

SHIH, Chih-Jen, Prof., Nanomaterials Engineering, D-CHAB, chih-jen.shih@chem.ethz.ch

SIGEL, Claudia, D-MATL, claudia.sigel@mat.ethz.ch

SIGRIST, Lukas, Dr., ETH School for Continuing Education, lukas.sigrist@sce.ethz.ch

SIMONOV, Arkadiy, Prof., Multifunctional Ferroic Materials, D-MATL, arkadiy.simonov@mat.ethz.ch

SKEVAKI, Eleni, Digital Building Technologies, D-ARCH, skevaki@arch.ethz.ch

SOUZA PLATH, André, Orthopaedic Technology, D-HEST, andre.souzaplath@hest.ethz.ch

SPINOLA, Miguel, Mechanics & Materials, D-MAVT, mspinola@ethz.ch

SPOLENAK, Ralph, Prof., Nanometallurgy, D-MATL, ralph.spolenak@mat.ethz.ch

STANKO, Štefan, Metal Physics & Technology, D-MATL, stefan.stanko@mat.ethz.ch

STEFFI, Chris, Dr., Bone Biomechanics, D-HEST, chris.steffi@hest.ethz.ch

STOICA, Mihai, Dr., Metal Physics and Technology, D-MATL, mihai.stoica@mat.ethz.ch

STRKALJ, Nives, Dr., Multifunctional Ferroic Materials, D-MATL, ns851@cam.ac.uk

STUCKI, Sandro, Wood Materials Science, D-BAUG, stuckis@ethz.ch

STUDART, André, Prof., Complex Materials, D-MATL, andre.studart@mat.ethz.ch

STUDER, Pascal, Soft Materials, D-MATL, pascal.studer@mat.ethz.ch

STYLE, Robert, Dr., Soft & Living Materials, D-MATL, robert.style@mat.ethz.ch

SUN, Qiyao, Food Process Engineering, D-HEST, qiyao.sun@hest.ethz.ch

SUTER, Benjamin, Nanoparticle Systems Engineering, Empa / D-MAVT, besuter@ethz.ch

SVANBERG, Sara, Bioanalytics, D-BSSE, sara.svanberg@bsse.ethz.ch

TALTS, Ulle-Linda, Optical Nanomaterial, D-PHYS, utalts@phys.ethz.ch

TIBBITT, Mark W., Prof., Macromolecular Engineering, D-MAVT, mtibbitt@ethz.ch

TIMPU, Flavia, Dr., Trapped Ion Quantum Information, PSI, D-PHYS, ftimpu@ethz.ch

TONCICH, Nensi, Nanometallurgy, D-MATL, nensi.toncich@mat.ethz.ch

TORZYNSKI, Alexandre, Soft & Living Materials, D-MATL, alexandre.torzynski@mat.ethz.ch

TOSIC, Tara, Materials Theory, D-MATL, tara.tosic@mat.ethz.ch

TRASSIN, Morgan, Prof., Multifunctional Ferroic Materials, D-MATL, morgan.trassin@mat.ethz.ch

TSIMOURI, Ioanna, Polymer Physics, D-MATL, ioanna.tsimouri@mat.ethz.ch

TUCKER, Michael, Dr., Advanced Manufacturing, D-MAVT, mtucker@ethz.ch

USUELLI, Mattia, Dr., Food & Soft Materials, D-HEST, mattia.usuelli@hest.ethz.ch

VAN BAALEN, Carolina, Soft Materials & Interfaces, D-MATL, carolina.vanbaalen@mat.ethz.ch

VAN KESTEREN, Steven, Soft Materials & Interfaces, D-MATL, steven.vankesteren@outlook.com

VERBEEK, Xanthe, Materials Theory, D-MATL, xanthe.verbeek@mat.ethz.ch

VOGEL, Alexander, Multifunctional Ferroic Materials, D-MATL, alexander.vogel@empa.ch

VOGLER-NEULING, Viola, Dr., Optical Nanomaterial, D-PHYS, voglerv@phys.ethz.ch

VOLLMANN, Morten, Micro- & Nanosystems, D-MAVT, mvollmann@ethz.ch

VON MENTLEN, Jean-Marc, Materials & Device Engineering, D-ITET, jean-marc.sujata@ife.ee.ethz.ch

WALSER, Tobias, Dr., D-HEST, tobias.walser@hest.ethz.ch

WANG, Xiaoyu, Dr., Computational Mechanics of Building Materials, D-BAUG, xiaoyu.wang@ifb.baug.ethz.ch

WENZLER, Nils, *Materials & Device Engineering, D-ITET*, wenzlern@ethz.ch
WESSELY, Viktor, *Metal Physics & Technology, D-MATL*, wesselyv@ethz.ch
WIED, Markus, *Materials & Device Engineering, D-ITET*, markus.wied@ife.ee.ethz.ch
WINTERSTELLER, Simon, *Chemistry & Materials Design, D-ITET*, simonwin@ethz.ch
WOBILL, Ciatta, *Food Process Engineering, D-HEST*, ciatta.wobill@hest.ethz.ch
WOHLWEND, Jelena, *Nanometallurgy, D-MATL*, jelena.wohlwend@mat.ethz.ch
WOLFISBERG, Gianna, *Soft & Living Materials, D-MATL*, gianna.wolfisberg@mat.ethz.ch
WOOLLEY, Lukas, *Soft Materials, D-MATL*, woolley@ethz.ch
WU, Chao, Prof., *Food & Soft Materials, D-HEST*, chao.wu@hest.ethz.ch
WU, Jiang, Dr., *Multi-Scale Robotics, D-MAVT*, jianwu@ethz.ch
XU, Dan, *Food & Soft Materials, D-HEST*, dan.xu@hest.ethz.ch
YANG, Chia-Jung, *Multifunctional Ferroic Materials, D-MAVT*, chia-jung.yang@mat.ethz.ch
YUTS, Yulia, *Drug Formulation & Delivery, D-CHAB*, yulia.yuts@pharma.ethz.ch
ZAUCHNER, Doris, *Bone Biomechanics, D-HEST*, doris.zauchner@hest.ethz.ch
ZHANG, Zhiyuan, *Acoustic Robotics for Life Sciences & Healthcare, D-MAVT*, zhiy Zhang@ethz.ch

ZHAO, Yaqi, *Computational Mechanics of Building Materials, D-BAUG*, zhaoya@student.ethz.ch
ZHUANG, Shengyang, *Acoustic Robotics for Life Sciences & Healthcare, D-MAVT*, szhuang@student.ethz.ch
ZIMMERMANN, Jan, Dr., *ETH Industry Relations*, jan.zimmermann@sl.ethz.ch
ZÜBLIN, Patrick, *Food & Soft Materials, D-HEST*, patrick.zueblin@hest.ethz.ch

THE ORGANIZING COMMITTEE

DIETSCHKE, Claudius, *Bioanalytics, D-BSSE*, claudius.dietsche@bsse.ethz.ch
DING, Yong, *Wood Materials Science, D-BAUG*, yoding@ethz.ch
ENRRIQUEZ, Nadia, *Complex Materials, D-MATL*, nadia.enrriquez@mat.ethz.ch
MORAGUES, Thomas, *Biochemical Engineering, D-CHAB*, thomas.moragues@chem.ethz.ch
SHEN, Xueting, *Soft Materials & Interfaces, D-MATL*, xueting.shen@mat.ethz.ch
ZUNZUNEGUI, Eva, *Food & Soft Materials, D-HEST*, Evamaria.zunzuneguibr@hest.ethz.ch
LAU, Barbara, *MaP*, barbara.lau@mat.ethz.ch
SCHEFER, Larissa, Dr., *MaP*, larissa.schefer@mat.ethz.ch

ETH Zurich
Competence Center for Materials and Processes (MaP)
Leopold-Ruzicka-Weg 4
8093 Zürich

www.doctoral-school.ethz.ch/events/grad-symp

© ETH Zurich, August 2022